Evaluation of a refrigerant/absorbent combination for vapour absorption refrigeration systems utilising solar heat.

Adegoke, C O

EVALUATION OF A REFRIGERANT/ABSORBENT COMBINATION FOR VAPOUR ABSORPTION REFRIGERATION SYSTEMS UTILISING SOLAR HEAT.

by

C. O. ADEGOKE

A thesis submitted for the fulfilment of the requirement for the Degree of Doctor of Philosophy in Mechanical Engineering of the University of London

Department of Mechanical Engineering
King's College, London (KQC)

1987

"Except the Lord build the house,
they labour in vain that build it;
except the Lord keep the city, the watchman
waketh but in vain"

-Psalm 127:1

To my mother Madam Maria
and my sisters Ruth, Comfort
and Abejide

Abstract

A new working fluid for absorption refrigeration system, using low temperature regeneration heat source, has been evaluated. In this working fluid, water was used as the refrigerant and a mixture of two moles of lithium bromide and one mole of zinc bromide as the absorbent.

The two most popular refrigerant/absorbent combinations for vapour absorption refrigeration systems are ammonia-water and lithium bromide-water. The lithium bromide-water combination is, however, more favoured for low regeneration temperature applications for air conditioning and other chilling purposes. The major limitation of the lithium bromide-water system however, is the low salt solubility which prevents the strong solution from the generator from being cooled to nearer the absorber temperature without salt crystallisation. The first attempt of this research work was therefore, to improve the solubility of lithium bromide in water with the derived solution also maintaining most of the advantages of the lithium bromide-water combination.

A solubility apparatus was built and zinc bromide was tested with acqueous solutions of lithium bromide within a solution temperature range of 25-80°C. Zinc bromide was found to improve the solubility of lithium bromide in water quite markedly.

A boiling point apparatus was designed and built to measure the normal boiling point of $2LiBr-ZnBr_2-H_2O$ solution. As there were no data available in the literature for the solution, the normal boiling point of $LiBr-H_2O$ solution was also measured and the results compared with published data to ascertain the accuracy of results obtained by this apparatus.

A vapour pressure apparatus was designed and built to measure the vapour pressure of the solution ($2LiBr-ZnBr_2-H_2O$). A Duhring plot was produced from these data which was also used in conjunction with the heat capacity measurement for one solution concentration made by the National Physical Laboratory, to produce the Enthalpy/Concentration chart.

An experimental absorption refrigerator was then designed, built and tested using the solution, $2LiBr-ZnBr_2-H_2O$. At a regeneration temperature as low as 64°C. an actual heat ratio of 0.57 was attained with an evaporation temperature of 13°C.

Acknowledgement

The author would like to express his sincere thanks to his supervisor, Professor W. B. Gosney for his invaluable contributions and indispensable advices throughout this investigation.

Thanks are also due to Mr M. Harrington and his workshop staff, notably Dennis Green, Carlyle Edwards, David Elgar and Leslie Clark, for their help in the construction of the experimental apparatus. His sincere thanks also go to David Cummings Word Processing for typing this thesis and to his wife, Olufunmilayo, for her understanding and support throughout the period of this work.

Contents

Chapter 4 DETERMINATION OF THE THERMODYNAMIC PROPERTIES OF THE SOLUTIONS

LIST OF FIGURES

Chapter Four

Chapter Five

Chapter Six

List of Tables

Table:

Chapter Four

Chapter Five

Chapter Six

Chapter Seven

LIST OF PLATES

Chapter Four

Chapter Five

NOTATION

A	Outside surface area, m^2
C	Specific heat
E	Total irradiation, J/m^2S
H	Heat of vapourisation
h	Specific enthalpy, KJ/kg
I	Solar insolation, W/m^2
k	thermal conductivity, W/mK
M	Molecular weight, Kg/kmol
m	mass flow rate, g/s
P	Pressure, mbar
Q	Total heat, KW or W
q	heat flux, KW/m^2
R	Fouling resistance or surface resistance, m^2 K/W
T	Absolute temperature, K
t	Temperature, °C.
U	Overall coefficient of heat transmission, W/m^2K
V	volume, m^3
v	Specific volume, m^3/kg
W	Work, KJ
α	Absorptance
ε	Heat ratio
η	Efficiency
λ	Circulation factor
ξ	Mass fraction of solution, %
μ	Dynamic viscosity, Kg/mS
ρ	Density, Kg/m^3
σ	Stefan Boltzman constant, J/m^2SK^4
	Surface tension of liquid; N/m
τ	Transmittance

SUBSCRIPTS

a	absorber, ambient
B	barometric
b	boiling point
c	condenser, solar collector
e	evaporator
g	generator
l	inside
o	outside
p	at constant pressure
L	lithium bromide
z	zinc bromide
s	strong solution, surface, solar
u	useful
w	weak solution

Other symbols are described in the text where used

Chapter One

1.0 Introduction

The unfavourable weather conditions within the environment in which man lives necessitates the efforts to look for ways of maintaining more comfortable living conditions. The early man burnt fossil fuel or wood to provide heat but cooling his environment when the ambient air is too hot presented a more complex problem. Hence his interest in the artificial production of cold.

The methods of producing cold by mechanical means is quite recent. In 1834, Jacob Perkins proposed a hand operated compressor machine working on ether to produce ice. This machine became the forerunner of the modern mechanical vapour compression system. However, Perkins work was not mentioned in the literature of the time and seemed to have remained unknown throughout nearly fifty years until Sir Frederick Bramwell described it in 1882 (1).

Sometime about 1850, James Harrison invented a hand operated machine which made ice. The working fluid was also ether but it was not known if Harrison knew of Perkins work or not.

Other refrigerants tried in mechanical refrigeration machines were Dimethylether by Charles

Tellier in 1864 and Sulphur dioxide by Raoul Pictet in 1874. Dimethylether did not come into general use but Sulphur dioxide was an important refrigerant for some sixty years.

In the 1870s, Linde developed a machine working on ammonia. Ammonia has since then been the most important refrigerant for large plants.

Franz Windhausen in 1886 used Carbon dioxide as a refrigerant. Although the system pressure was quite high, of the order of 80 atmospheres in the condenser. The safe nature of Carbon dioxide made it a principal refrigerant for use in ships until about 1955 when the relatively new fluorinated hydrocarbons displaced it. The properties of these new refrigerants of which the first promising one was dichlorodifluoromethane (Freon 12) was measured in the USA by Thomas Midgley in 1929-30.

Although the mechanical vapour compression refrigeration system has been more commonly used,one of the oldest refrigeration devices was based on the absorption principle. William Cullen in 1755 made ice by the distilling effect of evaporating ether. He placed some water in thermal contact with ether under the receiver of a vacuum pump. The operation of the pump caused accelerated evaporation of the ether and the temperature was lowered sufficiently to freeze the water. Because of the low vapour pressure of water a high vacuum was required for effective refrigeration.

This mechanical problems therefore, gave way to the first absorption machine with an absorbing agent.

In 1810, Sir John Leslie made ice artificially by using sulphuric acid as an absorbing agent to absorb pure water vapour. The modification of Cullen's machine was probably the basis of Vallance's Sulphuric acid machine invented in 1824 and of which Edmund Carre's machine, invented in 1850, was an improvement (2). Carre's machine consisted of a glass vessel containing water which under vacuum and in conjunction with a supply of sulphuric acid, froze rapidly.

Ferdinand Carre in 1860 invented the continuous acqua-ammonia system whereby ammonia was the refrigerant and water the absorbent. This development accounts for the major commercial and industrial application in the field of refrigeration.

A special form of acqua-ammonia system has been used in many domestic refrigerators. In this arrangement, the solution pump and the expansion devices are eliminated and the pressure in the whole system made uniform. The low-pressure side is then charged with a non-condensable gas which adds its pressure to that of ammonia to make a total pressure equal to that of the high-pressure side. Geppert in 1899 tried air as a non-condensable gas but he was unable to obtain a sufficient rate of evaporation until he used a fan to circulate the air, thus defeating the object of making a system without any

moving parts. In 1922, Carl Munters and Balzar Von Platen used hydrogen as the non-condensable gas with greater success. They, in addition, used the bubble pump principle to raise the strong solution to the top of the boiler, and provide a hydrostatic head to feed weak solution to the absorber.

More recently, the lithium bromide-water absorption machine was introduced and was operated on commercial basis in 1947 (3).

Before the OPEC cartel of 1973, non-renewable fossil fuels such as coal, oil and natural gas were cheap and so was electricity generated using them. Refrigeration machines were normally driven by burning fossil fuels or by steam or electricity. Since the 1973 Cartel, however, the search for alternative energy sources have been shifting towards the renewable and chemical pollution-free source, such as solar energy. Refrigeration machines are therefore now designed to utilise solar energy as the driving force. Such refrigeration systems that utilise solar heat are discussed in the following section.

1.1 Methods of Refrigeration for Solar Energy Utilisation

The world energy consumption is increasing at a fast rate whilst on the other hand the price and depletion rates of fossil fuel are increasing in recent years,

thus calling for the search for alternative energy sources. A single nuclear reactor, meticulously engineered, carefully tested and thoughtfully sited a safe distance of 150 million kilometres away,that is the Sun, is enough to provide the world energy requirement. The whole surface of the earth receives about 20,000 times the present world energy usage, so that the effect of man's incremental input to the environment is relatively small.

The technology for utilising solar energy is, however, at the present time poorly developed. The two major problems are:

a) the relatively low density at which the energy is available on the earth surface

b) Storage of the energy derived for use when collection is low or impossible.

As a result of these problems, even though solar energy is free for collection, the complete system for effective utilisation is quite expensive at the present time.

However, solar energy application to refrigeration is based on the following conventional methods:

i) the vapour compression system

ii) the vapour jet system

iii) the thermoelectric system

iv) the vapour absorption system.

1.1.1. The Vapour Compression System

It is possible to use concentrating solar collectors to produce steam, which in turn can be used to drive a steam engine that can be used to drive a conventional compressor of a compression refrigeration system. Temperatures around 5900°C. can be obtained by good concentrating collectors (4) which is far more than what is required to generate steam. However, this type of collector is expensive despite the fact that it can only collect direct radiation, thus rendering it inoperative on cloudy days.

According to Yellott (5), Baum and Kirpichev used concentrating collectors to generate steam which they used in driving the compressor of a compression refrigeration cycle. The cost of energy collection, however, did not allow commercialisation of this method. Teagan and Sargent (1973) proposed a vapour compression system whereby R114 was used for the power cycle whilst R22 was used for the refrigeration cycle with a solar collector temperature of 120°C and an air-cooled condenser, they aspired to a COP as high as 0.4

Prigmore and Barber (6), reported a cooling system consisting of a Rankine Power cycle operating on R113 and a vapour compression refrigeration system operating on R12. Solar energy was used to generate R113 vapour in the boiler of the Rankine Power cycle and the vapour was expanded through a high speed

turbine that drove the R12 refrigeration compressor. Utilising a flat-plate collector, with a water temperature of 102°C, they obtained an overall COP of about 0.71. They concluded that a higher COP could be obtained if concentrating collectors were used.

1.1.2. The Vapour Jet System

Like the case of the vapour compression refrigeration system, concentrating solar energy collectors can be used to operate a steam jet refrigeration system of conventional design.

According to Yellott (5), W.P. Green, in his investigation in 1936, used a concentrating collector to produce steam of a high enough pressure to operate a steam jet ejector that caused evaporation and chilling of water in a tank connected to the ejector. The low COP of the system and the cost of energy collection in view of tracking the sun's path required by concentrating collectors, did not make the system viable.

Kakabaev et al (7) reported the behaviour of a Freon-ejector solar cooler designed for summer time cooling. R12 was used as the refrigerant. However, the system efficiency was found to be relatively low compared with conventional absorption coolers for evaporating temperatures below 18°C.

Champoussin et al (8) using R-11 in a vapour jet system, reported for an evaporating temperature of 13°C, a COP of 0.73. This was particularly suited for low regeneration temperatures of between 65°C and 85°C.

1.1.3 The Thermoelectric System

Thermoelectric refrigeration is based on the discovery of Peltier in 1834 that when a direct current passes through two conductors of dissimilar metals, one junction becomes cool and the other becomes warm. Refrigeration based on the Peltier effect may be considered as using an electron gas as the refrigerant instead of the conventional refrigerants. The two dissimilar thermoelectric materials are named according to whether the current is carried by electrons (n-type) or by holes (p-type). The current flowing to the cold junction requires heat to be supplied which is taken from the materials at this junction. Work is done in the circuit and this work plus the energy peaked up at the cold junction is given off as heat. Comparing this system, the cold junction may be considered as the evaporator and expansion valve whilst the hot junction as the compressor and condenser (9).

For solar energy application in a thermoelectric system, solar cells which are photovoltaic semiconductor devices that convert solar energy

directly into electrical energy are used to generate d.c. output which can be used to drive the thermoelectric refrigerator. In a photovoltaic system module, individual cells are assembled in series and/or parallel combinations. The number of cells in series determines the module voltage and the number in parallel determines the module current capability. Modules are assembled together in a frame or support to form an array. A typical photovoltaic conversion system consists of arrays of solar cells, power conditioning equipment and storage facilities. A battery is normally used to store energy for use whenever the sun is down. A calcium-lead alloy instead of antimony-lead alloy employed in lead-acid batteries has been found to be more suitable (10). The d.c. output from a solar cell array can be either transmitted directly to the load or used to charge the battery.

Vella et al (11), suggested using solar energy to heat the hot junction of a thermoelectric generator (TEG), then using the d.c. output thus generated to drive a thermoelectric (TE) refrigerator. Their system would not refrigerate more than 25°C below ambient with flat-plate solar collectors. Moreover, separate heat sinks was required for the TEG and the TE refrigerator.

Field (12), reported on the photovoltaic generator driven thermoelectric refrigerator that cooled medicines down to 40°C below ambient under high

ambient temperature conditions. Unlike in the case of the TEG/TE refrigerator unit, no heat sink was specifically required for the operation of the photovoltaic generator as the natural convection cooling for the outdoor installed cells was adequate.

More recently, Sofrata (13), also used a photovoltaic solar collector to power a thermoelectric refrigerator. A temperature of -3°C was obtained in the refrigerator when environmental temperature was about 25°C

1.1.4. The Vapour Absorption System

The vapour absorption system is the most viable of all the refrigeration systems for solar application. This system can make use of low temperature heat that can be supplied by the relatively cheap conventional flat-plate solar collectors. The absorption refrigeration system can generally be classified into intermittent and continuous "closed" cycle. However, a third classification that has received a lot of attention in the USSR is the continuous "open" cycle.

The intermittent refrigeration cycle has two major operations; regeneration or charging and refrigeration. Figure 1.1 shows the essential components of a solar powered intermittent refrigeration system. In the regeneration mode, warm water from a flat-plate solar collector is circulated

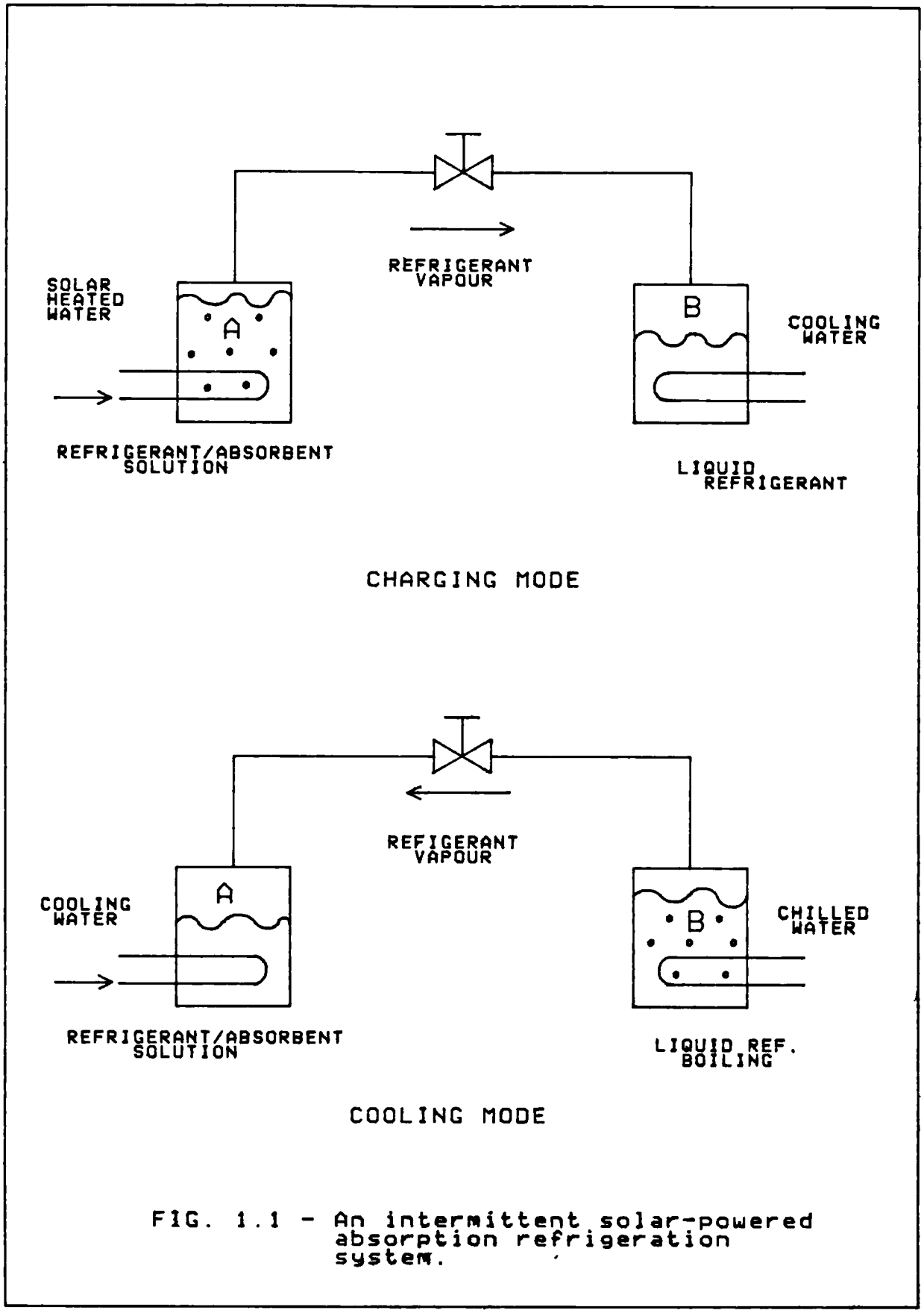

FIG. 1.1 - An intermittent solar-powered absorption refrigeration system.

through the heating coil in vessel A containing the refrigerant/absorbent solution. Refrigerant vapour is driven off the solution and is condensed in vessel B where cooling water is circulated through the coil. Vessel A in this case functions as a generator whilst vessel B functions as a condenser. Regeneration ends when the solution in vessel A ceases to vaporise, then the isolation valve in between the vessels is turned off. When heating stops, the vapour pressure in vessel A, which is now weak in the refrigerant, drops below the pressure in vessel B.

In the refrigeration mode, owing to the pressure difference between the two vessels the refrigerant in vessel B will vaporise when the valve is reopened. The vaporisation of the refrigerant absorbs heat from the surrounding of vessel B, thus producing some refrigerating effect. The vapour is then re-absorbed by the absorbent in vessel A after completing a full cycle. In this mode vessel B functions as an evaporator whilst vessel A functions as an absorber. The rate of evaporation, controlled by the valve, determines the refrigeration temperatures and the desired cooling rates.

In the continuous system, which can be further classified as closed or open, both regeneration and refrigeration are carried out simultaneously, resulting in a continuous cooling effect as long as the heat is supplied to the generator. The open cycle, however, differs from the closed cycle in that the

open cycle generates the weak absorbent solution by evaporating refrigerant to the atmosphere rather than to a condenser.

Figure 1.2 shows a diagram of a continuous close cycle absorption cooling system. This can be divided into three distinct sections:

i) the low temperature heat supply section,

ii) the absorbent solution section,

iii) the refrigerant or working section.

In the low temperature heat supply section, solar energy is collected and used to drive off the refrigerant from the absorbent solution in the generator. The hot fluid emerging from the collector at 3 enters the heating coil of the generator where it heats up the absorbent solution, thus vaporising some of the refrigerant. The heat supply fluid emerges at 1 and is returned to the solar collector to pick up more heat in the system.

In the absorbent solution section, dilute absorbent solution accumulating in the absorber is pumped by a solution pump (between 8 and 9) through a heat exchanger to the generator where the solution is regenerated. Part of the solution is recirculated into the absorber. The regenerated solution drops by gravity through the solution heat exchanger back to the absorber where it absorbs more vapour from the evaporator. The absorbent solution is the carrier of the refrigerant vapour, thus allowing a small pump to

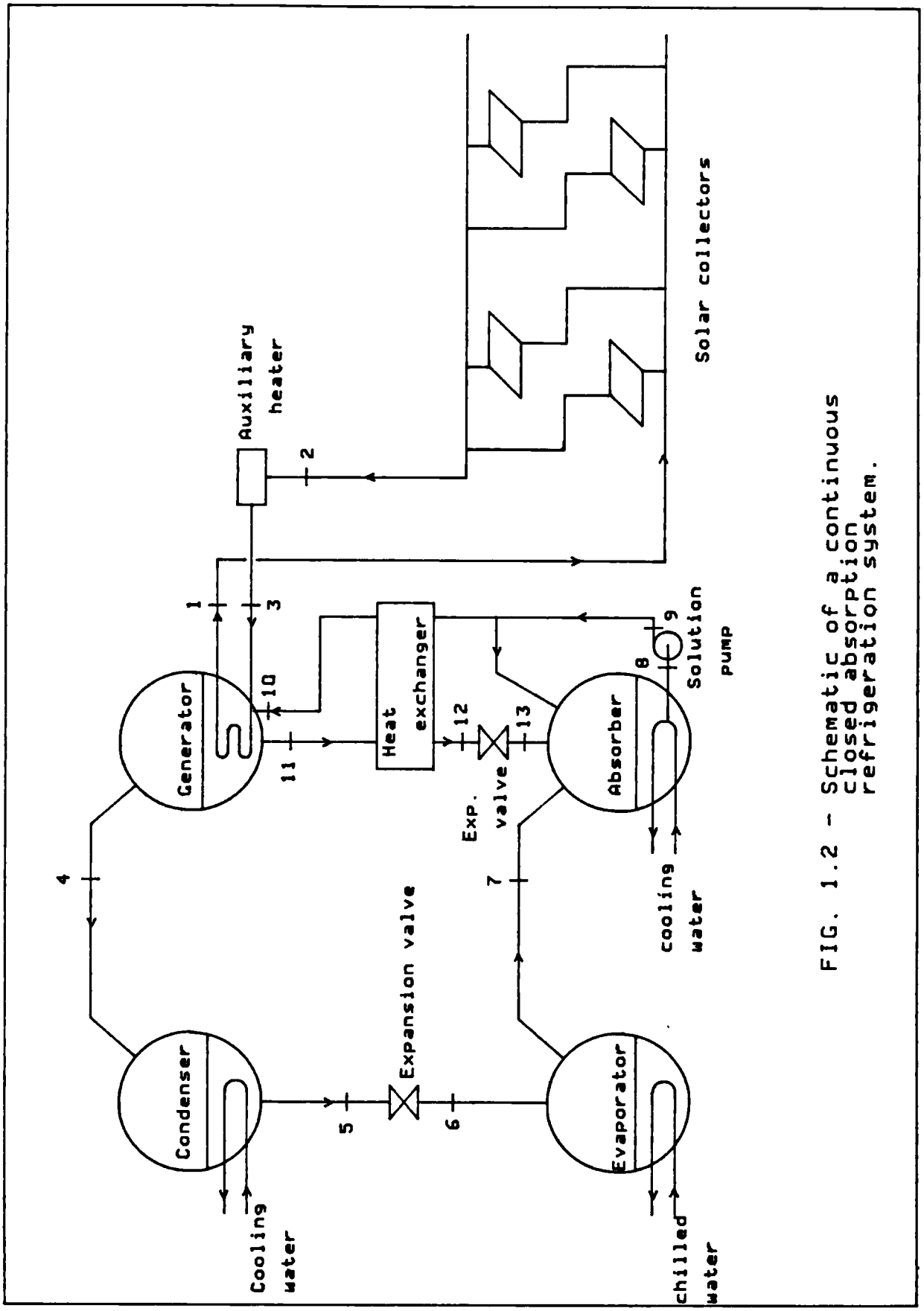

FIG. 1.2 - Schematic of a continuous closed absorption refrigeration system.

do what a large compressor could have been required to do.

The refrigerant section is the real working part of the system providing the cold. Refrigerant vapour from the generator goes into the condenser where heat is removed by cooling water or by air to condense the vapour. The condensate is throttled through an expansion device (between 5 and 6) into the evaporator. The expansion device lowers the temperature of the liquid-vapour mixture now at a lower pressure in the evaporator, the liquid refrigerant evaporates, absorbing heat from its surroundings. The vapour now enters the absorber at 7 where it is absorbed by the absorbent solution and carried to the generator to repeat the cycle.

The temperatures obtainable are a function of the solution concentrations, evaporation rates, pressures and supply water temperatures. These can be controlled to an extent by controlling the circulating rates in the various sections.

Figure 1.3 shows a diagram of an open cycle absorption cooling system. The weak solution from the absorber is pumped through a heat exchanger to the solar collector which is open to the atmosphere. Here the solution is heated and concentrated. The strong solution leaving the solar collector is sent into a liquid column which facilitates an efficient reduction in its pressure from atmospheric pressure. The

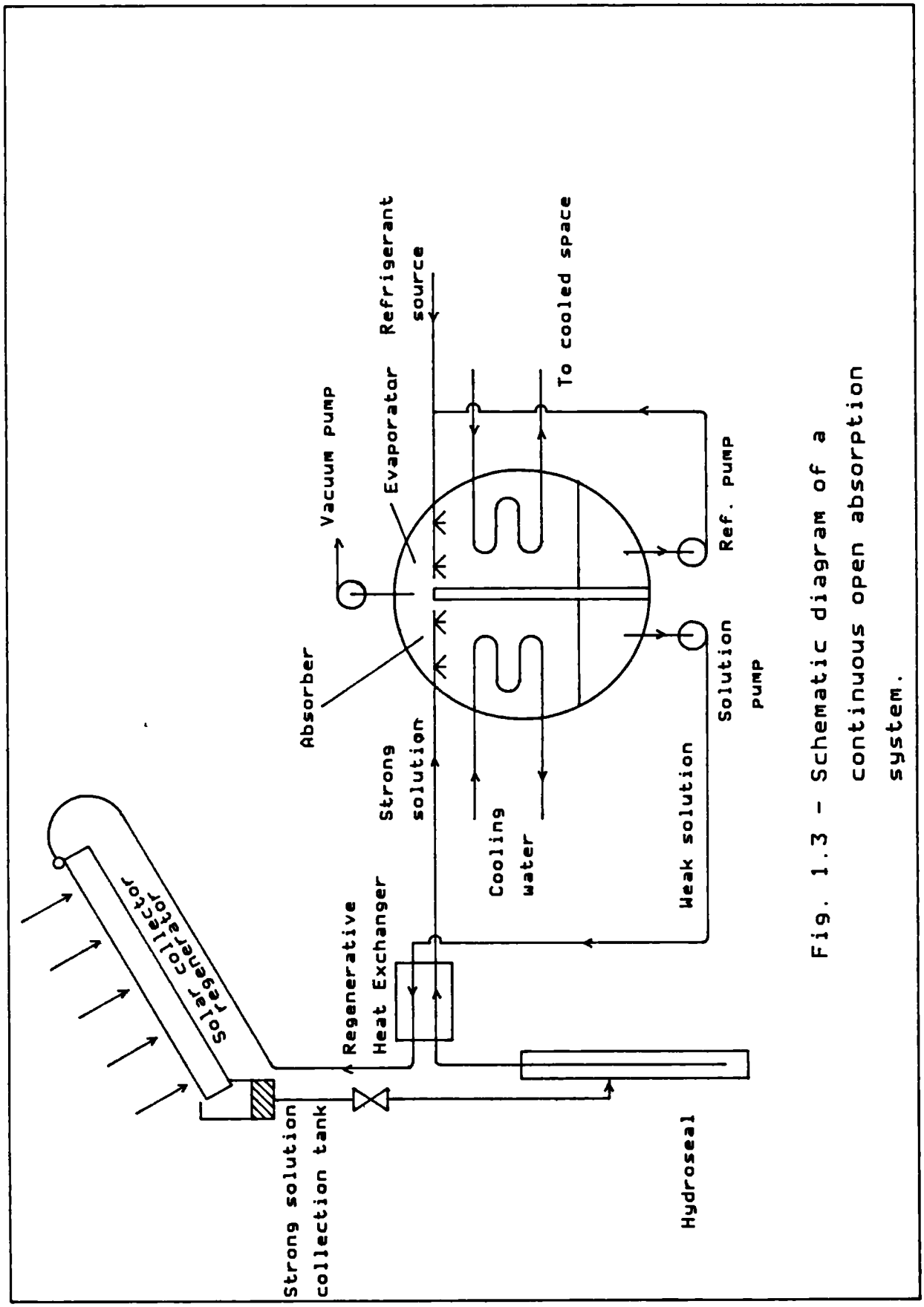

Fig. 1.3 - Schematic diagram of a continuous open absorption system.

solution then passes through the heat exchanger to the absorber where it absorbs the refrigerant vapour from the evaporator, the heat of absorption being removed by cooling water. In the evaporator, refrigerant from an external source is evaporated at reduced pressure, absorbing heat from the cooled space. The generated vapour is absorbed by the strong solution in the absorber and the resultant weak solution is pumped to the solar collector for regeneration thus repeating the cycle.

It should be noted that the condenser is eliminated in the open cycle system but an external source of refrigerant must be available. Hence, this cycle is at the present time feasible only when water is the refrigerant.

Many researchers have reported the use of solar energy for the absorption systems working in various refrigerant-absorbent combinations, namely ammonia-water (4, 14, 15), Lithium bromide-water (16-18), Lithium bromide-zinc bromide methanol (19), Lithium chloride-water (20-21). The cycles of operation were either intermittent or continuous - open or closed. Quite recently, Kumar et al (22) reported an analysis and comparison between closed and open cycle absorption cooling systems using water-Lithium bromide as working solution. They also compared an ammonia-water closed cycle with the water-lithium bromide closed cycle system. They confirmed that an open cycle system is better than a closed cycle system and that

systems using water-lithium bromide give higher COP values than systems using ammonia-water.

1.2 The Selection Of Refrigerant-Absorbent Combinations For Absorption Refrigeration Systems

A suitable refrigerant-absorbent fluid is probably the single most important item in an absorption refrigeration system. The selection of a suitable combination involves simultaneous consideration of various factors which include qualitative considerations of desirable properties as well as an analysis of its theoretical performance in a refrigeration system.

Hainsworth (23) reviewed various desirable properties of refrigerant-absorbent combinations and Buffington (24) studied these qualitative requirements. The desirable characteristics of refrigerant-absorbent combinations as listed by Buffington and other researchers (25-26), include:

- low vapour pressure of absorbent,
- low viscosity,
- high solubility of refrigerant in absorbent,
- good chemical stability,
- high thermal conductivity,
- high heat of vaporisation for the refrigerant,

- low heat capacity for the absorbent,
- non-corrosivity,
- non toxicity,
- large negative deviation from Raoult's law,
- low cost and availability,
- high thermal stability.

Macriss (27), who described the qualitative studies of Hainsworth, Buffington and others as neither systematic nor comprehensive, suggested that the selection of the fluid system be based on:

i) the chemical and physical properties of the fluids,
ii) acceptable ranges established for certain thermodynamic properties of the fluids,
iii) acceptable ranges for practical engineering quantities that affect the viability of a commercial unit, which in turn are affected by the fluid's properties.

The desirable properties he suggested for selecting refrigerants were:

- non toxicity
- good chemical stability
- non corrosivity
- ready availabity
- low cost

For absorbent the desirable properties were:

- good stability,
- non-toxicity,
- non corrosivity,
- mutual solubility with the refrigerant,
- normal boiling or melting point that satisfies the low volatility requirements.

The thermodynamic properties of a refrigerant-absorbent combination, different from the properties of the individual components is more critical in evaluating suitable solution for absorption refrigeration systems. Macriss further suggested that the criteria for the selection of suitable combinations should be based on the most important engineering parameters effecting performance in a practical system viz:

i) Coefficient of performance (COP).
ii) Pumping factor defined as the mass rate of generator solution circulated per unit mass of refrigerant produced in the generator.
iii) Pump work defined as the work to pump the absorber solution to generator pressure.
iv) Heat Transfer Rate - the rate of heat transfer in the solution heat exchanger between the absorber and the generator.
v) Gross Cooling Load - the sum of the useful cooling produced and the energy needed to provide for cooling the refrigerant liquid

between the temperature of the condenser and that of the evaporator.

Considering these points, the thermodynamic criteria for the selection and pairing of absorbents and refrigerants are:

i) Negative deviation from Raoult's law. The ability for a solution to exhibit negative deviation from Raoult's law is the result of strong intermoleculer attractions between the constituents of the solution. This could be either hydrogen bonding between the two dissimilar molecules of solution constituents or the ion-dipole bonding in case the absorbent is a metal salt such as lithium bromide.

ii) High solubility of refrigerant in the absorbent.

iii) Low solution viscosity.

iv) Low heat capacities.

No refrigerant-absorbent combination satisfies all these desirable conditions, so a careful choice should be made for a specific purpose and certain disadvantages must be accepted. It is even more difficult to select suitable combinations for solar refrigeration utilising a conventional flat-plate collector with its attendant low grade heat.

Even though the requirement for negative deviation

from Raoult's law is the single most important criterion in a successful combination, Gosney (1) suggested that a solution exhibiting a large negative deviation from Raoult's law in the absorber and the ideal solution behaviour or even a positive deviation in the generator would be more acceptable but unfortunately, no known solution exhibits this behaviour.

1.3 Outline Of Present Work

The main objective of this investigation is the utilisation of solar energy for an absorption refrigeration system. An absorption cycle requiring no electrical power and utilising solar energy as a source of heat supply for regeneration, could offer the possibility of providing refrigeration for an air conditioning system or the preservation of food at temperatures above 0°C if water is used as the refrigerant, in tropical developing countries where there is no regular supply of electricity.

Of all the refrigerant-absorbent combinations proposed for absorption refrigeration systems, the NH_3-H_2O and the H_2O-LiBr are most popular. For solar applications, especially for air conditioning purposes, the H_2O-LiBr system is more favoured for the following reasons:

i) It is simpler to operate as there is no need for a rectifying column, the absorbent salt being non volatile.

ii) It operates with higher COP and lower pump work.

iii) It is adaptable for using the low temperature heat that can be supplied by flat-plate solar collectors. Regeneration temperatures of about 93°C will operate a H_2O-LiBr whilst for NH_3-H_2O systems, regeneration temperatures of at least 120°C will be required.

iv) Water, the refrigerant is cheap, non toxic and safe.

The H_2O-LiBr system, however, have some limitations which include:

i) Low absorber temperature that cannot be maintained practically by air cooling.

ii) Lithium bromide salt is corrosive to metals.

iii) The lithium bromide salt is high in cost.

iv) The salt solubility is limited by temperature.

v) It can not be used to produce sub-zero temperatures.

However, the single most important limitation is that of salt solubility. If the solubility of lithium bromide in water can be improved, a stronger solution will result which can minimise the solution circulation ratio (between the absorber and the generator), and increase the temperature lift to

reduce the heat load in the generator. Thus at relatively lower operating temperature levels in the generator, refrigeration can be obtained. Vamvakidis (28), reported that even though lithium bromide is more soluble in water than in methanol, the addition of zinc bromide improved the solubility of lithium bromide in methanol.

A solubility apparatus was built and zinc bromide was tested with acqueous solutions of lithium bromide within 25°-80°C temperature range. A mixture of lithium bromide and zinc bromide was found to exhibit higher solubility in water than in methanol. These results necessitated the measurement of some of the properties of the derived solution to be able to establish it as a working fluid for absorption refrigeration systems.

A boiling point apparatus was built and used to measure the boiling points of:

i) LiBr - H_2O solution

ii) 2LiBr - $ZnBr_2$ - H_2O solution

iii) LiBr - Licl - H_2O solution

The LiBr - H_2O data was compared with those of Pennington (29). The solubility of LiBr - Licl in water was found to be relatively poor.

A vapour pressure apparatus was designed and built to measure the vapour pressure of the 2LiBr-$ZnBr_2$-H_2O

solution. The result was presented in chart form to make design calculations easier. Since the enthalpy for a solution with a nonvolatile absorbent can be calculated from vapour pressure data, knowing the heat capacity for only one concentration, the National Physical Laboratory measured the heat capacity of the solution for one concentration.

An experimental absorption refrigerator was then designed, built and tested using the solution 2LiBr-$ZnBr_2$-H_2O as the working fluid. Much emphasis was laid on obtaining some refrigerating effect at low regeneration temperatures.

Chapter Two

SOLAR ENERGY COLLECTION AND UTILISATION

The utilisation of renewable energy sources such as wind power, wave power, ocean thermal gradient, geothermal and solar energy are receiving attention in recent years but for refrigeration and air conditioning purposes, solar energy is most suitable. The potential for solar refrigeration will be more appreciated when it is noted that most countries that are poor in fossil fuels have abundant supply of solar energy and the need for refrigeration and air conditioning is greatest when the sunshine is highest.

The sun is a body with a surface temperature of about 6,000 K radiating mainly within the 0.3 μm to 3 μm spectrum, with maximum energy occurring at a wavelength corresponding to green light. The total energy radiated per second per unit area is proportional to the fourth power of the temperature, i.e.,

$$E = \sigma T^4 \qquad (2.1)$$

where E = Total irradiation
σ = Stefan Boltzman Constant
= 5.7×10^{-8} J/m^2. sK^4.

The radiation from the sun at a temperature of

6,000 K is given by:

$$E = 7.38 \times 10^{7} \ J/m^2 \ s$$

The total energy emitted by the sun assuming a hemispherical surface of diameter 1.39×10^{9}m is given as:

$$E_{TOT} = 2.24 \times 10^{26} \ J/S$$

The maximum possible energy reaching a unit area of the earth's surface, normal to the sun's rays and neglecting the losses in the passage of the rays can be estimated from the equation:

$$E_{max} = E_{TOT}/2\pi L^2 \qquad (2.2)$$

$$= 1.6 \ KW/m^2$$

with the distance from the earth to the sun, L, taken as 149×10^{9}m.

However, considering losses by absorption and reradiation in the atmosphere, the maximum solar energy reaching the earth's surface at the equator varies between 0.85 KW/m^2 and 1.135KW/m^2 with the maximum value in the United Kingdom nearer 0.75 KW/m^2 (30).

With the intermittent nature and the relatively low density at which solar energy is available on the earth's surface therefore, it is necessary to maximise its collection and storage for effective utilisation. The collection methods, storage and utilisation of solar energy for heating and cooling are discussed in

the following sections.

2.1 Solar Energy Collection Methods

The variability of supply and the diffuse nature of sunlight constitute major technical difficulties in harnessing solar energy. It does not come in concentrated easily stored forms as do the fossil fuels. Solar radiation data may be used to estimate the energy likely to be available for collection using either non-concentrating devices of the flat-plate or evacuated-tube types or the concentrating type which collects only direct radiation.

2.1.1. The Flat-Plate Solar Collectors

Cheremisinoff et al (31), made a comprehensive survey of solar energy collection and utilisation methods. According to them,the first experiment with flat-plate solar collectors was by H.E. Willsie and John Boyle, Jr. in 1902. This type of collectors collect both diffuse as well as direct solar radiation and thus is able to operate during more widely varying weather conditions. The heated water obtained by Willsie and Boyle's collector was used to vaporise some volatile liquids such as ammonia, sulphur dioxide, ether etc. The collector performance was such that in cold October weather, temperatures were high enough to vaporise sulphur dioxide to operate a solar engine.

Flat-plate collectors use either air or liquid to

transfer the collected heat to wherever it is needed but whatever heat transfer medium is used, the principle of operation involved is the same. The vast majority of the flat-plate collectors therefore, have the following basic components in common:

i) the absorber surface,
ii) the heat transfer interface / fluid passage,
iii) the glazing,
iv) the insulation,
v) the casing.

Figure 2.1 shows an exploded cross-section of a typical flat-plate solar collector. The absorber surface is the part that actually absorbs solar radiation and converts it to heat. It should lose as little heat as possible upward through the glazing and downward through the casing. Most collectors use plates made of copper, aluminium or galvanised steel but some are prefabricated of plastic for lower temperature applications. The top surface of the absorber will have either a black coating or a thin layer of a selective surface that will exhibit higher absorptivity of the short wave solar rays transmitted through the glazing and lower emissivity of the long wave radiation from the surface.

Hollands (32) reported on the improvement of the selectivity of an air heater collector plate by corrugating it to give a series of parallel vee-shaped

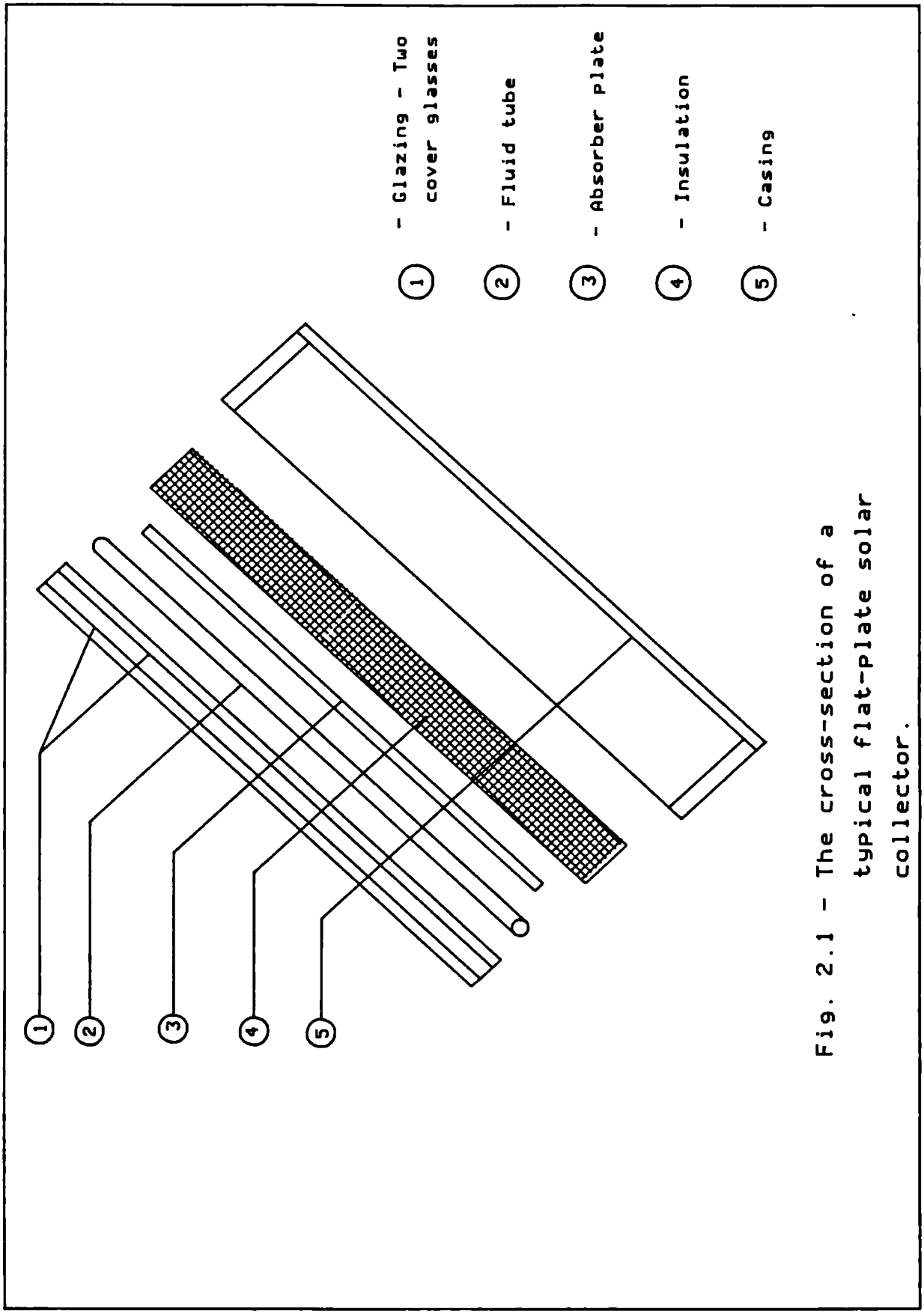

Fig. 2.1 - The cross-section of a typical flat-plate solar collector.

grooves. Solar radiation incident on the sheet undergoes multiple reflections in the vee-grooves, each surface absorbing some radiant energy. The vee-shaped corrugated sheets provide additional heat transfer surface and improved absorptance even though the increase in emittance is relatively small when compared with that of flat sheets.

In flat-plate solar collectors, the efficiency of energy collection drops drastically at high absorber temperatures. Furthermore, the energy collected is normally needed at a point away from the collector itself. Hence the need for a heat transfer fluid (which can be air or liquid) to perform the dual function of cooling the absorber to improve the collection efficiency and to transport the collected energy to wherever it is needed. In liquid cooled collectors, water or water/anti-freeze solution is commonly used as heat transfer fluids. It should be noted that for the same temperature rise, a unit mass of water absorbs over four times as much heat than air can. Hence air cooled flat-plate solar collectors have much larger fluid passages than water cooled ones thus increasing system cost. For space heating applications, however, this relatively high system cost of air cooled systems may be nearly offset by the fact that the heated air can be blown directly into the heated space without the need to circulate it through heat exchangers and tubes along walls as in hydronic systems.

Recently some researchers (33-36) have reported on flat-plate solar collectors with fluids undergoing phase change as working fluids rather than water or air. The phase change fluids used are R-11, acetone and petroleum ether. The relative advantages of these fluids over water or air include: Elimination of corrosion, fouling and freezing in cold climates. These systems find application in the field of Solar water heating,comfort conditioning, refrigeration and water pumps.

The glazing, whilst protecting the absorber surface against environmental weather conditions is also required to transmit solar energy to it. Glazing materials must therefore be capable of transmitting within the solar spectrum (0.3 - 3.0μm) the incoming short wave solar radiation, whilst only a negligible portion of the long wave radiation emitted by the absorber surface should be transmitted outward through it. Glass is known to possess the above qualities. Perspex even transmits more solar radiation within the solar spectrum than glass whilst being opaque to infra-red radiation (37). However, most usable plastics possess transmission bands in the middle of the thermal radiation spectrum and may have long wavelength transmittance as high as 0.40. Furthermore, plastics are generally limited in the temperatures which they can sustain without undergoing dimensional changes and even though they withstand hail and other stones, they are affected by the sun's ultra violet radiation when exposed for a long period of time.

When adequate glazing material has been selected, the optimum number of cover sheets to use must also be determined. It is generally believed that two or three collector covers are needed to provide insulating dead air spaces to minimise heat losses from a flat-plate solar collector. Thomanson (38), found that a single layer of ordinary window glass gives very good results and has many advantages for solar house heating. He found that whereas condensation formed in both transparencies when plastics plus glass are used as covers, there is less condensation and even the little that appear is clear and non-milky in appearance when glass only is used. During the summertime when the collector temperature can approach about 149°C, the use of only one transparency permits more of the excess heat to be reradiated outward to avoid collector damage. Also rain automatically washes clean a single transparency.

The insulation component of a flat-plate solar collector is installed at the base (behind the absorber surface) and sides of the protective casing to contain the heat within the solar collector unit. The protective casing serves to hold the entire unit together. It may be made with a wooden frame and a moisture-resistant hardboard backing or it may be constructed from sheet metal, painted for weather protection.

2.1.2 The Evacuated-tube Type Solar Collector

Another type of non-concentrating collector is the evacuated-tube type collector. Like the flat-plate collector, it collects both diffuse as well as direct solar radiation and it can use either air or liquid as the heat transfer fluid. It is, however, cylindrical in shape rather than being rectangular.

Figure 2.2 shows a sketch of a typical concentric evacuated-tube-type collector. They incorporate two concentric metal tubes situated within a glass tube. The inner metal tube provides the heat transfer fluid passage whilst the other one is the absorber surface. The heat transfer fluid flows through the inner tube to the opposite side undergoing some preheat as it does so. At the other end of the tube the fluid is directed to the annulus between the two metal tubes. It is along this pass that the major heat transfer takes place. The fluid is then discharged into a manifold which routes the flow to the next tube where the same process is repeated. The tubes are therefore connected in series, each one increasing incrementally the temperature of the fluid. A typical collector module may consist of up to 24 tubes.

The outer glass casing acts as the glazing and casing for the collector. The annular space between the absorber surface and the glass casing is evacuated to a very low vacuum (of the order of 10^{-4} torr) thus providing the insulation capability for the collector.

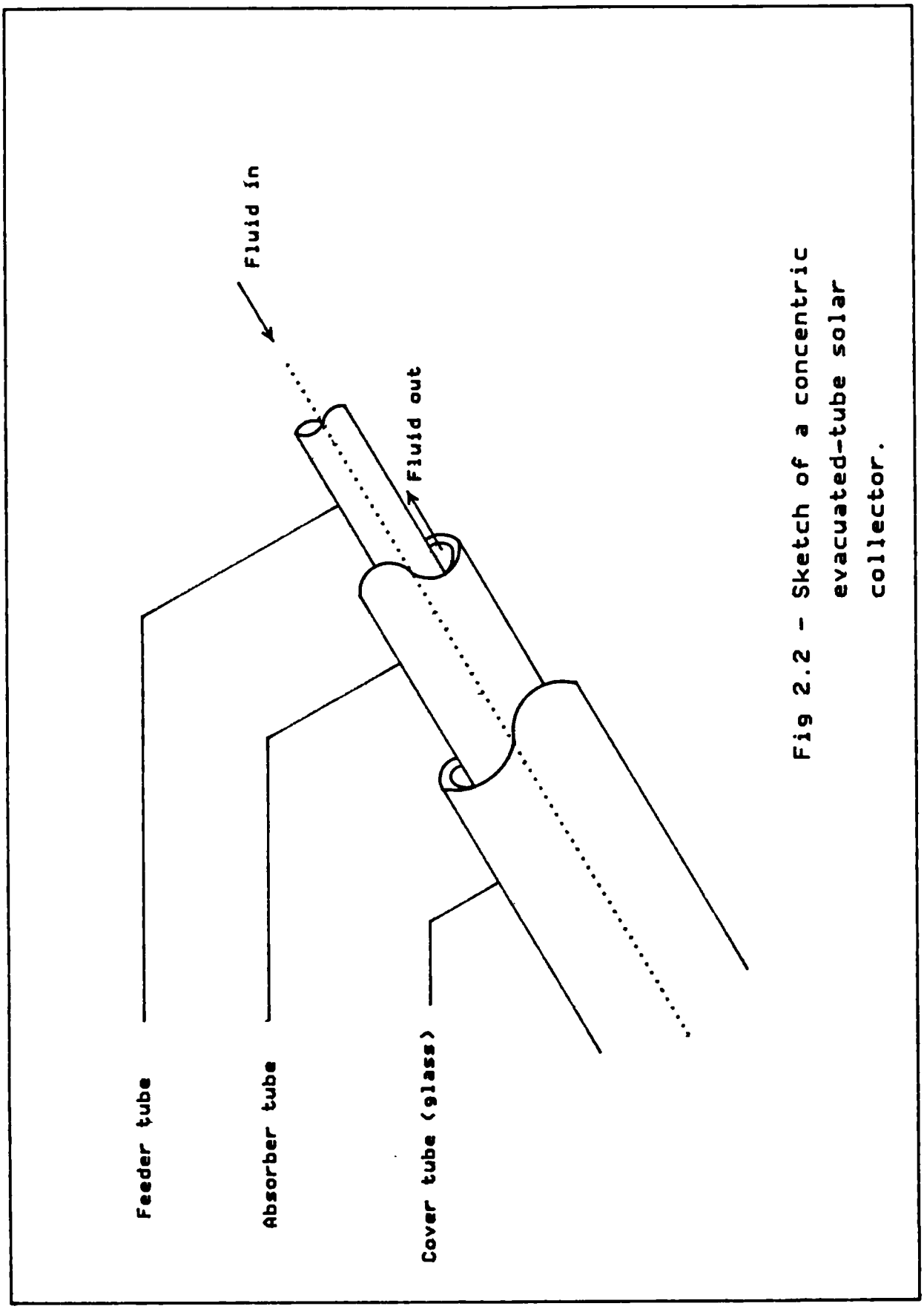

Fig 2.2 - Sketch of a concentric evacuated-tube solar collector.

With a selective absorbing surface temperatures of between 87° and 115.5°C can be obtained with this type of solar collector under high vacuum.

2.1.3 The Concentrating Solar Collectors

This type of solar energy collectors make use of paraboloidal concentrators to channel natural concentrations of energy falling on an area into significantly smaller area, that is, the focus of the system. Temperatures around 3871°C can be obtained by good concentrating devises (4). However, this type of collector can collect only direct radiation, hence the need for a tracking device for the sun's rays which makes them quite expensive. Furthermore, they can not function at all on cloudy or overcast days.

Two methods normally used for tracking the sun are altazimuth and equatorial mounting. The altazimuth method requires that the tracking surface change both its altitude and its azimuth to follow the movement of the sun across the sky. The equatorial mounting requires that the axis of the concentrator is pointed to the North and arranged to change its tilt angle to compensate for the varying declination of the sun.

A typical trough-like collector developed by Northrup Plants, Hutchins, Texas in the USA is shown in Figure 2.3. This makes use of a fresnel lens which directs the sun's rays onto a blackened metal tube located on the focus of the lens at the bottom of the

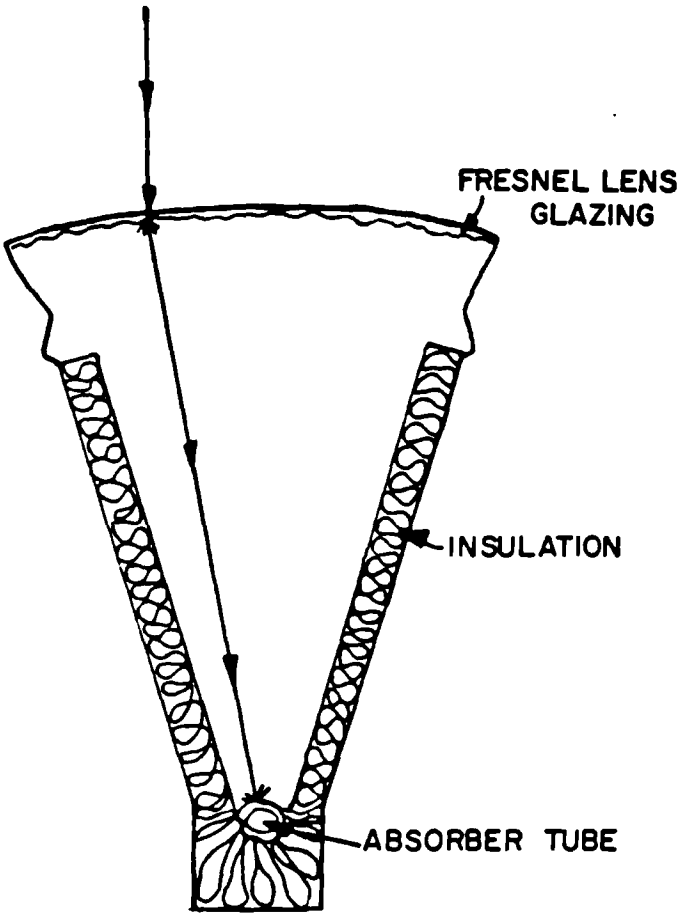

Fig. 2.3 The Northrup Concentrator

trough. Heat is transferred to the heat transfer fluid flowing into the tube. The casing of the collector is insulated to minimise thermal losses and the whole unit employs a tracking device which permits its movement from east to west.

A stationary type concentrator known as the Hot-Line Collector has been developed by Dan Lightfoot of the Alternate Energy Resources Company (AERCO) of Ottumwa, Iowa. This, as shown in Figure 2.4 employs a reflective sheet curved in two dimensions and focuses solar radiation into a line-shaped hot spot. The heat transfer fluid, usually air, is forced through the wedge shaped absorber channel coated with black paint. Although stationary, the reflective surface compensates for solar movements and can continuously focus both direct and diffuse radiation onto the absorber surface. The glazing, insulation and casing configuration are similar to flat-plate collectors.

2.2 Solar Energy Storage

The intermittent nature of the availability of solar energy on the earth's surface dictates the necessity for a means of thermal energy storage for continuous operation of solar operated systems. When applied to buildings with significant interior heat gains, some of which may be solar originated, thermal storage can serve to:

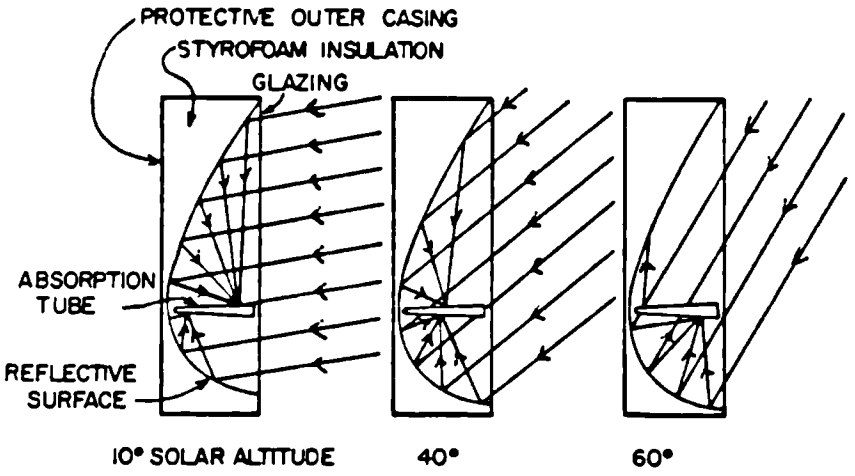

Fig. 2.4 Schematic of the Hot-Line Concentrator

i) save fuel,

ii) reduce electric cooling demand,

iii) reduce electric utility investment.

For some areas, energy storage may be on short term basis, i.e., storage during daytime for use during the night. However, long-term storage may be required in certain areas, i.e., storing the long hour summer sunshine for use during the following winter months.

The material in which the heat energy is to be stored can be divided into two broad types:

i) Those that store energy in the form of sensible heat.

ii) Those that undergo a change of state or physico-chemical change at some temperature within the practical range of temperatures obtainable by the solar heat collectors.

Water and rock pebbles have been found to be the most practical storage materials in the first category, heat being absorbed as their specific heat. Water, with its low molecular weight, has a very high specific heat per unit weight having at least 25% higher thermal capacity per unit volume than rocks. Water is therefore the best specific heat type heat-storage material for application below its boiling point. It is however, surpassed only by materials with phase change. The most economical way of storing hot

water (at 60°-120°C) if the volume is 100,000 m^3 or more is in unlined rock caverns (39). This is because for a rock cavern, the relative heat losses and construction costs decrease as the volume increases.

Choda and Read (40) have reported on the performance of a solar air heater with a collector area of 27.87m^2 and 9.62m^3 of rock storage system. The rocks, consisting of 1.9cm clean basalt rock screenings are contained in a 2.94m internal diameter, 1.83m high corrugated galvanised iron tank lined internally on the sides and top with 25.4mm polystyrene foam insulation. The rocks are supported by 9.5mm x 14 gauge galvanised wire mesh and located on a number of bricks which form a plenum chamber beneath the wire mesh. With a temperature rise above ambient of 26.7°C the storage capacity was estimated at 525.4 MJ. Taking the rock density and specific heat as 1377.7 Kg/m^3 and 878.6 J/Kg K respectively.

One major disadvantage associated with water and rock pebbles as heat storage materials is that their large bulk limits the period of storage to only a few days. A large space is therefore required for storing the heat requirement of an average home for only a day or two.

The second category of heat storage materials - that is the phase change materials - offer a considerable reduction in storage space. They also offer the possibility of storage of heat at higher

temperatures. However, a major problem with them is that considerable supercooling can take place during which period the materials do not part with their stored latent heat until either some crystal nuclei are introduced or some stirring is done.

Goldstein (41), undertook a survey of materials that could be used for phase-change heat storage. He surveyed many groups of substances selected from standard references such as Perry's Chemical Engineer's Handbook and the International Critical Tables. He classified his findings based on thermodynamic equilibrium grounds as follows:

i) Inorganic or organic substances having large heat of fusion and their melting point within the temperature range -1° to 93°C.

ii) Entectic mixtures of inorganic salts.

iii) Change-of-phase materials.

iv) Storage by chemical reaction in solution.

Goldstein concluded that aside from further thermodynamic data required to evaluate more precisely the storage capacities, data on the kinetics of the chemical or physical processes occurring are also required to ascertain if the rate at which they will store or deliver their energy is comparable to the rate required by the practical considerations.

Speyer (42) suggested that solar energy storage must be designed as a part of a solar energy system bearing in mind the six important parameters: cost, space, requirements, capacity, efficiency level and rate. The first two parameters having received much attention, Speyer defined the last four as follows:

i) Storage Capacity - the amount of energy that the storage system can furnish.

ii) Storage efficiency - the fraction of energy put into storage which is still available at some later date.

iii) Storage level - ordinarily the storage temperature.

iv) Storage rate - the power (e.g. in Watts) put in or withdrawn from storage.

The storage capacity is inversely related to collector capacity as a reduced collector area will be required for energy collection to supplement the stored energy if storage capacity is high. Furthermore, a high storage efficiency can usually result in reduced collector capacity even though storage efficiency by itself has a very slight effect on required collector area. The efficiency of storage required for a solar house is based on two superimposed duty cycles, i.e., daily variation in temperature and seasonal variations. For long term energy storage, at least 50% of the energy put into storage must be recoverable after three months.

The storage level depends on the use the solar energy system is designed for. Even for air conditioning systems, it depends on whether a solar-powered compressor in a mechanical system or an absorption cycle system is in use. However, in proven absorption cycles such as used in the Servel system, collection temperatures of at least 85°C are required. The rate of storage or withdrawal is not, usually, a problem in space heating or cooling unless heat-of-fusion is stored in which case supercooling may require the introduction of some crystal nuclei or stirring the solution.

To reduce supercooling of heat-of-fusion materials which normally occur when they are heated and cooled repeatedly in sealed containers, nucleating agents should be present in the sealed containers. Nucleation can be produced by using solid crystals which are isomorphous or partly isomorphous with the salt hydrate crystal and are sparely soluble or practically insoluble in the melt. Maria Telkes (43) reported that Glauber salt which melts at 32.2°C with a heat of fusion of 251.64 KJ/Kg, when mixed with 3 to 4% borax to serve as a nucleating agent, forms a mixture with a melting-freezing temperature of 29.4°C. When mixed with thickening or suspending additives, this heat storage material can be repeatedly heated and cooled in sealed containers without any supercooling or segregation.

Other problems associated with the heat-of-fusion materials are: the lack of demonstrated reliability in the recycling process (44); the need for the salts to be encapsulated within the water circuits because of their corrosivity; and if used for heating and cooling storage, their volume must be duplicated since a different material is required for each temperature range.

Jaffrin et al (45) employed the heat-of-fusion storage method to horticulture in heating up a professional greenhouse devoted to rose production in La Baronne, France. Heat storage was achieved partly through phase-change processes taking place in 13.5 tons of calcium chloride hydrate and partly though the heat capacity of the soil. To maintain acceptable temperatures in the closed greenhouse during the sunny days, the original calcium chloride hexahydrate, chliarolithe, melting at 28°C was modified by excess water so that phase-change takes place between 25°C and 15°C. The latent and sensible heat of the material add to a total of 154.91 MJ/m^3. 9,000 flat bags made of a polyester-aluminium-polyester complex, sealed air tight, each with a capacity of 1 dm^3 are used for latent heat storage. They are distributed on 500 m^2 of horizontal asbestos-cement shelves, piled up on five levels in semi-cylindrical concrete tunnels buried in the ground. Reinforced concrete slabs which provide convenient parallel paths between the rose lines are used to cover the tunnels. Sixty tons of concrete, and about seventy-five tons of surrounding soil

contributed to the latent heat material to take care of the daily incident solar radiation in winter. With 100% solar overcast, however, the economical aspect of this prototype solar greenhouse is not very attractive. Furthermore, the phase-change material bags developed do not represent the optimum combination of latent heat content and fusion temperatures.

In recent time, there has been an interest in the chemical storage of solar energy involving the utilisation of sunlight to induce endoergic covalent structural changes in organic molecules. A portion of the incident photon energy is converted to and stored as increased chemical potential energy of the photo products. Talbert et al (46) have made an analysis and economic study of a photochemical solar energy system compared with a conventional hot water system. Based on clear day operation, they recorded the following advantages in favour of the photochemical system:

i) Lower cost of collector

ii) Smaller storage tank.

iii) Room temperature storage capability.

iv) Cloudy day effectiveness (i.e., operates every day, all day, with constant conversion efficiency.

v) Stored energy available at constant energy level both winter and summer.

The following disadvantages are, however, worthy of

note:

i) Higher cost of fluid.

ii) Time decay in degradation of the chemical properties.

iii) Constraints related to fire and health hazards.

Many more technical problems are still to be overcome but little work has been done so far.

There is another solar energy collection device generally known as 'Solar Ponds', which, combines collection with storage. Solar Pond can be classified as: (1) shallow or convective type;2)the saturated salt type; and (3) the salt gradient, non-convective type.

The theory and technology of shallow solar pond is predominantly that of conventional flat-plate collectors. They are used mainly for producing hot water for domestic and industrial applications and they can be of large scale installations or of portable compact sizes. Figures 2.5(a) and 2.5(b) show sketches of a built in storage solar water heater and a shallow solar pond water heater. Kudish et al, (47), constructed and tested a prototype unit of a portable, shallow solar pond which they then proposed for supplying hot water for recreation and military use. Their compact shallow pond consists of a clear PVC bag placed within an insulated wooden box equipped with a hinged cover and a 0.1mm thick Tedlar film upper glazing. The inner side of the insulated hinged cover

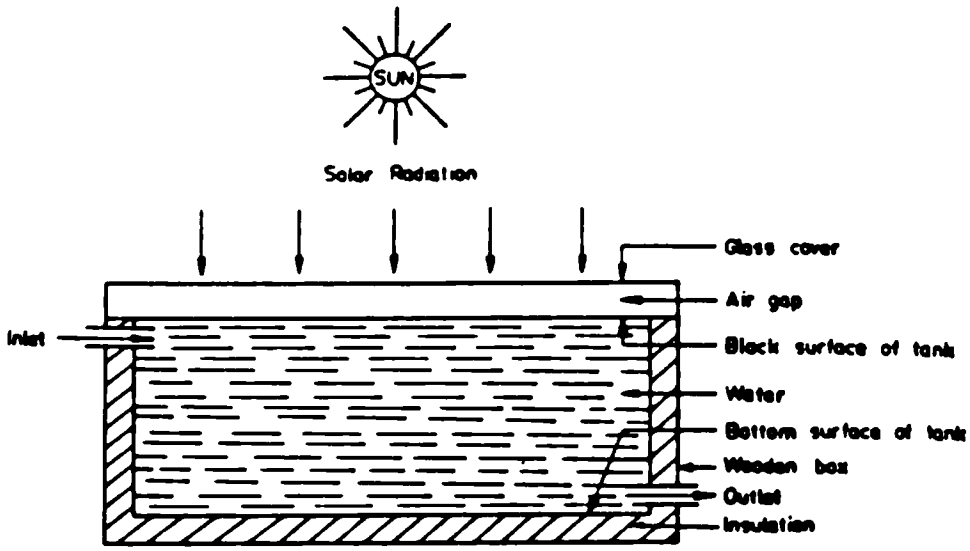

2.5 (a)

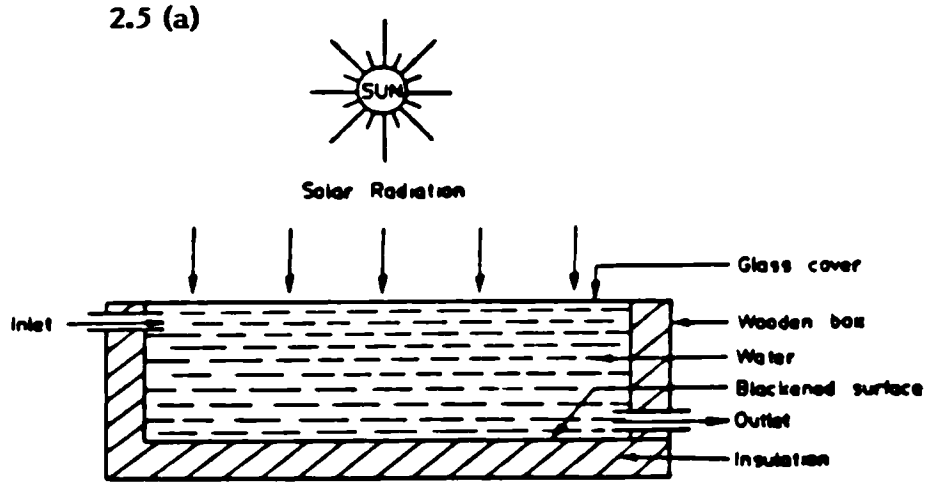

2.5 (b)

Fig. 2.5 (a) Sketch of a built-in storage solar water heater

Fig. 2.5 (b) Sketch of a shallow solar pond water heater

has an aluminised mylar film which serves to reflect solar radiation to the pond during the day. When covered after sunset, the box serves as an overnight storage of the heated water.

In the saturated salt solar pond, the pond is filled with saturated solution of a salt which exhibits a high increase in solubility with increase in temperature. Borax and Potassium nitrate are typical salts that can be used for this purpose. Convection and expansion due to heating are prevented by placing additional solid salt at the bottom of the pond so that if the pond heats up at the bottom, more salt will dissolve thereby increasing the density there. Even though this type of solar pond has been demonstrated on a small scale, it has not developed to the stage of the salt gradient ponds.

The salt gradient pond is a body of saline salts housing a higher salinity at the bottom than at the surface. As shown in Figure 2.6, it consists of three zones. The surface layer is a convective layer, the thickness of which is affected by wind mixing, penetrative convection, evaporation and diffusive action. This layer should be kept as thin as possible. The bottom layer, also a convective zone acts as a store for the absorbed solar radiation. A non-convecting gradient zone is formed in the middle which separates these zones and serves as an insulating layer.

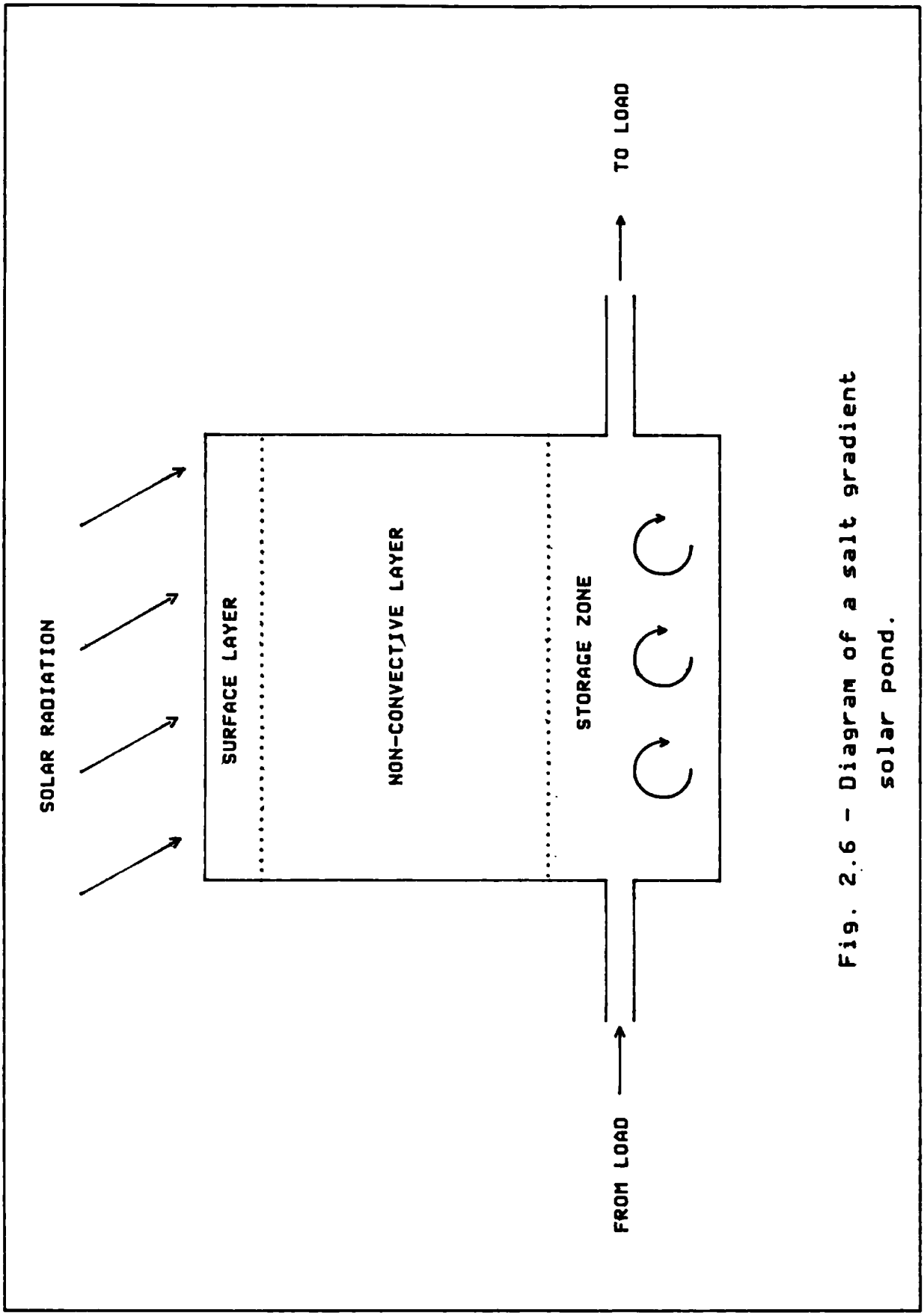

Fig. 2.6 - Diagram of a salt gradient solar pond.

Magnesium chloride, or sodium chloride is normally employed in a salinity-gradient solar pond. The maintenance of the salt gradient requires brine injection to the bottom and replacement of saline water at the surface with fresh water at regular intervals (48, 49). Neilson et al (50) described a flow system for maintaining the salt gradient in solar ponds.

The energy reaching the bottom of the pond decreases as the depth increases. The absorption of solar radiation at the bottom can therefore be increased by making the bottom black and by limiting the depth of the pond. Tabor (48), reported that temperatures in excess of 100°C could be obtained at the bottom of an artificial pond, 1-2m deep, with 85-90°C as practical working temperatures.

Upward heat conduction in the ponds can be reduced by increasing the thickness of the non-convective zone whilst side and bottom heat losses can be reduced by insulating the pond. Beniwal et al (51) made theoretical estimation of the steady state heat losses from the sides and bottom of a salt gradient solar pond. They considered as insulating materials: dry sand, mud powder, dry cement, marble dust and mica powder and found mud dust with an insulation thickness of 0.20m to be the best choice.

2.3 Solar Energy Collector Performance And Utilisation

Before discussing the solar energy collector performance and utilisation, it is pertinent to mention some problems associated with solar collectors. "Freeze-up" and "Stagnation" are common to both concentrating and flat-plate collectors. Freeze-up is caused by the outdoor air temperatures being below freezing when collectors are idle. The stagnation temperature is the collector absorber temperature which will be reached if no heat is being removed from the collector by the fluid passing through it. At stagnation temperature, no heat is transferred to the fluid which is either not circulating or has been drained from the collector hence the efficiency is zero. Furthermore, an appreciably high temperature can be reached within the collector which can affect the material used for the construction and hence the reliability and life of the collector.

Padillo (52) has suggested some solutions to the freeze-up and stagnation problems. For freeze-ups, he suggested the addition of anti-freeze mixtures to the system's liquid medium. In this case a heat exchanger will be needed between the collector and the storage tank for economy of the system first cost or else the entire storage system will have to be treated against freezing. Padillo also suggested some designs

incorporating drain-down systems to combat freeze-ups. However, the drain-down systems have certain disadvantages. These include:

i) Increased control complexity.

ii) Increased rate of corrosion in the collector as a result of alternate exposure to air and water.

iii) There is the risk of failure of drain-down controls which will eventually result in freeze-up.

For stagnation temperature protection the simplest method is to cover the collectors. Stagnation is, however, easier to control in concentrating collectors in that whenever power fails, the system will automatically defocus itself thereby eliminating any stagnation possibilities. If, power is available but water flow stops, the control system will defocus the collector.

2.3.1 The Performance Of Solar Energy Collectors

The thermal performance of a solar collector array depends upon a number of factors which include: collector area, type, tilt angle, the temperature of the heat transfer fluid entering the collector and shading. The thermal performance of a collector can be calculated from a first law energy balance which for a

flat-plate collector can be represented by the equation:

$$Q_u = I_c A_c \tau_s \alpha_s - U_c A_c (t_c - t_a) \qquad (2.3)$$

where Q_u = rate of useful energy gain, W

I_c = global insolation on plane of collector, W/m^2

A_c = Area of collector that absorbs radiation, m^2

τ_s = net solar transmittance of glazing

α_s = solar aborptance of collector plate

U_c = Overall heat loss coefficient, W/m^2K

t_c = average collector plate surface temperature, °C.

t_a = ambient air temperature, °C.

To improve the thermal performance of a solar collector therefore, it is necessary to reduce either the overall heat loss coefficient or the area from which energy is lost. U_c can be reduced by either placing a second glazing over the absorber or by evacuating the space around the absorber. The reduction of area from which heat is lost will require the concentration of the solar radiation on a smaller area. The heat loss for concentrating collectors is therefore reduced at large temperature differences than for flat-plate collectors.

Collector tilt angles will depend on whether the installation is for heating or cooling. Solar angles

are low in winter. For best performance in most parts of the world, solar collectors should face due south and be tilted at the local latitude plus 10-15° (10, 54). For combined heating and cooling systems, the optimal collector tilt is the local latitude except in the southern hemisphere where the tilt is the local latitude less 10° (10).

The temperature of the fluid required by heating or cooling equipment has a strong effect on solar system performance utilising flat-plate collectors. Bisset and Monaghan (53) observed that by reducing energy storage tank temperature from 88°C to 41°C for a heating system, collector performance improved by about 90%. For absorption cooling systems, higher temperatures are required than for space heating. Collector performance drops with rising absorber temperature but the COP improves.

Shading by other buildings or other collectors can affect the incident radiation on the collector surface and hence the thermal performance of a collector.

The thermal efficiency of a collector (η_c) defined as the ratio of the useful energy collected or derived by the collector to the total insolation on the collector aperture, is given by the equation:

$$\eta_c = \frac{Q_u}{A_c I_c} \qquad (2.4)$$

From equations (2.3) and (2.4)

$$\eta_c = \tau_g \alpha_g - U_c \frac{[t_c - t_a]}{[I_c]} \qquad (2.5)$$

Equation 2.5 is awkward to use because the absorber temperature, t_c, is difficult to determine accurately. This equation is therefore modified by introducing a correction factor to both right hand terms which will allow use of the more readily measured collector fluid inlet temperature. Hence:

$$\eta_c = F_R \tau_g \alpha_g - F_R U_c \left[\frac{t_i - t_a}{I_c}\right] \qquad (2.6)$$

where

F_R = A correction factor such that the thermal efficiency as calculated by equations 2.5 and 2.6 are the same.

$$= \frac{I_c \tau_g \alpha_g - U_c (t_c - t_a)}{I_c \tau_g \alpha_g - U_c (t_i - t_a)}$$

t_i = the temperature of the fluid entering the collector, °C.

The efficiency of a collector decreases with small flow rates because such flow rate leads to high collection temperature with increased heat losses (55).

Instantaneous efficiency during the middle of the day when incident angles are favourable are generally higher than day-long efficiences which take into account unfavourably high incidence angles which prevail during the early morning and late afternoon periods. It is customary to present a collector performance by plotting the collector's efficiency against a parameter given by the difference in the temperatures of the absorber and the ambient divided

by the incoming solar irradiation - $(t_c-t_a)/I$. However, in ASHRAE standard 93-77, this relationship was used in a slightly modified form to make use of the inlet fluid temperature instead of the absorber temperature. This gives a more useful efficiency relationship as the inlet fluid temperature is known to the designer whilst the absorber mean temperature cannot be known until the efficiency is known.

Figure 2.7 shows peak efficiency curves for three flat-plate collectors. The parameter $[(t_i-t_a)/I]$ makes use of the fluid inlet temperature to the collector. Two of the collectors have flat black absorbers, one with a single cover and the other with two covers.The third collector has a selective absorber but with a single cover. At large values of $[(t_i-t_a)/I]$, the two cover collector has a higher efficiency than the black absorber single cover collector. This is because at high fluid inlet temperatures corresponding to high $[(t_i-t_a)/I]$ values, the second cover reduces heat loss resulting in smaller U_c, and a reduced slope. At small values of $[(t_i-t_a)/I]$, however, the single cover collector has higher efficiency because it has a higher transmittance. Using a selective absorber with a single cover has the advantages of both high transmittance and a lower heat loss.

Husain et al (56) made an analytical study of the effects of the variations of the depth of water, its flow velocity and the lengths of the absorbing plate

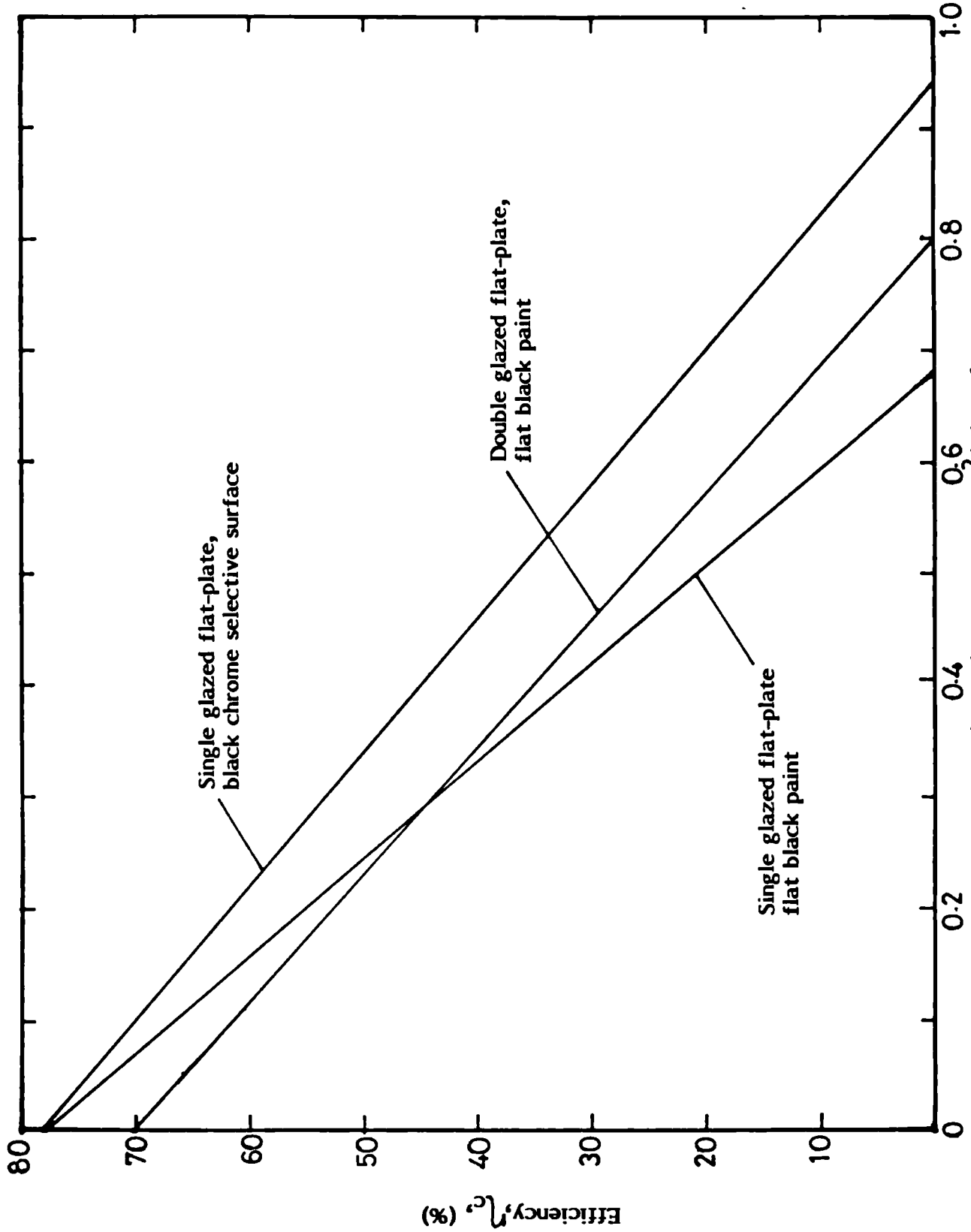

Fig. 2.7 Typical flat-plate collector instantaneous efficiency curves (Ref. 10)

on the performance of a solar collector/storage water heater in which water is flowing at a constant rate between the glass cover and the absorbing plate. They observed that at very low flow rates, the temperature of the water is not influenced by the length of the collector, whereas, for the same flow condition and the collector area being $1m^2$, the variation of the water thickness has a significant effect on the water temperature. As flow rate increases, the temperature of the water decreases but the rate of heat gained by the water increases. The rate of heat gained also increases with increases in the thickness of the water.

2.3.2 Utilisation Of Solar Energy In Buildings

The three basic uses of solar energy in buildings are: domestic water heating, space heating and space cooling. The most cost effective of the solar systems is the domestic hot water system. This is because inlet water temperatures are low so collector efficiency is high thus allowing for less collector area for the same heat collection. Furthermore, all the heat collected is useful as the temperature level required for water heating is much lower than for space heating where a minimum useful temperature level will be about 37°C (57).

Every solar hot water system has to be able to absorb

solar energy, transmit it to water and then store the hot water until it is needed. Three methods of doing this are:

a) absorbing and storing in the same unit,
b) absorbing and storing in separate units,
c) dual circulation system.

System (b) is the most common type. An absorber collects the solar energy and a separate well insulated tank is used for the storage of the hot water. The water flows by natural convection between the absorber and the storage tank if the tank is installed at a higher level than the absorber or else circulation is achieved by means of a small pump. For design purposes, a daily consumption of 91 litres of 60°C hot water per person per day is recommended for the average family (54).

In space heating, solar energy in the form of medium temperature air or liquid is used directly. Air systems are used particularly for residences and storage is typically rock pebbles. Air has the advantage that it does not freeze but more volume is required for rock storage than for water. Whenever the storage tank temperature is below a level useful for heating in solar energy space heating systems, a fossil fuel auxiliary energy must be used. For buildings requiring cooling as well as heating, this disadvantage can be overcome by combining a heat pump with a solar energy system for winter heating duty.

Bliss (58) has used south-facing tube-in-strip collectors to collect heat at moderate temperatures during winter. The ceiling of the building interior was made of the same tube-in-strip material as for the roof panel. Warm water was circulated through the ceiling panel to heat the building during winter whilst cold water was circulated through the ceiling to cool the building. An insulated tank was used for energy storage. The Bliss system delivered 37245 GJ/year to the building for heating purposes and a total of 6942.6 MJ/year were removed from the building by the cooling system.

Space cooling by solar energy is more technologically difficult than space heating as heat needs to be converted into cooling by some means. The two basic methods of using thermal energy to generate cooling are:

i) absorption cycle refrigeration,

ii) Rankine cycle refrigeration.

The absorption systems are more widely used and will be discusses further in the next chapter. The Rankine cycle uses thermal energy to develop mechanical energy which can then be used in conventional ways to develop cooling.

Even though solar energy is free, the high cost of apparatus used to collect and store the heat, the

controls and auxiliary heating systems for sunless days have made the cost of using it for heating or cooling alone prohibitively high. Systems are then designed for winter heating and summer cooling. In some cases, domestic hot water is also included. Thomason (59) made use of a south facing simple inexpensive solar heat collector to collect solar energy used for heating the building during winter, for cooling during summer and for heating most of the domestic hot water. The collector absorber surface is made of blackened corrugated sheet metal, the corrugation running down the incline. The efficiency of the Thomason collector is very high in its normal working range (approximately 40-75% in boosting water temperatures in the range of 0°-57°C). In this system (Figure 2.8), a 191 litre fresh water tank is placed in a 1250 litre drum. Hot water from the solar collector flows into the 1250 litre drum and heats up the fresh water in the smaller tank. The water then flows from the 1250 litre drum into a 7274 litre tank surrounded by 50,800 Kg of stone for temporary storage. The heat from the 7274 litre tank heats up the stone which stores the heat while water cools down ready to take more heat on the next sunny day. Whenever heat is needed a thermostatically operated blower automatically switches on. The cold air is circulated to the bottom of the heat storage bin. As the air rises, it picks up the heat from around the warm drum and the warm stones. The warmed air is then distributed through registers in the living rooms. The blower cuts off automatically when the house is warm

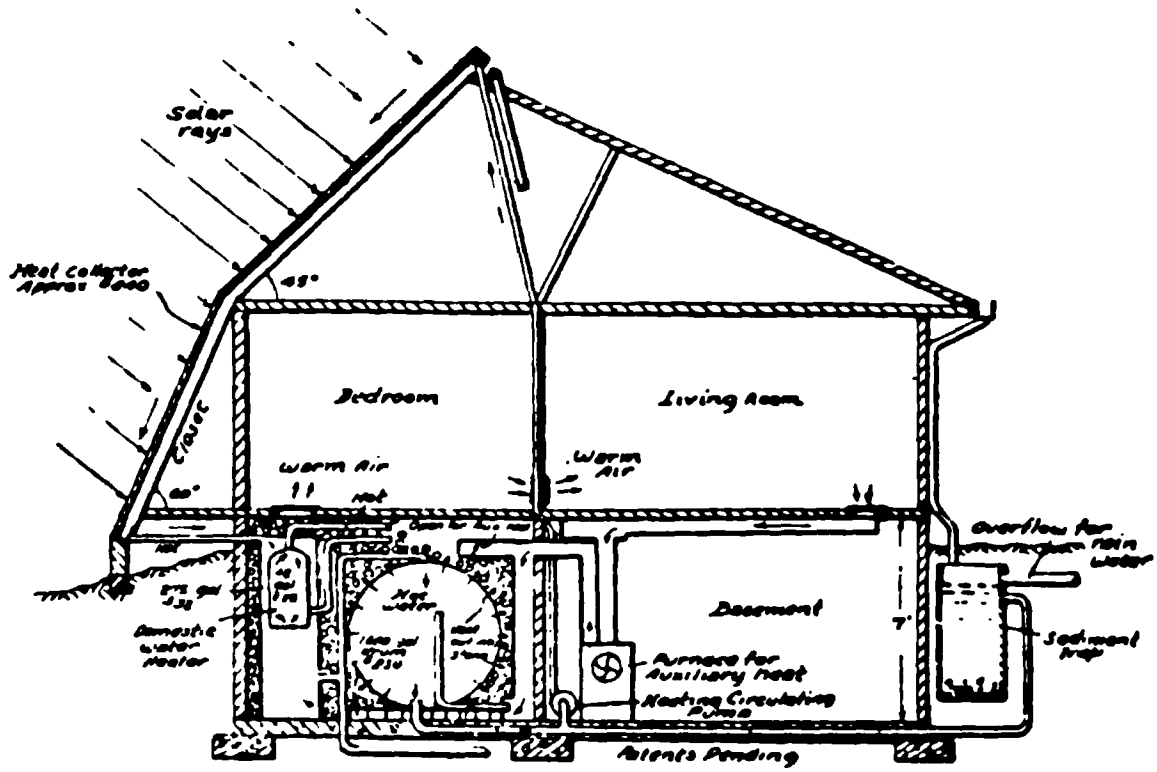

Winter Heating Cycle

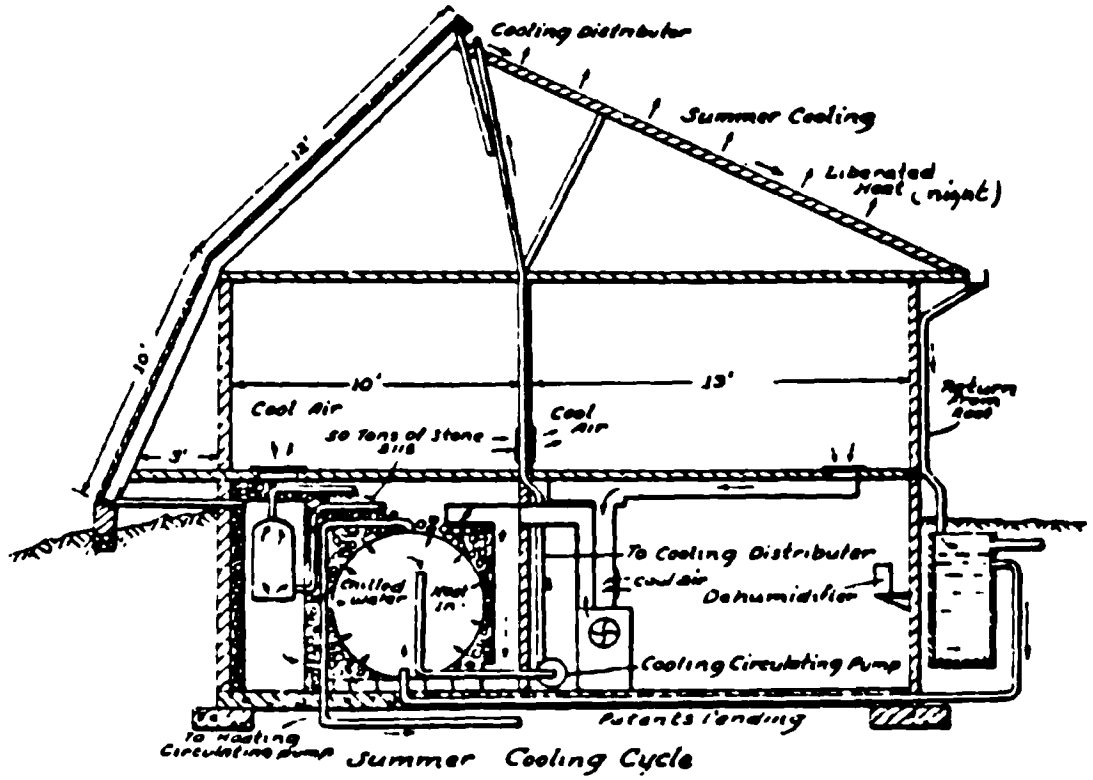

Summer Cooling Cycle

Fig. 2.8 The Thomason Solar System

enough (22°-24°C).

During the summer, the heat collector continues to heat the domestic water supply. However, warm water from the 7274 litre tank is circulated to the north sloping roof at night to cool the water now stored in the tank to cool the stones. Air blown through the drum is supplied to the house cooled and dehumidified.

Dunkle (60) described a method of solar air conditioning for hot, humid tropical and subtropical regions. This system with air-water mixture as the working fluid is based on adsorption dehumidification of the air coupled with regenerative evaporative cooling. The design conditions chosen are:

- outside conditions - 35°C d.b and 27.7°C W.B,
- inside conditions - 25°C and 65% relative humidity.

A ventilation heat load of 3.5KW, peak building load of 5.3KW and a mean building load of 2.93KW over a 24 hour period are assumed. A rock pile energy storage of about 42.5m^3 of rock screenings is proposed for the size of the system. Dunkle suggested that the air heater and rock pile can be used for heating in cold weather. However, no working system based on this proposal has yet been built.

Chapter Three

Review Of Absorption Refrigeration Systems For Solar Energy Applications

Absorption refrigeration is an attractive method for utilising low temperature heat such as industrial waste heat, solar energy and geothermal energy. Engine waste heat could be a source of energy supply for producing refrigeration but such systems present problems not encountered in conventional refrigeration plants. Whereas a conventional plant would be installed to cater for a particular load and at a desired location, refrigeration may not be required at the engine installation sites and even when it is required, the available refrigeration may not match particular requirements. Furthermore, it may not be easy to arrange for a heat recovery refrigeration unit where the need for cooling exists. For instance, a waste heat operated absorption plant for refrigerated road transport would need air cooled equipments.

Solar energy is a promising low temperature heat source for absorption refrigeration systems even though it has its own limitations also. Four types of systems deserve practical consideration at the present. Those in which ammonia is the refrigerant, those having a halogenated hydrocarbon as the refrigerant, those in which alcohol is the refrigerant and those with water as the refrigerant. The few solar

operated systems so far put on the market are of the ammonia and water types but recently there has been a growing interest in the use of the alcohol system. This is, however, still at an experimental stage. Even though systems with halogenated hydrocarbons are not common for solar energy applications, the regeneration temperature levels for some reported systems in the literature fall within what can be supplied by well designed flat-plate solar collectors.

Before going into the review of the different systems mentioned above, some problems associated with the use of solar heat for cooling, which could contribute to the delay in its economic acceptability, will be discussed.

3.1 The Problems Of Using Solar Heat For Absorption Refrigeration

For a solar operated NH_3-H_2O system, a high regeneration temperature is usually required hence a concentrating device is more suitable but with its associated high cost, such a system is not viable even at the present level of fossil fuel cost. The LiBr-H_2O system can operate on a relatively lower regeneration temperature that can be attained by the relatively cheaper flat-plate solar heat collectors. The cost of the solar heat collection and its associated equipments even for this type of system may only be justified in parts of the world where conventional energy sources are either not available or scarce.

Hence, although the technical feasibility of solar-powered refrigeration has been established at he experimental stage over the years, the system may, however, not be viable or accepted until it is economically acceptable depending on higher cost of other conventional energy such as electricity, gas or kerosene.

The availability of solar radiation is intermittent, hence for a refrigeration system for continuous operation, an auxiliary heating device is necessary whenever the energy level from the collector is low or unavailable. To a certain extent, this problem can be solved by incorporating a heat storage facility in the system. The types of storage systems have been discussed in Chapter Two. The addition of the storage system adds to the installation cost of solar operated refrigeration systems. However, for intermittent refrigeration cycles, the intermittent availability of solar energy is taken care of by regenerating the system when solar radiation is available whilst refrigeration takes place at night. The intermittent absorption unit, however, although it requires no mechanical part and is most suited for underdeveloped areas of the world, requires constant attention during its operation thus making such operation unwieldy.

In systems using ammonia as a refrigerant,low evaporation rate of ammonia in the evaporator has been reported for intermittent units, owing to poor mixing

and reabsorption of ammonia in the absorber (65, 67). Better absorber design can, however, improve this problem.

In a solar operated absorption system, the collected energy is usually used to heat up a heat transfer fluid flowing through a coil submerged by the working solution in the generator (Figure 1.2) Some problems could arise on the layout of the collector arrays and the generator. In cases where the insulated energy storage tank is installed at a lower level than the collectors, forced circulation will be necessary. For optimum performance, a flat-plate collector is generally mounted so that it faces the south with a tilt (to the horizontal) of the latitude plus or minus 10°-20° depending on the season of the year when maximum output is needed. Shading from other buildings and the orientation of the building could limit the amount of energy reaching the collector even on clear days. Also, aside from the collector cost, the heat transfer fluid pipings and the circulation pumps contribute to increased installation cost for a system that may still need an auxiliary heating source. Although the maintenance cost of a solar operated system will be small when compared with a conventional system and though the installation costs may be recouped over a few years through savings in energy and maintenance costs, the initial costs will contribute to making such a system economically unacceptable.

The cooling medium temperature and the flow rates determine the temperature of the absorber and condenser. The absorbing temperature and the evaporating temperature which establishes the low side design vapour pressure, determine the absorbent solution temperature. The generator temperature that can be used with any given condensing pressure is limited by the upper limit concentration, which is normally chosen to avoid crystallisation in the lines ($LiBr-H_2O$ system). An increase in cooling water temperature leads to reduced capacity and higher minimum evaporator temperature. However, with lower condensing and absorbing temperatures, a lower generating temperature can be successfully utilised for a given evaporating temperature. Hence, application of solar heat may be more favourable in places with abundant radiation combined with a moderately low air temperature.

3.2 Cycles With Ammonia As The Refrigerant

Williams, Chung, Lof, Fester and Duffie (61) used a solar energy regenerated intermittent absorption refrigeration cycle for the operation of some experimental coolers. The system utilised ammonia-water as the working solution. Generator-absorbers were containers with liquid seals in the tops and tubes to introduce refrigerant vapour into the bottom of the container to improve mixing. Evaporator-condenser vessels were cylindrical in shape with extended heat transfer area on the outside of the

metal walls.

For regeneration, the generator was insulated with a glass wool blanket which covered the vessel except a blackened area at the bottom to allow concentration of solar energy. The condenser was immersed in a 22.7 litre container of water, for water cooling in certain experiments, or exposed to the atmosphere for air cooling in some of the experiments. A parabolic reflector was used to focus solar energy onto the exposed bottom part of the generator. The paraboloids with a focal length of 45.7cm had 106.7cm aperture presenting an area of 0.773m^2 to the sun. On clear days, 2110 to 2638 KJ/hr of direct solar radiation was received by the reflectors.

When the maximum generator temperature was reached, heating was stopped by removing the reflector. Insulation around the generator was then removed and in some experiments, the generator was immersed briefly in water to facilitate cooling and rapidly initiate refrigeration. The solar regenerated unit was operated for four consecutive days cooling a 0.064m^3 box on the refrigeration cycle. They concluded that intermittent absorption refrigeration cycles with solar regeneration can be useful for refrigeration especially in small household food coolers in non-industrialised areas.

Trombe and Foex (62) developed an intermittent solar refrigerating machine with ammonia-water

solution as the working fluid. The general set up of the system is shown in Figure 3.1 and it functions as follows: Ammonia-water solution flows from a cold reservoir that has higher ammonia concentration at the upper part than at the lower part, through a pipe placed at the focal line of a cylindro-parabolic reflector to the generator. Ammonia vapour released from the generator is cooled in the condenser coils placed in a pool of water. The condensate flows into the evaporator which consists of a coil wound around a container used as the ice box. In producing cold after the disappearance of solar heating, the ammonia vapour is rerouted through the bottom of the boiler. As the cooling of the boiler progresses, the pressure is lowered, thus instigating the distillation of the ammonia gas from the evaporator coil to produce some cooling effect.

The cylindro-parabolic reflector measured 1.5m^2 and was oriented east-west. In prototype trials, the daily production of ice was about 6Kg or 4Kg/m^2 for four hours of solar heating.

Chinnapa (63) performed an experimental study of an intermittent vapour absorption refrigeration cycle with regeneration temperatures in the region of 121°C. An artificial heat source comprising two immersion heaters, 4KW and 2 KW respectively, with variable power supply and heating rate were employed to obtain these temperatures because of the location and time of the experiments, but such temperature levels could

well be obtained by well designed solar heat collectors in areas of high insolation. Ammonia-water and ammonia-lithium nitrate were the two binary solutions investigated. The schematic diagram of Chinnappa's refrigerator is shown in Figure 3.2. Results showed that the COP of the NH_3-$LiNO_3$ system is slightly better than that of the NH_3-H_2O system but for the latter, more refrigeration per Kg of solution is possible. Where the same vessel serves as both condenser and evaporator as is the case in some intermittent cycles, the available cooling is less than the actual effective cooling as the vessel has to be cooled at the start of the refrigeration stage. Hence for larger units, Chinnappa recommended that the condenser be separate from the evaporator. It was further observed that flat-plate solar energy collectors can operate the intermittent refrigerators with maximum solution temperatures of 93°-104°C and values of the COP of about 0.30 for evaporating temperatures around 0°C.

A flat-plate collector operated intermittent refrigerator with ammonia-water as working fluid was built by Chinnappa (64). The flat-plate collector comprised a 1.524m x 1.067m x 0.76mm thick copper sheet painted dull black. Six 6.35mm diameter steel pipes were soldered to the plate at 152.4mm intervals and their ends welded to headers. The absorber surface with 10.2mm thick cork board insulation behind it had three glass covers. Maximum solution temperatures of

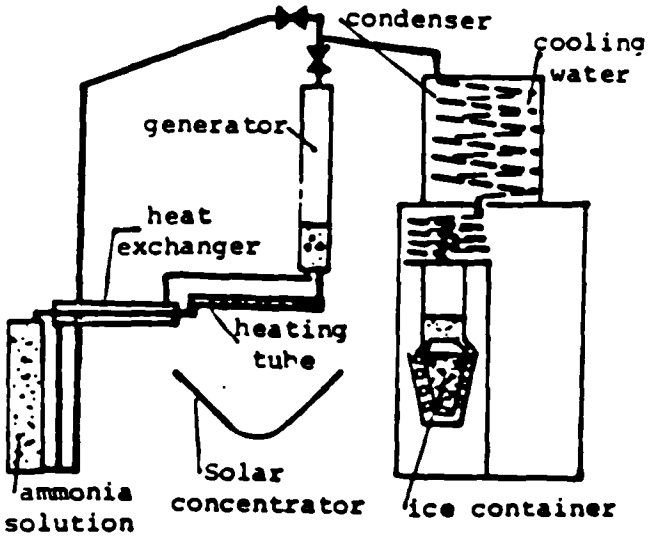

Fig. 3.1 Intermittent Absorption Refrigerator built by Trombe and Foex (62)

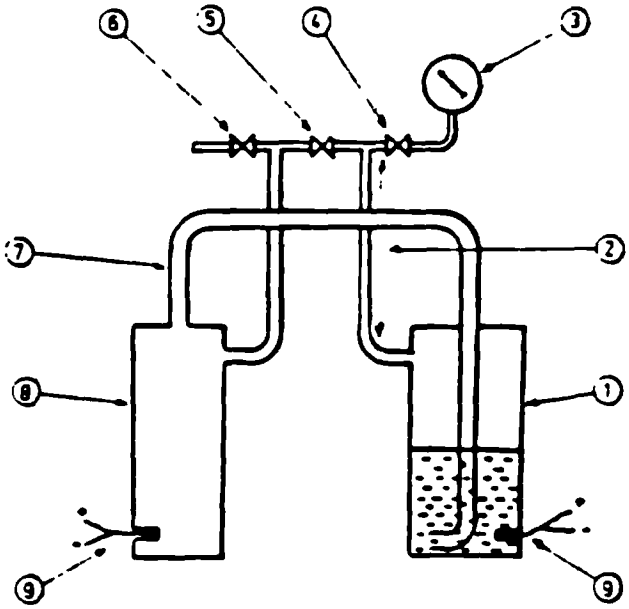

1. Generator Absorber
2. Rectifying section of distillation pipe:
   not insulated for NH_3 H_2O vapour
   insulated for NH_3 H_2O vapour
3. Pressure Gauge
4. Gauge valve A
5. Valve B open during regeneration
   closed during refrigeration
6. Valve C for charging
7. Absorption pipe
8. Condenser evaporator
9. Thermocouples.

Fig. 3.2 Schematic diagram of Chinnappa's experimental refrigerator (63)

about 100°C was attained during the experiments. This investigation indicated that temperatures as low as -12°C could be attained with a flat-plate collector operated refrigerator. Furthermore, 1Kg of ice a day was produced per 0.72m² of solar collector surface, and it was pointed out that the yield could have been improved with the use of a selective solar collector absorber surface.

An intermittent ammonia-water absorption refrigeration unit was built by DeSa in Dacca, Bangladesh (65). The unit consisted of two vessels placed together, with a pipe incorporating a valve for isolating the vessels. The generator-absorber was 15.24cm diameter, 22.86cm long and contained ammonia-water solution. A liquid seal in this vessel prevented water vapour from passing into the evaporator-condenser vessel. For the regeneration cycle, the generator with the bottom painted black and the body covered with insulation, was placed at the focus of a 1.37m parabolic solar reflector with aluminized Mylar film. The reflector was mounted normal to the sun and adjusted to continuously focus solar radiation on the generator. The ammonia vapour given off by the solution in the generator was condensed in the condenser which was immersed in a tank of water for water cooling operations or exposed to the atmosphere for air cooling operations. Heating was stopped when the maximum operator pressure (nearly 13.8bar) was reached and the interconnecting valve closed.

For the refrigeration cycle, the insulation cover on the generator-absorber was removed and the vessel immersed in water to facilitate cooling. The interconnecting valve was opened and ammonia liquid in the condenser-evaporator vessel evaporated thereby lowering the temperature of the vessel. The vapour so released was re-absorbed by the weak solution in the generator-absorber vessel.

For a generator temperature of 93°C and an ammonia concentration of 54.5%, an evaporator temperature in the order of -11°C was obtained. DeSa observed that the design of the generator-absorber and the condenser-evaporator could influence considerably the performance of an intermittent absorption refrigeration system. He pointed out the need for further tests for the effective design of the absorber and evaporator vessels for solar operated systems.

Farber (4) discussed the fundamental principles of using solar energy directly for refrigeration and air conditioning. He described the performance of three different actual refrigeration or air conditioning systems consisting of: a standard continuous system operated by solar energy concentrating device: a 1.76KW intermittent system operating on a flat-plate solar collector device; and a special 10.55KW continuous system using flat-plate solar collector. The flat-plate collector operated continuous system was described more fully in another paper (66).

In the first system, solar energy from a concentrating device was used to drive a conventional Servel absorption refrigerator using cotton seed oil as the heat transfer fluid. the oil was preheated in a flat-plate collector to about 93°C before flowing through a pipe at the focal line of a 1.83m x 2.44m concentrating solar collector where the temperature was raised to about 287°C. The hot oil then flowed into a well insulated storage tank from where a thermostatically controlled circulating pump circulated it around a heating coil in the generator to heat up the working fluid. Although this system functioned well, it was not pursued further because of the high cost of the solar energy collection by the concentrating device.

The intermittent system utilised ammonia-water as the working fluid and the operation is subsequently as described earlier in the basic intermittent solar refrigeration system. Results of this investigation showed that an ammonia-water system with high concentrations (50-60% ammonia by weight) could operate well within the temperature levels obtainable by flat-plate solar energy collectors.

For the 10.55KW continuous system utilising a flat-plate solar heat collector, the absorbing surface consisted of ten flat tube-in-strip copper sheets with a total area of 37.2m^2 and coated with black paint. They were placed inside galvanised metal boxes with 50mm thick foam glass insulation behind and a single

glazing over them. They were arranged in high parallel rows, south facing and inclined at about 10° to the horizontal to maximise the collection of solar energy. Water supply temperatures varied from 60° to 100°C with the most satisfactory operation obtained at temperatures of 79°C and above. At an operating temperature of 79°C and with a collector area of 37.2m², 13.015W of cooling was provided by the system under optimum conditions. Farber et al concluded that the performance of the system could be improved by raising the generator solution temperature possibly by combining the generator and absorber into one unit thus eliminating heat transfer resistance through solid surfaces and liquid films.

An intermittent absorption refrigerating unit working on ammonia-water solution was built and tested by Swartman et al (14). Figure 3.3 shows the schematic diagram of the refrigeration unit which used a flat-plate solar energy collector as the generator-absorber. The collector-generator unit consisted of 12.7mm steel pipes connecting a 50mm feed pipe to a 152mm header. Thin copper sheets were soldered to the tubes and the whole absorbing surface with a total area of 1.67m² was encased in a wooden box with two glazing covers. The generator was charged with ammonia-water solution of the required concentration and at the commencement of regeneration, the valve between the upper header and the condenser was opened. At the end of regeneration, the condenser was isolated

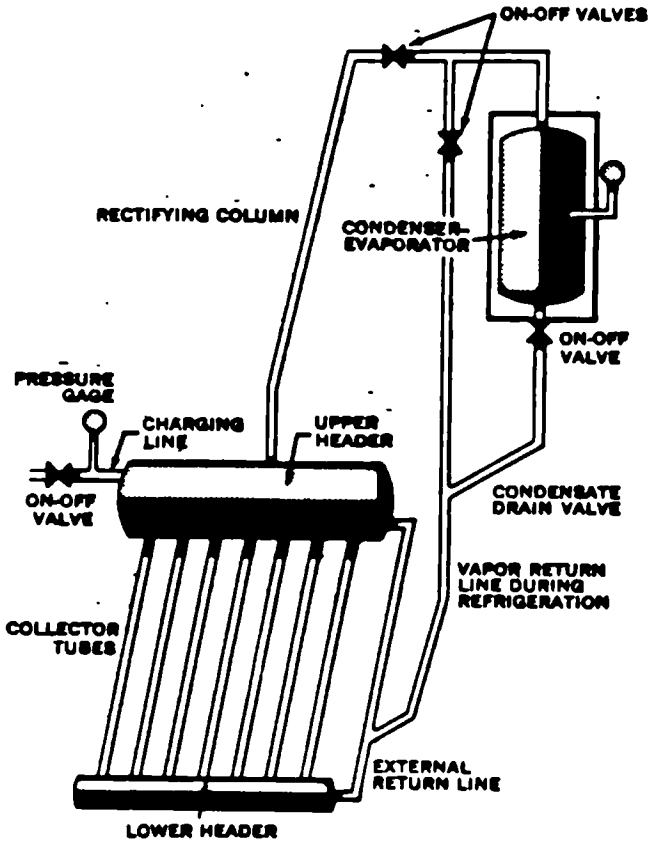

Fig. 3.3 Schematic diagram of the intermittent absorption refrigeration system built by Swartman et al (14)

from the rest of the system and the generator allowed to cool.

For the refrigeration cycle, the valve on the vapour return line was opened and the ammonia in the condenser-evaporator began to evaporate thus producing some cooling effect. Evaporator temperatures as low as -12°C were attained and for solar insolation of about 765.6 W/m^2, 4.5 to 6.8Kg of ice was produced from water originally at 27°C. It was concluded that a solar powered intermittent absorption refrigeration system has an important role and can compete favourably with conventional systems in many parts of the world.

The refrigerant-absorbent combination giving the best performance in intermittent refrigeration systems is the NH_3-H_2O under the assumption that no water is transferred to the condenser. It is, however, difficult in practice to prevent water from getting to the condenser during regeneration, hence the need for a rectifying column to minimise the transfer of water. An absorbent that gives a good combination with ammonia as a working fluid without the need for rectification is Sodium thiocyanate (NaSCN). Ammonia-sodium thiocyanate solutions are relatively cheap, non toxic, non explosive and non-corrosive to iron. They have relatively low vapour pressures, viscosities, high thermal condutivities and heats of vaporisation. Chung (67) built and operated an intermittent refrigeration system that worked on the NH_3-NaSCN

solution. He used common shop grade mild steel to construct the generator/absorber and the condenser/evaporator vessels and a flexible hose to connect them. The solar collector device was a 1.22m diameter reflector which concentrated solar heat unto the lightly insulated generator. A final regeneration temperature of 121°C was achieved. About 4Kg of ice was produced per cycle with winter sun through a window when the available radiation was below 906.5 W/m^2. At the time of Chung's experiment, however, the Temperature-Enthalpy data needed to evaluate the cooling efficiency of the NH_3-NaSCN combination was lacking.

Sergent and Beckman (68) measured the heat capacity data for NH_3-NaSCN solution at temperatures above 25°C. Their results were used in combination with the available data for heat$^{of}_{\Delta}$solution at 0°C to generate a Temperature-Enthalpy diagram for the solution. Using an idealised intermittent cooling cycle, they evaluated the ideal cooling ratios which they found to be identical to those of the NH_3-H_2O combination. However, the NH_3-NaSCN has the added advantage of not requiring a rectifier to prevent transfer of absorbent to the condenser.

According to Swartman et al (15), results of an earlier investigation by Swartman, Ha and Swaiminathan on the comparison of NH_3-NaSCN and NH_3-H_2O systems showed that the COP of NH_3-NaSCN ranges from 0.11 to 0.27 whilst that of NH_3-H_2O ranges from 0.05 to 0.14.

It was concluded that the NH_3-NaSCN have better performance than NH_3-H_2O systems and that the low volatiity of NaSCN salt which eliminates the need for a rectifier offered lower equipment cost.

Muradov and Shadiev (69) reported on the performance of an intermittent absorption refrigerator utilising ammonia as the refrigerant and calcium chloride as the absorbent. The machine which was of welded construction consisted principally of a generator, condenser and evaporator. The generator was a double glazed, flat-plate solar energy collector with an area of $2m^2$. Results showed that with a generator temperature of between 120° and 130°C, freezing temperatures were achieved within 1-2 hours of the refrigeration period and about 2Kg of ice was produced. It was concluded that the device can function successfully as an ice maker, is sturdy, reliable and needs no constant attention.

Some problems associated with the use of solid absorbents in ammonia refrigeration systems include: the large swelling of the salts upon absorption of ammonia; migration of the salts, in which case the absorbent is placed where it is wanted in a heat transfer structure but it will not stay there. Clausen and Worsoe-Schmidt (70) in their work on an intermittent ammonia-calcium chloride refrigeration system explored the possibility of solving these problems by the suspension of the absorbent (Calcium chloride) in a suitable liquid. Heptanol was found to

be the best for the establishment of suspensions of $CaCl_2$ and $SrCl_2$, another solid absorbent for ammonia, earlier proposed by Buffington (7/). Clausen and Worsoe-Schmidt reported that solid $CaCl_2$ has a much larger active content of ammonia on a mass as well as on a volume basis than have the fluid absorbents such as the $CaCl_2$/heptanol, water and sodium thiocyanate which have been previously suggested for solar applications. Furthermore, the disadvantages of using salt suspensions clearly outweighs the advantages when the operation of the system is complicated by the necessity for stirring the suspension.

3.3 Cycles With Halogenated Hydrocarbons As Refrigerant

Even though Refrigerant-12 (CCl_2F_2 is the most commonly used refrigerant today, it is not proposed as an absorption refrigerant because it shows only Raoult's law solubility in liquids that can be used as absorbents. Halogenated hydrocarbon refrigerants having at least a hydrogen atom in the molecule have shown the highest solubilities in absorbent liquids and are therefore of interest as absorption refrigerants. Eiseman (72) evaluated six fluoroalkanes and a nonfluorinated compound in dimethyl ether of tetraethylene glycol (DMETEG). The fluoroalkanes were: Refrigerant 21 ($CHCl_2F$); Refrigerant 22 ($CHClF_2$); Refrigerant 133a (CH_2ClCF_3, Refrigerants 31 (CH_2ClF); Refrigerant 124a ($CHF_2.CClF_2$) Refrigerant 134 ($CHF_2.CHF_2$. The non fluorinated compound was Refrigerant 30 (CH_2Cl_2), commonly used as a refrigerant in vapour compression systems.

Calculated COP values of 0.375 and 0.268 were obtained for Refrigerant 21 and Refrigerant 22 respectively. Refrigerant 21 with the best COP value has poor chemical stability hence Refrigerant 22 with excellent chemical stability as well as good thermodynamic properties is the preferred halogenated refrigerant. The Refrigerant 22 system showed good stability under the relatively severe conditions represented by 90 days at 176.7°C. Even though solar energy was not considered in Eiseman's studies, it is

expected that a solar concentrating device will produce such operating generator temperature of 176.7°C.

Thieme and Albright (73) investigated the solubility of Refrigerants 11, 12 and 22 in several organic compounds containing nitrogen atoms. They found that the two best solvents for Refrigerants 21 and 22 were dimethyl formamide (DMF) and diethyl formamide (DEF). These two solvents produce mixtures that have COPs about 15 and 2% respectively, better than mixtures containing DMETEG. Thieme and Albright, however, pointed out that even though DMF and DEF are good solvents on stability basis, both have relatively low boiling points which might cause problems in an absorption refrigeration system.

Williams et al (61) built solar operated intermittent coolers using Refrigerant 21-DMETEG as working fluid. The apparatus used and the procedure were essentially the same as those previously reported in the earlier reference for the ammonia-water system. The performance of the synthetic refrigerant systems suffered from low latent heat of the refrigerant and the requirements for relatively large amounts of absorbent. The maximum cooling ratio was about 0.26 compared with 0.32 for the ammonia-water system. Williams et al concluded that the ammonia-water system is superior to the Refrigerant 21 - DMETEG system.

De Silva (74) investigated the use of exhaust gas

heat of a diesel engine to operate an absorption refrigerator working on Refrigerant 22 - Dibutyl Phthalate solution. Several advantages were reported for this combination over the ammonia-water and water-lithium bromide combinations. These are: non toxic refrigerant that can be used for refrigeration and air conditioning; DBP with a boiling point of 329.4°C is noncorrosive and has negligible vapour pressure under generator operating conditions. Furthermore, the combination is capable of operation with generator temperatures down to about 66°C. This temperature level can be obtained from conventional flat-plate solar collectors. For a generator temperature of 94°C and a condensing temperature of 19°C an actual Coefficient of Performance of 0.55 was reported for an evaporation temperature of 7°C. However, De Silva conceded that the heat ratio for the R22-DBP system is considerably lower than that of $LiBr-H_2O$ system at the evaporating temperature of 5°C.

Borde et al, (75) investigated some refrigerant-absorbent combinations for absorption units powered by low grade heat sources. Refrigerant 22 was chosen as the refrigerant because of good chemical stability and thermodynamic properties. The absorbents investigated were: Methyl -Caprolactam (MCL); dimethyl methyl phosphate (DMMP); dimethyl ether of tetraethylene glycol (DMETEG); and dimethyl Formamide (DMF). They analysed an absorption cycle based on solubility measurements of the different combinations and compared their performance characteristics for

refrigeration and heat pump operations. Data on the Coefficient of Performance were presented for two typical conditions: in a refrigeration application with evaporation temperature of 0°C and condensing temperature of 30°C, and in a heat pump application with evaporation temperature of 5°C and condensing temperature of 45°C. Generator temperatures for both operations ranged from 60 to 140°C. Results of their analysis for both applications showed that R22-DMF performed best followed by R22-DMMP, R22-DMETEG and finally by R22-MCL. Again, the generation temperatures fall within what can be supplied by solar energy collectors, the lower range by flat-plate collectors and the higher range by solar concentrating devices.

3.4 Cycles With Alcohol As Refrigerants

There has been growing interest in solutions of inorganic salts in methanol as absorption refrigeration machine working fluids since the work of Aker et al in 1965 (76). Investigations were made of vapour pressures of mixtures of methanol or ethanol and various salts such as lithium bromide, lithium chloride and zinc bromide. A mixture containing 2 moles of lithium bromide and 1 mole of zinc bromide in methanol was found to be the best overall combination. Several investigators as reported in the comprehensive survey of Olama (25), investigated other thermodynamic properties such as specific gravity, viscosity, solubility, and specific heats for LiBr - CH_3OH and $(2LiBr + ZnBr_2)/CH_3OH$ combinations.

Grossman and Zhuravlenka (77) built an experimental absorption machine working on LiBr - CH_3OH solution. The evaporator, absorber, generator and condenser were of the shell-and-tube type. A gear pump was incorporated to recirculate absorber solution as well as pump solution to the generator. Evaporation temperature as low as -18.6°C was achieved with a generating temperature of 85°C, condensing temperatures of 20.6°C and an absorbing temperature of 23°C. The actual heat ratios for the machine ranged from 0.44 to 0.48 whilst the theoretical heat ratios ranged from 0.62 to 0.65

Olama (25) investigated the thermodynamic properties of a few methanol/salt solutions. The properties measured were vapour pressure, specific heat and heats of mixing. He built an absorption refrigerating machine working on $(2LiBr + ZnBr_2)/CH_3OH$ solution. The machine incorporated a circulation pump in the working solution circuit. Evaporation temperatures as low as -11°C was achieved with a generation temperature of 96°C, condensing temperature of 20°C and an absorbing temperature of 23°C. Olama concluded that an actual heat ratio of 0.45 was expected at an evaporation temperature of 10°C but concluded that the absorption process in the absorber was inadequate.

Alloush (78) modified Olama's experimental refrigerator and built a second version that utilised

the vapour bubble pump principle for the circulation of the solution. Both refrigerators functioned on the same working solution - (2LiBr + $ZnBr_2$)/CH_3OH. In the first version refrigerator, experimental data were obtained at constant generation temperatures of 95°C and 75°C respectively. In both cases, the condensing temperature was also constant at 20.1°C. At 95°C generation temperature, the evaporating temperatures varied from -10°C to -1.4°C whilst the absorbing temperatures varied from 22 to 26.5°C. The actual heat ratio varied from 0.357 to 0.612 whilst the theoretical heat ratio varied from 0.72 to 0.75. At 75°C generation temperature, the evaporating temperature varied from -7 to 1.7°C and the absorbing temperature varied from 22 to 25°C. The actual heat ratio varied from 0.413 to 0.563 whilst the theoretical heat ratio varied from 0.77 to 0.79.

For the second version refrigerator, sets of readings were taken for constant generation temperatures of 100, 90, 80 and 70°C. The condensing and absorbing temperatures for all runs were constant at 20 and 25°C respectively. The lowest evaporating temperatures corresponding to the generation temperatures were -20, -14, -8 and -4°C. Similarly the corresponding maximum actual heat ratios were 0.625, 0.625, 0.615 and 0.60 whilst the maximum theoretical heat ratios were 0.75, 0.77, 0.78 and 0.81.

It was concluded that absorption refrigeration machines operating on the (2LiBr + $ZnBr_2$)/CH_3OH

solution can be useful for solar energy applications as they perform efficiently at low regeneration temperatures that are easily attainable by flat-plate solar heat collectors. Furthermore, the utilisation of the vapour bubble pump for solution circulation will eliminate the need for auxiliary power and make the system more reliable.

El-Shamarka (2) investigated the use of (2LiBr + $ZnBr_2$)/CH_3OH solution for thermally operated heat pumps. He measured the following properties of the mixture in the temperature range of interest for heat pump operations: vapour pressure, specific heat, viscosity, relative density, solubility, thermal conductivity, surface tension. An experimental intermittent absorption heat pump was constructed and found to be capable of pumping heat from -10°C up to 74°C. El-Shamarka, however, recommended that the chemical stability of the mixture be further investigated over a working temperature range of 150 - 200°C to ascertain its suitability for real heat pump machines.

3.5 Cycles With Water As Refrigerant

Absorption refrigeration systems with water as refrigerant and acqueous salt solutions as absorbents are normally non-poisonous and odourless. Water is a good refrigerant in terms of its high ratio of latent heat to specific heat but its low vapour pressure leads to high specific volumes at evaporator

conditions. Also its freezing point of 0°C prevents its exploitation as a fluid at sub zero temperatures. However, it is useful for air conditioning refrigeration and other chilling applications. Lithium salts (most especially lithium bromide) have been found to be particularly efficient absorbing agents for water vapour. According to Lower (79), investigations in the USA showed that a saturated solution of lithium bromide at 30°C and 46% concentration by weight reduces the relative atmospheric humidity to 11% whilst a saturated calcium chloride solution yields only 30% of atmospheric humidity.

Several investigators (29,79 , 80) have studied the thermal and physical properties of the binary system $LiBr-H_2O$, that are necessary for the evaluation of absorption machines. Duhring charts and Enthalpy-Concentration diagrams have been constructed from the data so obtained to facilitate the calculation of processes connected with heat operated machines.

Duffie and Sheridan (81) described a flexible method for the analysis of a system consisting of a solar collector, a lithium bromide-water absorption refrigerator and an air conditioner. They gave calculated performance of a particular system for a tropical design day operation in a Western Queensland town in Australia. The $LiBr_2-H_2O$ cooler was a 10.55KW Arkla DUC-2, operated with hot water from a solar collector with neither energy storage nor auxiliary

energy for the operation. Even though the cooler was originally designed for operation with atmospheric steam, there was no apparent basic technological problems when it was solar operated.

The solar collector consisted of a copper tube-in-strip absorber plate with selective coating of emissivity 0.40 placed in a double glazed casing with polyurethane foam insulation at sides and back. The total area was 5.92m^2.

Results of Duffie and Sheridan's analysis show that the increase in the collector area has the effect of increasing the temperature of the collector, the temperature drop across the generator and the generator temperature. The cumulative effect of these is an increased system capacity. However, the increase in output is not proportional to the added area hence the collector area required per unit load is increased. On the other hand, decreasing the collector area to too low a value reduces the generator temperature resulting in diminished output. Furthermore, the cooling water temperature and flow rate determine the temperature in the absorber and condenser. An increase in cooling water temperature leads to reduced capacity and higher minimum evaporator temperature.

They concluded that the result of their analysis was encouraging enough to justify the use of solar energy in operating the $LiBr-H_2O$ refrigerator but that

the operation with available cooling water temperatures and with energy storage should be studied further before the economics of the system will be understood.

Two basic requirements of major concern to the designer of a solar powered air conditioning unit that distinguish it from conventional fuel fired systems are:

i) the need to operate at a low temperature of heat source; in the range of 60 to 90°C for systems utilising flat-plate collectors.

ii) the need for a back up system to supply the cooling load at times of insufficient or no energy at all from the sun.

Grossman et al (82) presented a theoretical evaluation of two design improvements made in an attempt to solve these problems for a lithium bromide absorption machine. One was the addition of a solution pre-heater between the heat exchanger outlet and the generator, which allowed for a considerable reduction in generator size and cost and improved performance at part load. The other aimed at solving the back up problem was the addition of an auxiliary generator. The first generator was powered by solar energy whilst the auxiliary one was powered by conventional energy, both operating in series to supply the full load without interference with each other. A computer

programme was written and used for the evaluation of the absorption chiller.

Figure 3.4 shows diagrammatically an absorption chiller with a pre-heater. In the pre-heater the solar heated water leaving the generator is used to pre-heat the LiBr-H_2O solution entering the generator. However, the fraction of the generator load which can be supplied by the pre-heater is limited by the requirement that the temperature of the solar heated water leaving the generator must be greater than the temperature of the solution entering the generator. Results of analysis on a 703.2KW machine show that with 20% of generator load supplied by the pre-heater, the generator area requirement was reduced by 21% and resulted in a 7.1°C superheat in the solution entering the generator instead of 10.4°C subcool formerly at the design point. The pre-heater also contributes some improvements in the COP and capacity of the machine at part load.

For the auxiliary generator, two configurations were considered and are shown schematically in Figures 3.5 and 3.6 respectively. The first configuration (Figure 3.5) employs both generators in the same shell. The solution leaving the first generator drips directly into the second, with one condenser handling the vapour generated in both. In the second configuration (Figure 3.6), two separate shells each containing one generator and one condenser are considered. The dilute solution from the absorber is

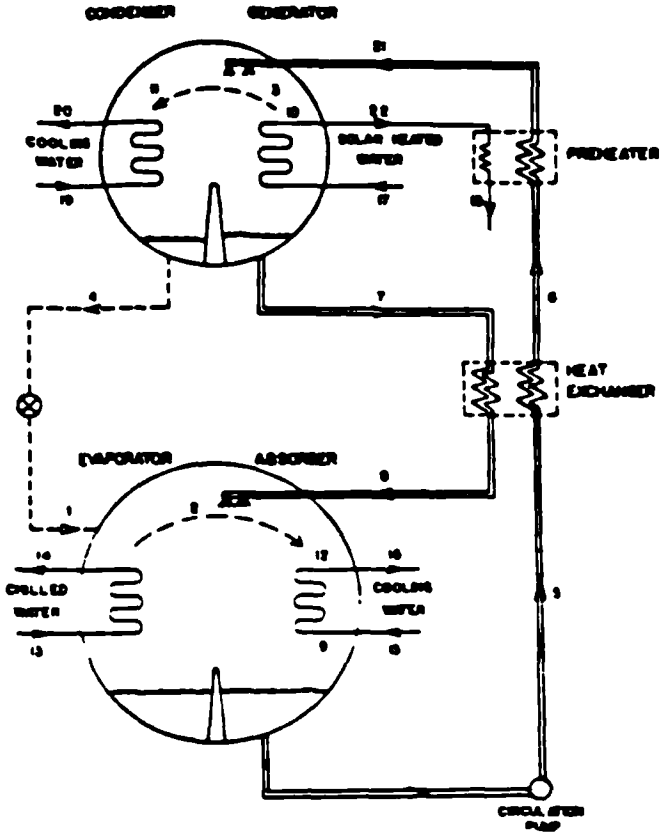

Fig. 3.4 Schematic diagram of the absorption chiller with the major sub-units, including a preheater, reproduced from Grossman et al (82)

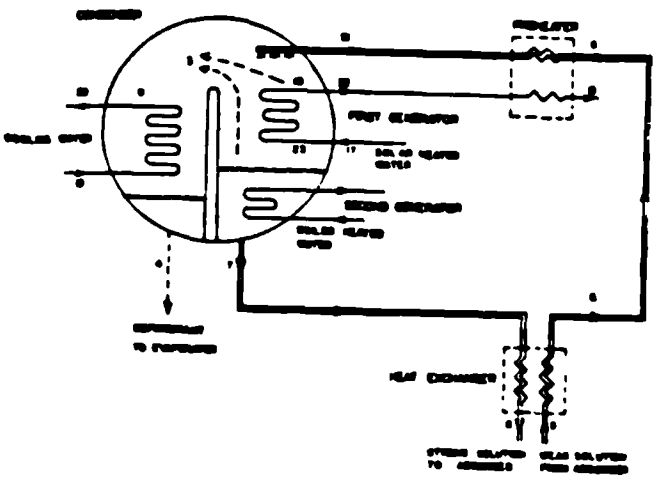

Fig. 3.5 Schematic diagram of auxiliary generator in the one-shell configuration, reproduced from Grossman et al (82)

pre-heated then concentrated in the first generator to an intermediate concentration by the solar heated water. The vapour generated is condensed in the first condenser. The solution is then passed to the auxiliary generator powered by conventional fuel where it is concentrated further before returning to the absorber. The vapour generated in this generator is condensed in the second condenser. The cooling water flows in series from the cooling tower through the first to the second condenser before returning to the cooling tower and in so doing, the two condensers require no more cooling water than the one condenser in the one shell configuration.

Results of the analysis show that the two shell configuration is superior to the one shell configuration. Even though the two shell configuration is more costly, it enables the machine to utilise effectively solar-heated water at lower temperatures. Furthermore, the two shell configuration can operate at overall capacities up to 150% of the nominal with relatively little interference of the conventional back up heating with the solar heating.

Zhang and Yu-chi (83) analysed and compared energy consumption for single stage and double stage cycle lithium bromide-water absorption refrigeration systems utilising a low temperature heat source (below 90°C) that can be supplied by industrial waste heat, solar energy or geothermal energy. Results of their analysis

show that the two-stage cycle is more suitable to low temperature heat source than the single stage cycle. It is even more advantageous as the heat source temperature decreases. An exergetic analysis of a two stage cycle was also carried out and it was found that the generation process has the largest exergy loss in the cycle. It was suggested that a study of how to decrease the irreversible loss of the heat transfer and mass transfer in the generation process be made so as to increase the thermodynamic perfection of absorption refrigerator cycles.

Carey, Khahra and Smith (84) considered the use of a sodium-hydroxide/water solution for the operation of an absorption heat pump. They designed and built a 3-KW heat pump using industrial glassware for much of the construction to enable them to observe the behaviour of the system. Electric heaters were used to supply energy to the generator and evaporator. It was expected that a 70% concentrated solution of NaOH in water at temperatures above 65°C should be capable of providing an equilibrium temperature lift of from -10°C to 100°C. Although they did not operate their machine at such high solution concentration, they achieved a temperature lift of 50°C with 60% solution concentration at a generation temperature of 150°C. They concluded that the expected high temperature lift capability of the NaOH-H_2O solution should be realised in the near future.

Quite recently, Gutkowski and Ryduchowski (85)

reported on a continuous operating solar air conditioning system utilising a desiccant absorption system in which $CaCl_2$-H_2O was used as the absorbent. Figure 3.7 shows the system flow diagram. The $CaCl_2$-H_2O solution absorbs vapour from the air which is in counterflow with it in the absorber. The dry air leaving the absorber then flows with water through an adiabatic cooler, then blown into the conditioned space by a thermostatically controlled circulating fan. The weak solution leaving the absorber flows by gravity to a storage tank from where it is discharged to the absorber, part of it being fed to the solar collector where it flows by natural convection over the flat surface to encounter the oncoming ambient air and remove the desorbed water as vapour. Heat exchangers are provided for heat recovery. In the crystalizer, crystals of calcium chloride salt are formed from the high concentration solution coming from the solar collector. The storage tanks contains a saturated solution which when feeding the absorber, raises the humidity of the air close to saturation.

The solar collector used was a low cost double glazed flat-plate type, made of a thin panel of waterproof material, insulated underneath and at the edges to prevent heat losses. The dimensions of the absorber are 1180 x 380mm and of the air cooler are 700 x 500 x 200mm. The volume of the storage tank is $0.3m^3$ and it is able to operate for 24 hours without any solar radiation. The unit can provide a cooling capacity of 5KW under extreme tropical conditions.

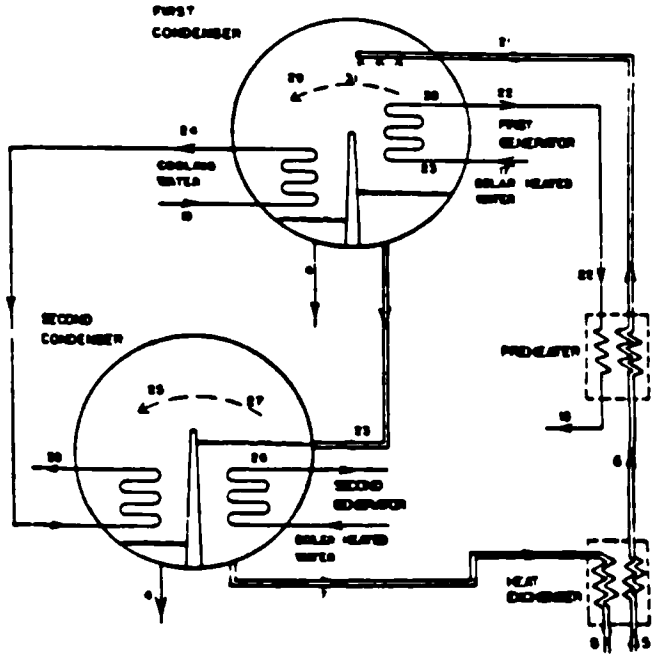

Fig. 3.6 Schematic diagram of auxiliary generator in the two-shell configuration, reproduced from Grossman et al (82)

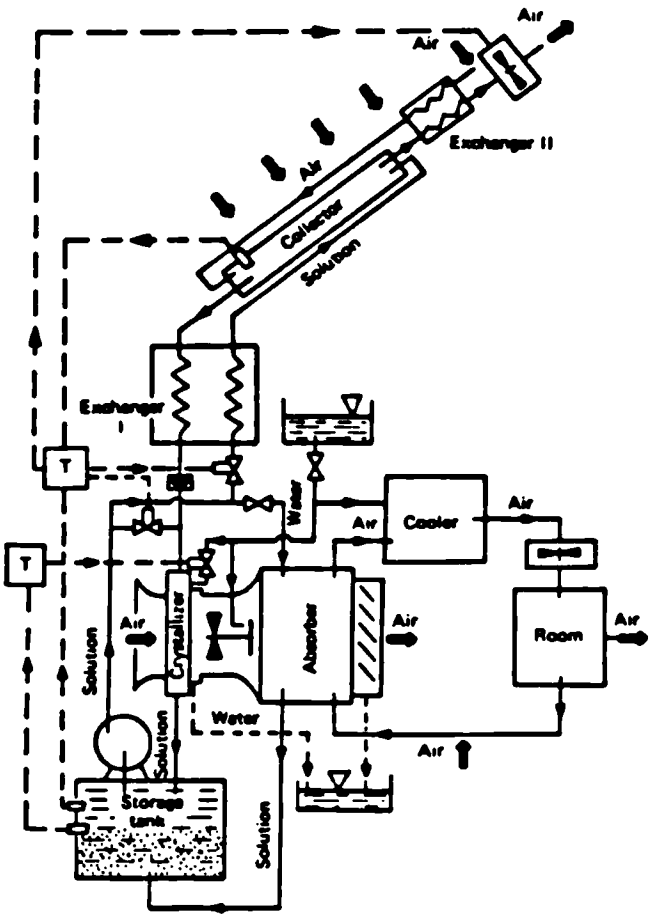

Fig. 3.7 Air conditioning system flow diagram, reproduced from Gutkowski and Ryduchowski (85)

The coefficient of performance for the system is within the range 0.4 - 0.8 and the temperature of cooled air leaving the cooler is between 21.5 and 15°C, for a wet bulb temperature ranging from 22 to 34°C. The desorption temperature is within the range of 47 to 66°C. Gutkowski and Ryduchowski claimed that the overall efficiency of the system, defined as the product of the Coefficient of Performance and the solar collector coefficient of thermal efficiency was the highest of all the presently known systems.

Chapter Four

4.0 Determination Of The Thermodynamic Properties Of The Solutions

In order to effectively evaluate a working solution for an absorption system, a knowledge of the thermal and physical properties is essential. Thermodynamic properties such as vapour pressure, specific heat capacity and solubility characteristics are necessary to fully understand the driving potential of the system. Thermophysical properties such as thermal conductivity, viscosity , relative density and surface tension are also essential for better understanding of heat and mass transfer processes within the system. Whilst it is desirable to have a complete knowledge of these properties for any working solution, the availability of thermodynamic data that can be presented in enthalpy/concentration and pressure/temperature diagrams is most helpful as a starting point for new working solutions.

The main objective of this investigation is the utilisation of solar energy for an absorption refrigeration system. In view of the high cost of solar energy collection with concentrating devices, flat-plate collectors with collector temperatures of the order of 93°C and below are preferred. The low

temperature level of energy collection associated with flat-plate collectors, therefore requires that a refrigerant- absorbent combination should satisfy the following conditions.

i) There should be high solubility of the solute in the solvent. The use of a mixture of high solubility could allow for a higher difference between the concentrations of the strong and weak solutions leaving the generator and absorber respectively. This could reduce the solution circulation factor, increase the temperature lift and reduce the heat load in the generator.

ii) A solution of high solubility will allow the cooling down of the strong solution leaving the generator to a temperature nearer the absorber temperature without crystallisation of salts. This could improve the performance of the heat exchanger and can in effect reduce the heat load in the generator.

iii) The refrigerant and absorbent should be non-toxic, non-inflammable, non-corrosive, cheap and readily available.

The $LiBr-H_2O$ system which has been favoured over the NH_3-H_2O system for low temperature heat application, should have been useful here except that the first two conditions which are functions of salt solubility are not met. A new refrigerant-absorbent combination that

has evolved from this research work, which satisfies the above conditions is $(2LiBr-ZnBr_2)/H_2O$. In the following sections, the measurements of such properties as solubility, boiling point at atmospheric pressure, vapour pressure and the specific heat of this solution is described. The generation of the pressure/ temperature and the enthalpy/concentration diagrams are also described for the solution.

4.1.0 Solubility Measurements

One of the most serious problems of the $LiBr-H_2O$ system is the crystallisation of salt in the strong solution return line to the absorber. The solubility of lithium bromide in water is low at low temperatures hence an attempt to cool a highly concentrated solution to nearer the absorber temperature could result in salt crystallisation which could cause stoppages in the solution circuits and result in loss of efficiency.

In this study, the possibility of improving the solubility of lithium bromide in water was investigated. A solubility apparatus was designed and constructed and zinc bromide, which was known to improve the solubility of lithium bromide in methanol, was tested in the lithium bromide-water system to determine the temperature and concentration at which crystallisation occurs. The solubility of lithium bromide in water was also measured and the results compared with published data, to check the accuracy of

the apparatus.

A solution stability test was carried out by comparing solutions of $LiBr+ZnBr_2$ in water, of different molar ratios and mass fractions and observing them over some time. The first solution with salts mass fraction of 69.73% had a molar ratio of 7.1:1. The second solution with salts mass fraction of 68.9%, had a molar ratio of 8.6:1 whilst the third solution with salts mass fraction of 75.0% had a molar ratio of 2:1. After one day, some salt crystals appeared in the first solution. After three days, salt crystals appeared in the second solution. In the case of the third solution, however, the solution remained liquid even after four days under atmospheric conditions. The result of these tests shows that stable high concentration solutions should be of low molar ratio. The result falls in line with those of past investigators who have used two moles of Lithium bromide plus one mole of zinc bromide in methanol as an experimental absorption working fluid (25, 78). The same approach has been followed inthis work by using two moles of Lithium bromide and one mole of zinc bromide in water.

4.1.1 Apparatus

In solubility measurements, an accurate determination of the saturation concentration of the solution is essential whilst the solution temperature should be kept constant for any specific measurement. To maintain

a constant solution temperature, an insulated oil bath was designed and constructed and the bath temperature was maintained to within ± 0.2°C of the nominal temperature under investigation by the combined operation of a contact thermometer, an immersion heater and an electric motor driven stirrer. Figure 4.1 shows the schematic diagram of the solubility apparatus. A second thermometer was used for more accurate checks on the bath temperature whilst another thermometer (not shown in the diagram) was inserted inside the solution cell to constantly check the solution temperature.

Liquid paraffin was used in a pyrex glass beaker, 210mm internal diameter and 265mm deep. The beaker was placed inside a rectangular shaped wooden box, 280mm x 275mm x 300mm high with a viewing window, 50mm wide and 260mm deep, covered with a 3.2mm thick clear perspex so that the content of the solution cell could be easily viewed during the experiment. The space between the box and the glass beaker was filled with fibre glass insulating material, except the viewing window.

The contact thermometer and the immersion heater were connected to a relay switch. The contact thermometer used was a 0-100°C x 1°C, direct reading,adjustable, mercury filled and sealed, with an accuracy of±0.1°C over its measurement range. It had two opal glass scales, the upper scale for setting the required temperature and the lower one for indicating the temperature. The contact thermometer was used to

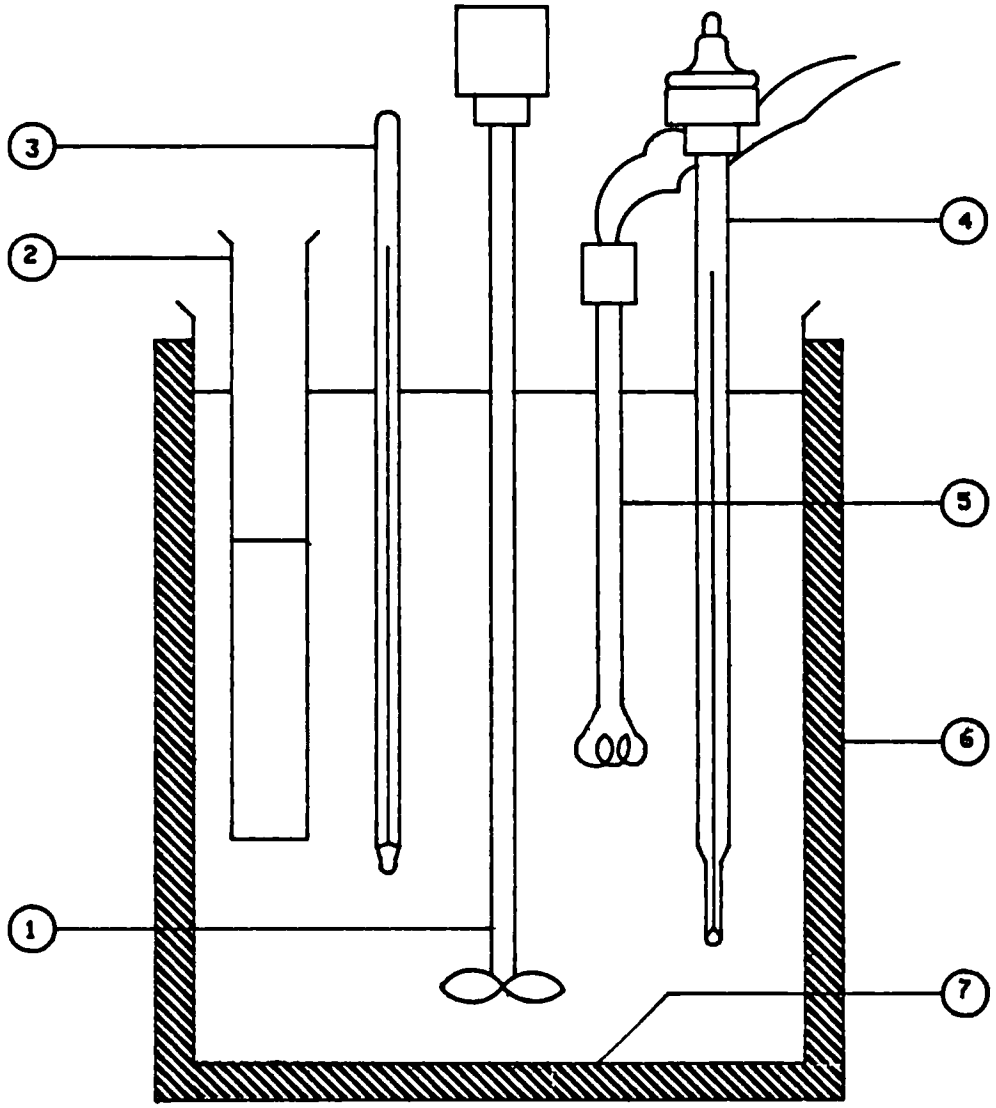

1 - STIRRER

2 - SOLUTION CELL

3 - THERMOMETER

4 - CONTACT THERMOMETER

5 - ELECTRIC HEATER

6 - WOODEN BOX

7 - INSULATED GLASS BEAKER

FIG. 4.1 - THE SOLUBILITY APPARATUS.

operate the relay which cuts in and out, the electrical supply to the heater as required by the setting of the thermometer. The relay and inverter circuits were enclosed in a die cast box, and a neon bulb visible from outside was fixed in the circuit to indicate when the heater was switched on or off. Once the bath temperature was raised to the desired level, the heater was switched off. It would be automatically switched on again only when the bath temperature dropped to about 0.1°C below the preset temperature on the contact thermometer.

The stirrer was used to agitate the oil in the bath so as to maintain a uniform temperature within the bath.

4.1.2 Experimental Procedures

Normal solubility measurements

Saturated solutions of lithium bromide and water, then the mixture of the two moles of lithium bromide, one mole of zinc bromide and water, were prepared using the apparatus described above (Figure 4.1) and the salt concentration for each prepared solution at temperatures of 25°C, 40°C, 60°C and 80°C were found.

a) Lithium Bromide in Water

An amount of distilled water was put in the solution

cell (2), placed in an oil bath whose temperature was raised to the desired level. A small amount of anhydrous lithium bromide salt was added at a time to the distilled water in the solution cell and the solution stirred with a glass rod until the salt had completely dissolved. At first the solution temperature was observed to be higher than the preset bath temperature because of the heat of mixing of the solution but as more salt was added, the temperature dropped. The process of adding more salt a little at a time and stirring was continued until saturation point was reached whence no more salt could go into the solution. At this point, the solution temperature was again checked to make sure it was within±0.1°C of the desired value. Stirring of the solution was continued for some time, then allowed to settle for about 2-3 hours.

A 10ml pipette was then used to draw two samples of clear solution into two preweighed 25ml flasks and closed with rubber stoppers. The flasks were allowed to cool down to room temperature and reweighed to find the weight of the sampled solution. The flasks were then placed on a 1000W, variable output, Barlow Whitney,process heater type HP10/V and the water evaporated slowly from the solutions. The rubber stoppers were replaced, the flasks removed from the heater and allowed to cool to room temperature , then reweighed to within 0.0001gram using a Mettler H311 type weighing machine. The weight of the dry salt in

each flask was found and the concentration of lithium bromide in the solution was calculated at that solution temperature. The concentrations found in these cases were found to be generally quite close but the average of the total samples was taken as the solution concentration at that temperature.

Another sample was taken and the concentration found as above, to compare with the result of the first samples. Generally, there was good agreement between sample results.

The bath temperature was then raised and more salt added to the solution in the cell and stirred to obtain a saturated solution at the new temperature. The process of sample taking and evaporation was repeated to find the concentration at that temperature. To prevent crystallization of samples inside the pipette when taking highly concentrated samples at higher temperatures, the pipette was preheated prior to sample taking at temperatures from 40°C and above.

b) Lithium Bromide plus Zinc Bromide in Water

In preparing a saturated solution of lithium bromide plus zinc bromide in water, an amount of the salts made up of two moles of lithium bromide and one mole of zinc bromide was put inside the solution cell then placed inside the oil bath maintained at the predetermined temperature. Distilled water was added a little at a

time to the salt mixture and stirred until a saturated homogeneous solution was obtained at the set temperature. The solution was then allowed to settle for about three hours.

The same method used for lithium bromide-water solution was used to obtain the concentration of lithium bromide plus zinc bromide in the solution.

4.1.3 Results

Solubility measurements were made of lithium bromide in water and of two moles of lithium bromide plus one mole of zinc bromide in water within a temperature range of 25°C and 80 °C to determine the temperatures and concentrations at which crystallisation occurred. In each case, measurement was made at four selected temperatures between 25°C and 80°C (inclusive). The experimental data for lithium bromide in water, shown in Table 4.1 were fitted to obtain the equation:

$$\%_L = A + Bt + Ct^2 + Dt^3 \qquad (4.1)$$

where A = 47. 734028

B = 0. 783407

C = -1. 207435E-2

D = 6. 638527E-5

$\%_L$ = the mass fraction of lithium bromide in the solution, %

t = the solution temperature, °C

Table 4.2 shows the comparison of the experimental data with those of McNeely (80) and Lower (79) also shown graphically in Figure 4.2. There is better agreement with McNeely's data with the maximum deviation in the region of 1.0%. There is reasonably good agreement between the experimental data and those of Lower with maximum deviation been 6.5%. Lower's values, however, seem generally quite high as it is not practicable to obtain acqueous lithium bromide solutions with salt concentrations much higher than 61% at 25°C solution temperature.

Table 4.3 shows the experimental data for the solubility of ($2LiBr + ZnBr_2$) in water, also shown graphically in Figure 4.3. These data were fitted to obtain the equation:

$$\%_{L,Z} = a + bt + ct^2 + dt^3 \qquad (4.2)$$

where a = 64. 983119

b = 0. 920664

c = -1. 604707E-2

d = 9. 790041E-5

$\%_{L,Z}$ = the mass fraction of lithium bromide plus zinc bromide in the solution, %

t = the solution temperature, °C

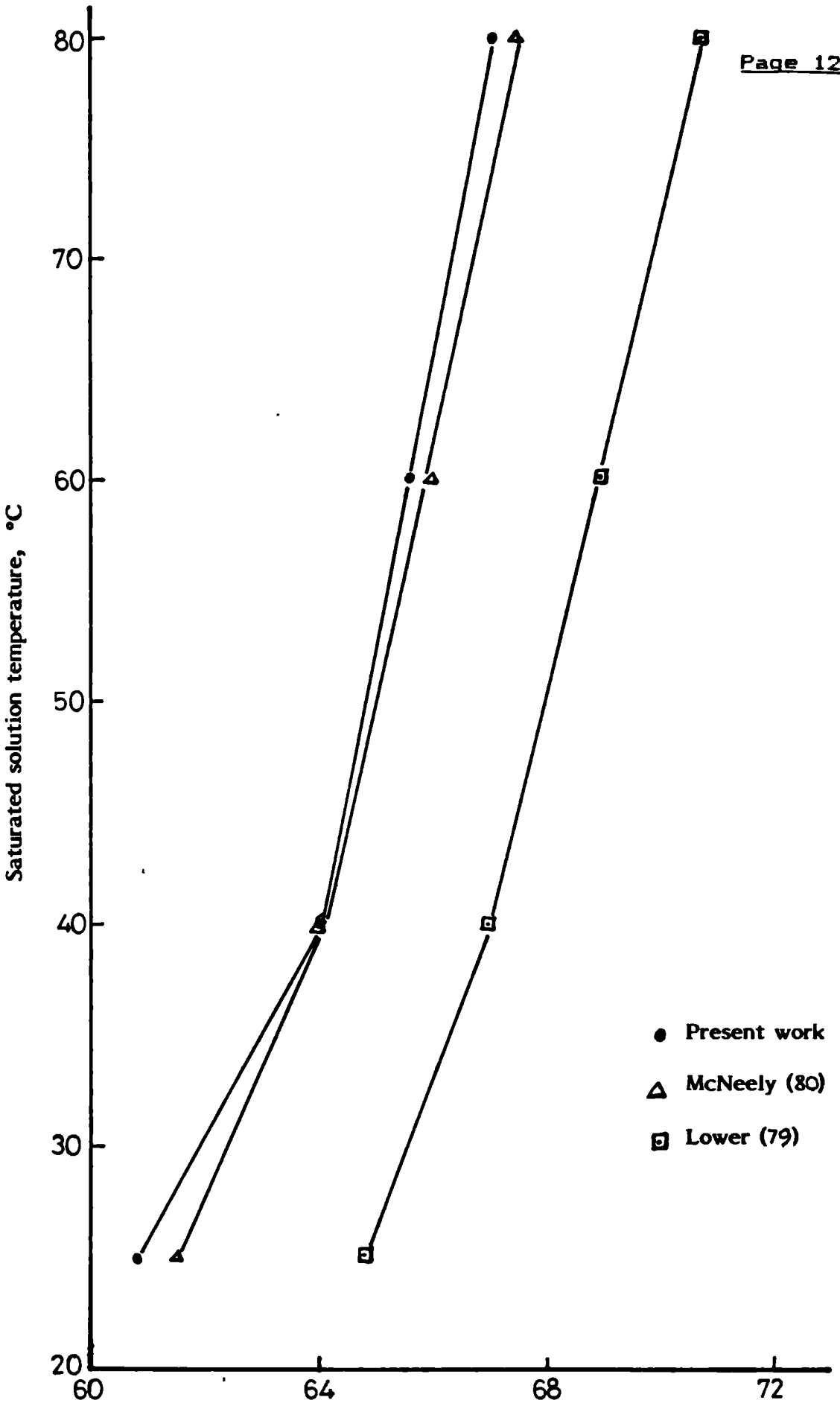

Fig. 4.2 Solubility of LiBr in water

The saturated solution concentrations for solution temperatures from 20° to 100°C are calculated in steps of 10° using equation 4.2 and the results shown in Table 4.4. Whereas extrapolation of data are more reliable at higher temperatures, it is not very reliable at temperature ranges lower than the experimental minimum.

Table 4.5 shows the comparison of the solubility of (2LiBr + $ZnBr_2$) in water and Vamvakidis's (28) measurements in methanol. This comparison, including that of LiBr - H_2O solution is also shown graphically in Figure 4.4. The (2LiBr + $ZnBr_2$)/CH_3OH solution shows only slightly higher solubility than LiBr - H_2O solution at saturated solution temperatures below 60°C. However, the (2LiBr + $ZnBr_2$)/H_2O solution shows a markedly higher solubility than both LiBr - H_2O and (2LiBr + $ZnBr_2$)/CH_3OH solutions over the entire temperature range investigated.

With the solubility characteristics displayed by the (2LiBr + $ZnBr_2$)/H_2O solution, it is expected that a lower solution circulation rate will be possible in the system and the strong solution from the generator can be cooled to temperatures nearer that of the absorber without crystallisation of salts in the lines. The cumulative effect of these will be a reduced heat load on the generator thus resulting in higher heat ratios. Cooling may also take place at relatively lower generator temperatures, the heat requirement of which the conventional flat-plate solar energy collector may supply.

Saturated Solution Temperature (0°C)	Solution Concentration ξ_L, (%)
25	60.81
40	64.00
60	65.61
80	67.12

Table 4.1 - Experimental data for the solubility of lithium bromide in water.

Saturated Solution Temperature °C		25	40	60	80
Solution Concentration = $\frac{m_L}{m_L+m_w}$ %	$LiBr/H_2O$ Present investigation	60.81	64.00	65.61	67.12
	$LiBr/H_2O$ (McNeely 1979) (Ref 80)	61.5	64.00	66.00	67.5
	$LiBr/H_2O$ (Lower - 1960) (Ref 79	64.80	67.00	69.0	70.8

Table 4.2 Comparison of the solubility of lithium Bromide in water

Saturated Solution Temperature °C	Solution Concentration $\xi_{L,Z}$, (%)
25	79.50
40	82.40
60	83.60
80	86.06

Table 4.3 Experimental Data for the solubility of (2LiBr +$ZnBr_2$) in water

Saturated Solution Temperature, (°C)	Solution Concentration $\xi_{L,Z}$, (weight %)
20	77.76
30	80.80
40	82.40
50	83.14
60	83.60
70	84.38
80	86.06
90	89.23
100	94.48

Table 4.4 Solubility of (2LiBr +$ZnBr_2$) in water

Saturated Solution Temperature °C		25	40	60	80
Solution Concentration (%)	$\underline{2LiBr + ZnBr_2}$ / $2LiBr + ZnBr_2 + H_2O$ (Present Investigation)	79.5	82.4	83.6	86.06
	$\underline{2LiBr + ZnBr_2}$ / $2LiBr+ZnBr_2+CH_3OH$ (Vamvakidis (28))	63.0	64.80	67.07	73.28

Table 4.5 Comparison of the solubility of $2LiBr + ZnBr_2$ in water and in methanol.

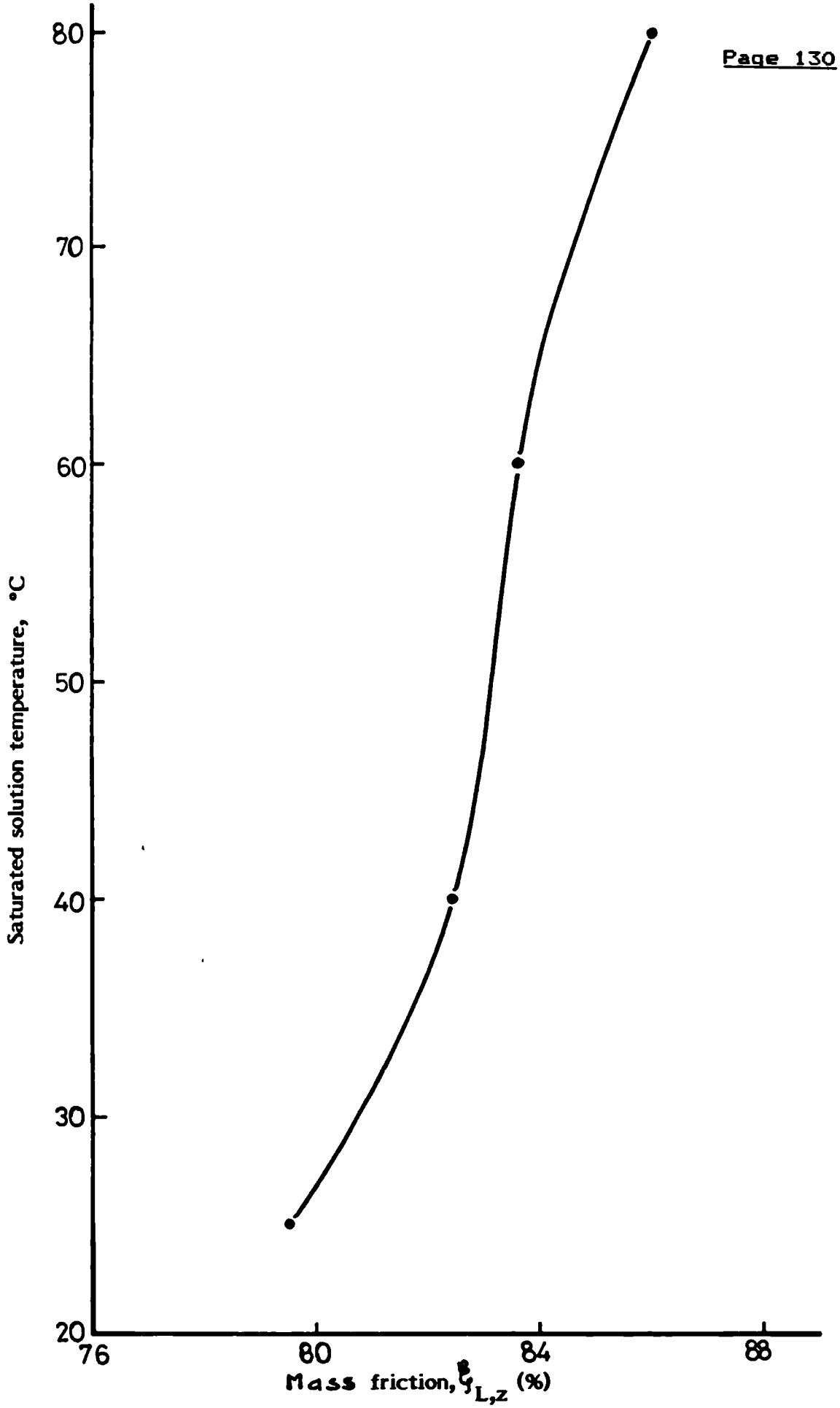

Fig. 4.3 Solubility of ($2LiBr + ZnBr_2$) in water

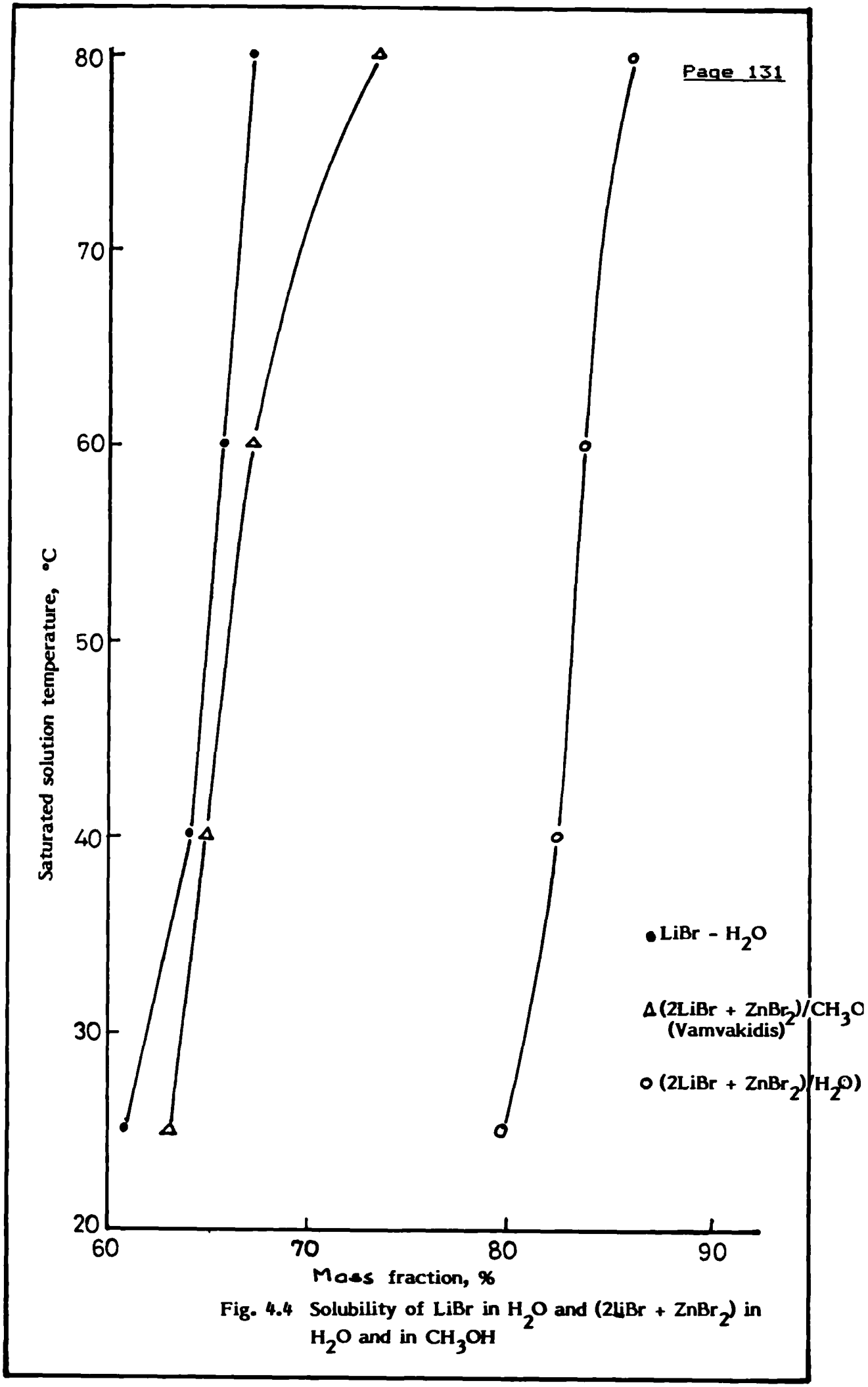

Fig. 4.4 Solubility of LiBr in H_2O and ($2LiBr + ZnBr_2$) in H_2O and in CH_3OH

4.2.0. Boiling Point Measurements

Following the encouraging results of solubility measurements of (2LiBr + $ZnBr_2$) in water, it was proposed to measure the normal boiling points at salt concentrations ranging from 50% to 75% by weight for this solution and for (LiBr + Licl)/H_2O solution to indicate which would be worth investigating more fully for vapour pressure. The activity if the solvent in a solution can be determined from the measurement of the rise in boiling point.

For a pure liquid, the true boiling and condensation temperatures are equal but for a solution the condensation temperature differs from the boiling temperatures owing to fractionation. An apparatus was therefore designed and made to measure the boiling point of LiBr-H_2O solutions and the results compared with those of Pennington (29), to check the accuracy of the apparatus and method. The same apparatus was used to measure the boiling point of (2LiBr + $ZnBr_2$)/H_2O and (LiBr + Licl)/H_2O solutions.

4.2.1 Boiling Point Apparatus

It is more difficult to determine the boiling temperature of a solution than that of a pure liquid. For a pure liquid, the condensing temperature can be simply determined by a thermometer in the condensing vapour and this temperature taken as the boiling point.

However,for a solution, the condensing temperature can differ from the boiling temperature by up to 37°C at certain concentration.

A boiling liquid is generally superheated by the heating device used, because it boils under the pressure at the surface plus the hydrostatic pressure at the level in the liquid at which the temperature is measured. In the determination of boiling point of a solution, the thermometer must be in contact with solution rather than with condensed vapour and the elimination of superheating of the liquid is of paramount importance (86). The first requirement was accomplished by the use of the Cottrell principle whereby the thermometer was hung in the vapour above the solution and a stream of boiling liquid was sprayed on the thermometer above the bulb by a simple vapour pump. The liquid on emergence from the pump was slightly superheated. However,on flowing down the thermometer it very quickly comes to equilibrium with the surrounding vapour, cooling slightly by evaporation. The liquid from the bulb is therefore at its true boiling point. Overheating was minimised by heating the distilling flask in an electrically heated beaker of oil.

The all glass apparatus shown in Figure 4.5 and in Plate 4.1 consisted basically of a round bottomed distilling flask, a condenser, the vapour pump and the heating devices.

The round bottom distilling flask which held the solution had a 19/26 ground glass joint on the side for connecting the condenser and a 60/46 ground glass joint at the top to hold the cover on which the vapour pump was mounted through an inner tube. The condenser, made of an 18mm outside diameter inner and a 40mm outside diameter outer glass tube with vapour flowing through the inner tube and cooling water through the annulus, condensed the vapour and the condensate returned to the flask. The flask cover consisted of a central 14/23 ground glass joint with two others, each of 10/19 ground glass joint. The three connections were covered by glass stoppers. The two side connectors provided access to withdraw a portion of the solution for concentration checks during the experiment. The central connection had the inner glass tube attached to the underside and the glass stopper was made to take a calibrated thermometer used in measuring the boiling point of the solution ensuring that the thermometer was submerged in the solution vapour. The vapour pump was attached to the bottom of the inner glass tube which acted as a radiation shield and prevented the cold condensate return from getting onto the thermometer.

The vapour pump consisted of an inverted funnel with a central tube and three vertical spouts. When assembled, the inverted funnel just cleared the bottom of the flask, immersed inside the solution. The funnel was to catch the bubbles of vapour and direct them through the central tube to the spouts. In so doing, three sprays of the mixture of solution and vapour were directed to the stem of the thermometer, any superheated solution came to equilibrium with the vapour by the time it got to the thermometer bulb.

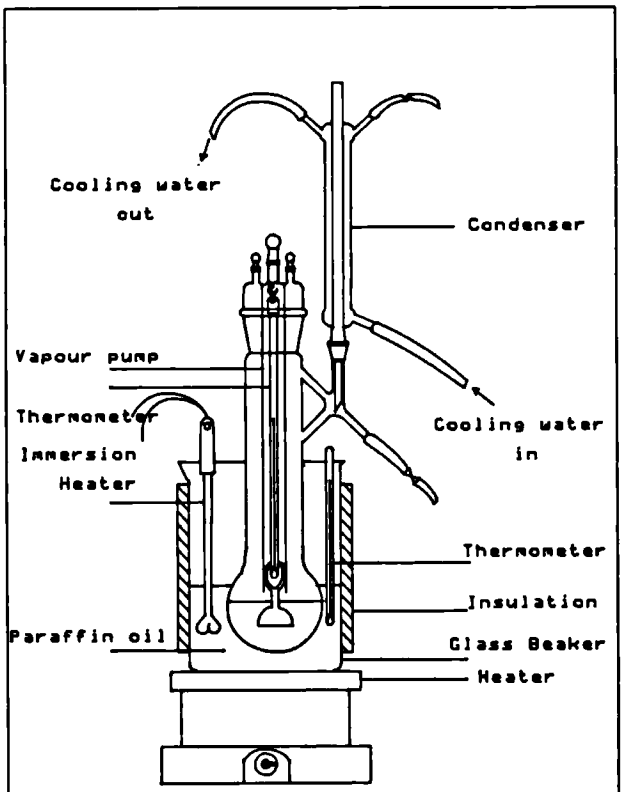

Fig. 4.5 - The Boiling Point Apparatus.

Plate 4.1

The Boiling Point Apparatus

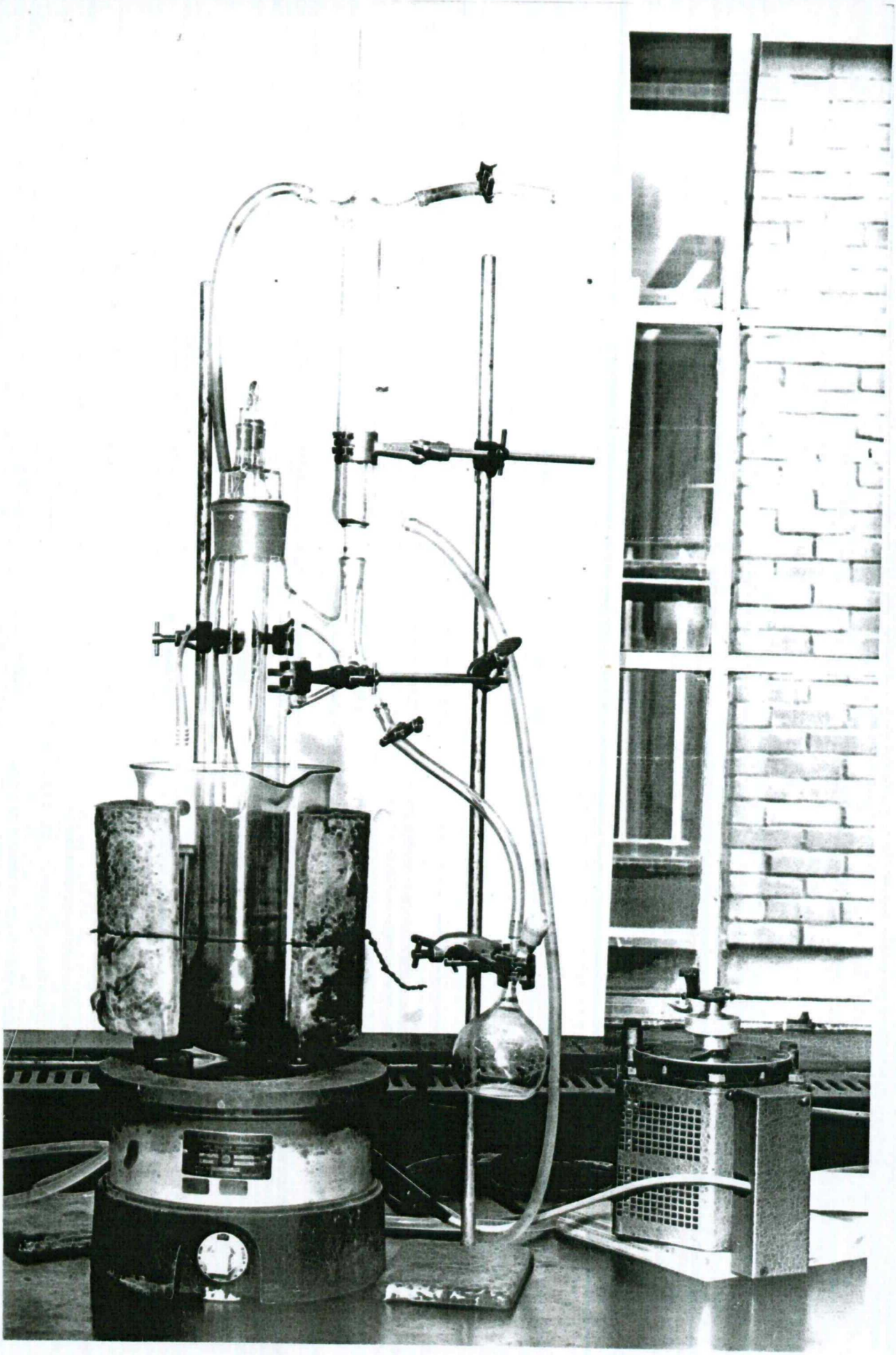

The distilling flask, condenser and vapour pump were mounted vertically on retort stands inside an insulated oil bath consisting of a pyrex glass beaker, 210mm i.d and 265mm deep, filled with a high boiling point Shell Thermia B oil. Heating of the bath and thus the solution was provided by a variable power Barlow Whitney process heater type HP 10/V, in conjunction with a 1KW immersion heater operated through a variac. A calibrated high temperature range thermometer was used to measure the temperature of the oil bath which was much higher than the boiling temperature of the solution in the flask. Some pieces of porcelain rings were placed in the solution during heating to avoid bumping.

4.2.2 Experimental Procedure

Concentrated solutions of $LiBr/H_2O$, $(LiBr + ZnBr_2)/H_2O$ and $(LiBr + LiCl)/H_2O$ respectively, were prepared before each boiling point measurement.

A sufficient quantity of solution to submerge the inverted funnel of the vapour pump was placed in the distilling flask and the cover was replaced. The heaters were turned on and regulated to steadily but slowly raise the oil bath temperature and hence that of the solution to boiling temperature. When equilibrium

was reached, characterised by a slight fluctuation of the temperature about a mean value for at least fifteen minutes, the temperature of the submerged thermometer and the barometer reading in the room were taken.

As boiling progressed, some portion of the vapour was condensed in the condenser and the condensate returned to the distilling flask. However, since the whole vapour given off could not be condensed as the condenser vapour line was open to the atmosphere, the concentration of the solution should vary. Hence at the instant of taking the temperature and pressure readings, a portion of the solution was also taken and the concentration measured by evaporating the water in the sample.

For LiBr/H_2O solutions, the normal boiling temperature were measured for five mass fractions between 53 and 62%. For (%LiBr + $ZnBr_2$)/H_2O solutions, thirteen measurements were made for mass fractions ranging between 50% and 73%, whilst for (LiBr + Licl)/H_2O solutions, only four measurements were made for mass fractions between 51% and 58% because of poor solubility.

The boiling temperatures were corrected for the thermometer calibrations as well as for variations in atmospheric pressure. The method used in the correction for pressure variations is shown in Appendix A.

4.2.3 Results

i) $LiBr/H_2O$ solution.

The experimental data for the boiling points of $LiBr/H_2O$ solution was plotted as shown in Figure 4.6. This shows a straight line relationship with the smoothing equation given as:

$$t = 2.8448 + 2.5517\S_L \qquad (4.3)$$

where: t = boiling temperature, °C

$\S_L$ = mass fraction of LiBr in water, %.

Table 4.6 shows a comparison between the observed and the smoothed data calculated from equation 4.3. Apart from the boiling temperature for the 56.13% salt concentration which was clearly off the fitting straightline, the maximum deviation between the observed and smoothed data was 0.24°C and even this was at an end point, to which in experimental work, less weight should be given than to the other points of the plot (87). Table 4.7 shows the smoothed values of boiling temperatures for solution mass fractions in the range between 50% and 70%.

ii) $(2LiBr + ZnBr_2)/H_2O$ Solution

The experimental data for the $(2LiBr + ZnBr_2)/H_2O$ solution was plotted as shown in Figure 4.7 to indicate the best fit. For the purpose of interpolation, however, the following quadratic

smoothing equation was obtained using a polynomial fitting computer programme:

$$t = A_1 + B_1 \xi_{L,Z} + C_1 \xi_{L,Z}^2 \qquad (4.4)$$

where A_1 = 267.0281143

B_1 = -6.8707891

C_1 = 7.3043843E-2

t = the boiling temperature of the solution, °C

$\xi_{L,Z}$ = the mass fraction of lithium bromide and zinc bromide salts in solution, %.

Solution concentration ξ_L , (weight %)	Boiling Temperature (°C)		Deviation (K)
	Observed	Calculated from equation 4.3	
53.47	139.48	139.28	-0.2
55.96	145.49	145.64	+0.15
56.13	149.50	146.07	-3.43
58.52	152.02	152.17	+0.15
61.72	160.58	160.34	-0.24

Table 4.6. Comparison of observed and smoothed data for the boiling point of $LiBr/H_2O$ solution.

Solution Concentration ξ_L , (weight %)	Boiling Temperature (°C)
50	130.4
52	135.5
54	140.6
56	145.7
58	150.8
60	155.9
62	161.1
64	166.2
66	171.3
68	176.4
70	181.5

Table 4.7 Boiling point of $LiBr/H_2O$ solution.

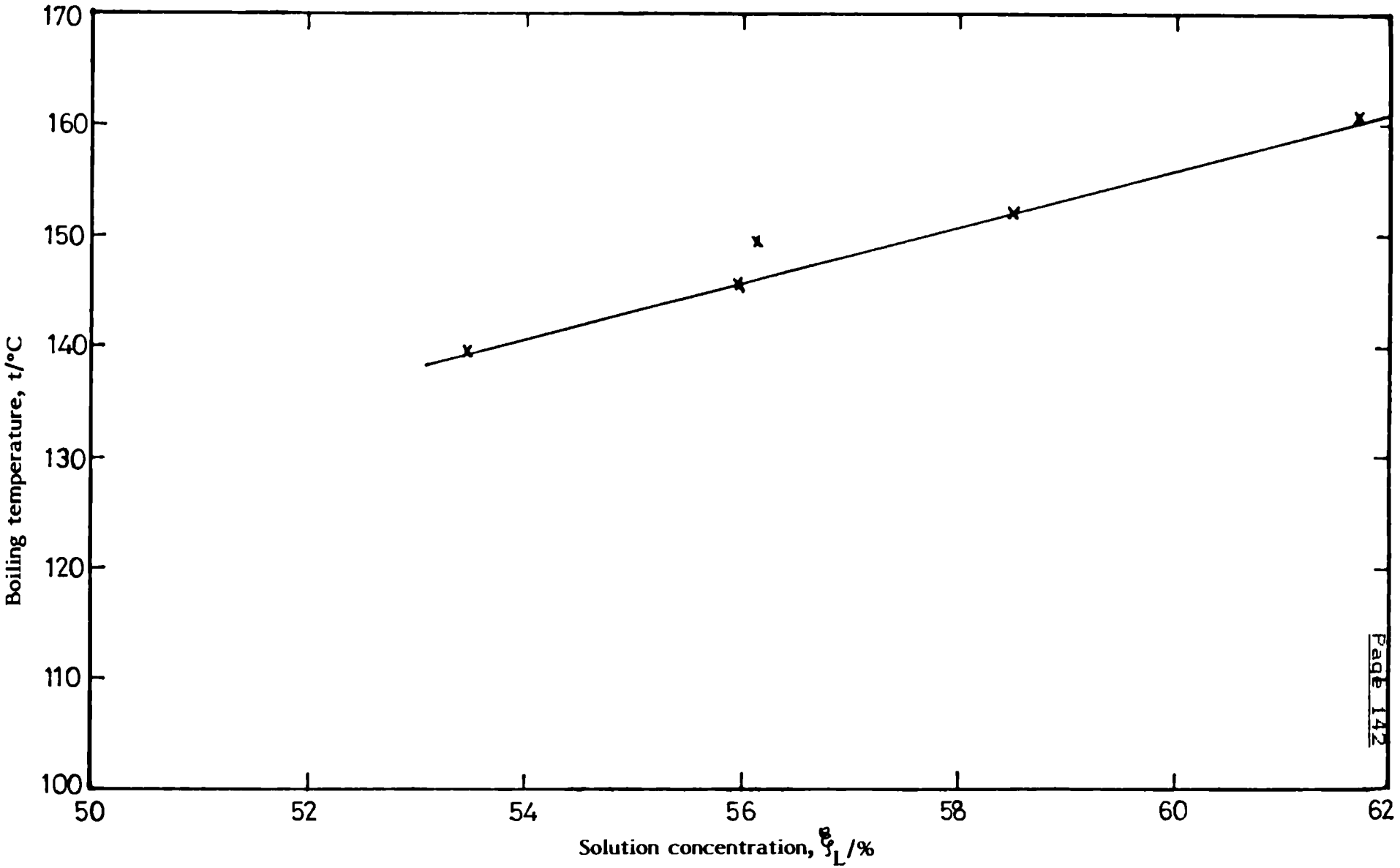

Fig. 4.6 Boiling temperature Vs solution concentration for LiBr - H_2O solution

olution Concentration ξ_L, (weight %)	Boiling temperature (°C)		Deviation (K)
	Present Investigation	Fennington Data	
50	130.4	131.9	-1.5
54	140.6	140.7	-0.1
58	150.8	150.2	+0.6
62	161.1	160.7	+0.4
66	171.3	173.4	-2.1
68	176.4	181.7	-5.3

Table 4.8 Comparison of $LiBr/H_2O$ Solution Boiling Point data compared with those of Pennington (29).

Solution Concentration $\xi_{L,z}$ (weight %)	Boiling temperature (°C)		Deviation (K)
	observed	calculated from equation 4.4	
51.96	107.94	107.23	-0.71
53.06	109.26	108.11	-1.15
57.89	111.88	114.07	+2.19
59.27	114.50	116.32	+1.82
61.57	117.17	120.81	+3.64
62.59	123.50	123.14	-0.36
62.71	124.41	123.41	-1.00
64.11	129.95	126.76	-3.09
65.94	133.31	131.57	-1.74
67.15	137.54	135.02	-2.52
70.22	142.28	144.73	+2.45
71.87	149.86	150.52	+0.66
73.02	154.86	154.79	-0.07

Table 4.9 Comparison of observed and smoothed data for the Boiling Point of $(2LiBr + ZnBr_2)/H_2O$ Solution.

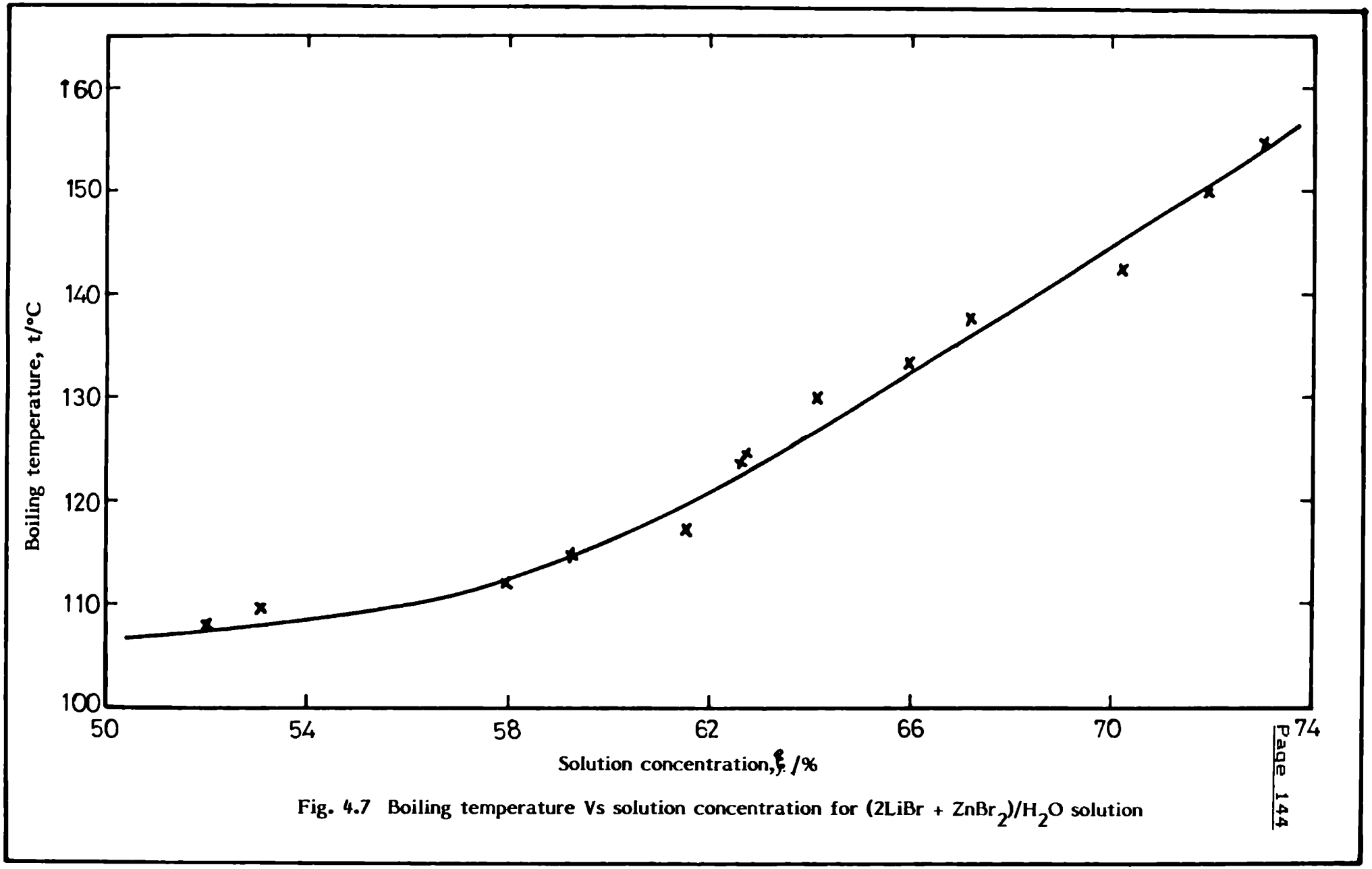

Fig. 4.7 Boiling temperature Vs solution concentration for (2LiBr + $ZnBr_2$)/H_2O solution

Table 4.9 shows the comparison of the observed results with the smoothed data calculated from equation 4.4. The maximum deviation was 3.64°C over a concentration range between 51.96% and 73.02% lithium bromide and zinc bromide salts by weight.

The boiling point of the solution was calculated for concentration range between 50% and 80% of salts by weight and the results shown in Table 4.10. The boiling temperatures of the (2LiBr + $ZnBr_2$)/H_2O solution are observed to be in general relatively lower than those of LiBr/H_2O solution for the concentration range investigated. The boiling points, however, increases with increase in concentration.

iii) (LiBr + Licl)/H_2O solution

The boiling point of (LiBr + Licl)/H_2O solution was also investigated to find out if it could be a better candidate than the (2LiBr + $ZnBr_2$)/H_2O solution. The result is shown in Table 4.11. The investigation was, however, not pursued further because of poor solubility of the salts in water. It was not possible to obtain solution concentrations higher than 58%. This solution, however, boils at slightly higher temperatures than the LiBr/H_2O solution at same concentrations.

Solution concentration (β_{LiBr}, weight %)	Boiling temperature (°C)
50	106.1
52	107.3
54	109.0
56	111.3
58	114.2
60	117.7
62	121.8
64	126.5
66	131.7
68	137.6
70	144.0
72	151.0
74	158.6
76	166.7
78	175.5
80	184.8

Table 4.10 Boiling Point of (2LiBr + $ZnBr_2$)/H_2O Solution.

Solution Concentration (weight %)	Boiling temperature (°C)
51.63	146.16
51.94	147.26
54.89	153.82
57.98	154.98

Table 4.11. Experimental data for the boiling point of (LiBr + Licl)/H_2O Solution

4.2.4 Accuracy of Results

The main sources of error in these experiments are in the temperature and concentration measurements. To minimise the error in temperature measurements, the mercury-in-glass thermometers used were calibrated at the National Physical Laboratory and it was ensured that the one for measuring the boiling temperatures was completely immersed in the solution vapour. Temperature measurements were made to within 0.1°C. Such error for example would represent 0.2% and 0.6% respectively for the boiling point elevation at 60% salt concentration by weight for $LiBr/H_2O$ and ($LiBr + ZnBr_2$)/H_2O solutions.

In determining he concentration of the solutions, water was evaporated and the cooled, dried salts in 25ml conical flasks weighed to within 0.01 gram. In all the cases, the samples extracted for concentration measurements were a homogeneous liquid. Electric heating of the flask was slow to avoid splashing of solution. Rubber stoppers were also used to close the flasks just before removing them from the heater and weighing was done only when the flask had cooled to room temperature to avoid the effect of any variation in the buoyancy of the flask with temperature. The variation of the internal environmental temperature was low enough to neglect the effect of buoyancy of the flask.

As earlier mentioned, corrections were made for the variation in atmospheric pressure. This amounted to a maximum of 0.42°C and 0.51°C for the $LiBr-H_2O$ solution and the $(LiBr + ZnBr_2)/H_2O$ solution respectively.

The experimental boiling point data for the $LiBr/H_2O$ solution for this investigation and those of Pennington (29) were plotted together in Figure 4.8. These data also show a straight line relationship. The maximum deviation of Pennington data was 1°C whilst the maximum deviation for this investigation was 2.5°C, neglecting the data point at $\%_L^B$ = 56.13% which is assumed to be ill-determined. The smoothed data were also compared in the concentration range between 50% and 68% by weight. This comparison is shown in Table 4.8. There was better agreement for solution concentrations between 50% and 62% (the experimental range), with a maximum deviation of 1.5°C. However, at higher concentrations, Pennington's data were relatively high thus resulting in a maximum deviation of about 5.3°C at 68% concentration. Pennington, however, did not indicate whether corrections were made for variations in atmospheric pressure during his measurements. There is no data in the literature to compare the results of the $(2LiBr + ZnBr_2)/H_2O$ and $(LiBr + LiCl)/H_2O$ solutions with.

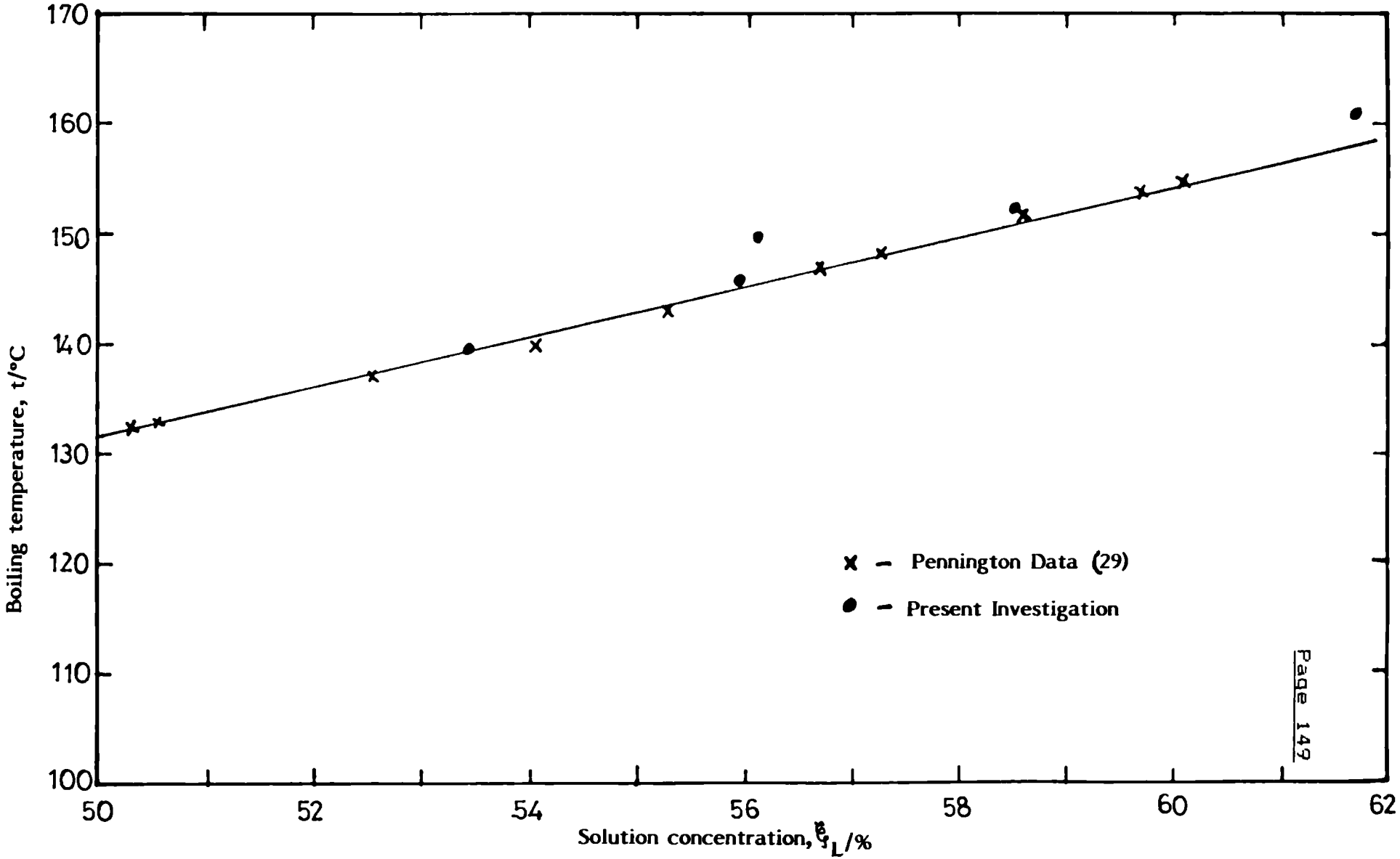

Fig. 4.8 Boiling temperature Vs solution concentration for experimental data of the Present Investigation and Pennington's for $LiBr/H_2O$ solution

4.3.0 Vapour Pressure

The vapour pressure of a solution is an equilibrium property from which other thermodynamic properties required for the evaluation of new working fluids for absorption refrigeration systems can be calculated. Solution properties such as the heat of dilution and enthalpy can be calculated from vapour pressure data.

The methods used for vapour pressure measurements can be classified as static or dynamic. In static methods, the liquid is contained in a bulb connected to a mercury manometer and a vacuum pump and the pressure measured directly or indirectly. Dissolved air or other permanent gases are the greatest sources of error in this method. In dynamic methods, the boiling points of the liquid is determined at a series of pressures.

In this investigation, an apparatus was designed and constructed to measure the vapour pressure of the promising solution, $(2LiBr + ZnBr_2)/H_2O$, based on the static method. Because there is no known data in the literature on this solution, the apparatus was used to measure the vapour pressure of distilled water and the results compared with published data to check the accuracy of results obtained by the apparatus. A full description of the method used in this investigation is given in the following sections.

4.3.1. Apparatus

The major sources of error in the static method of vapour pressure determination are:

i) temperature errors arising from the difficulty of adequately stirring a tall bath full of liquid.

ii) pressure measurements are usually uncertain as every part of the mercury column is normally not held at the same temperature as the vapour chamber.

iii) impurity of the substances, as gases and moisture from the air may be absorbed or dissolved in the solution or adhere to the walls of manometer tubes.

These sources of error were carefully considered in the design of the vapour pressure apparatus. To take care of the first two problems, a smaller U-tube manometer containing a confining liquid was incorporated between the solution cell and the mercury manometer that indirectly measured the pressure of the solution. This U-tube manometer was easily submerged in a smaller oil bath where effective stirring was possible and the temperature was kept to within $\pm 0.1^{\circ}C$ of the nominal value. Provisions were made to evacuate he system to 0.03mm Hg absolute pressure to remove any gas or moisture that might have got into the system.

The apparatus (Plate 4.2) shown schematically in

Plate 4.2

The Vapour Pressure Apparatus

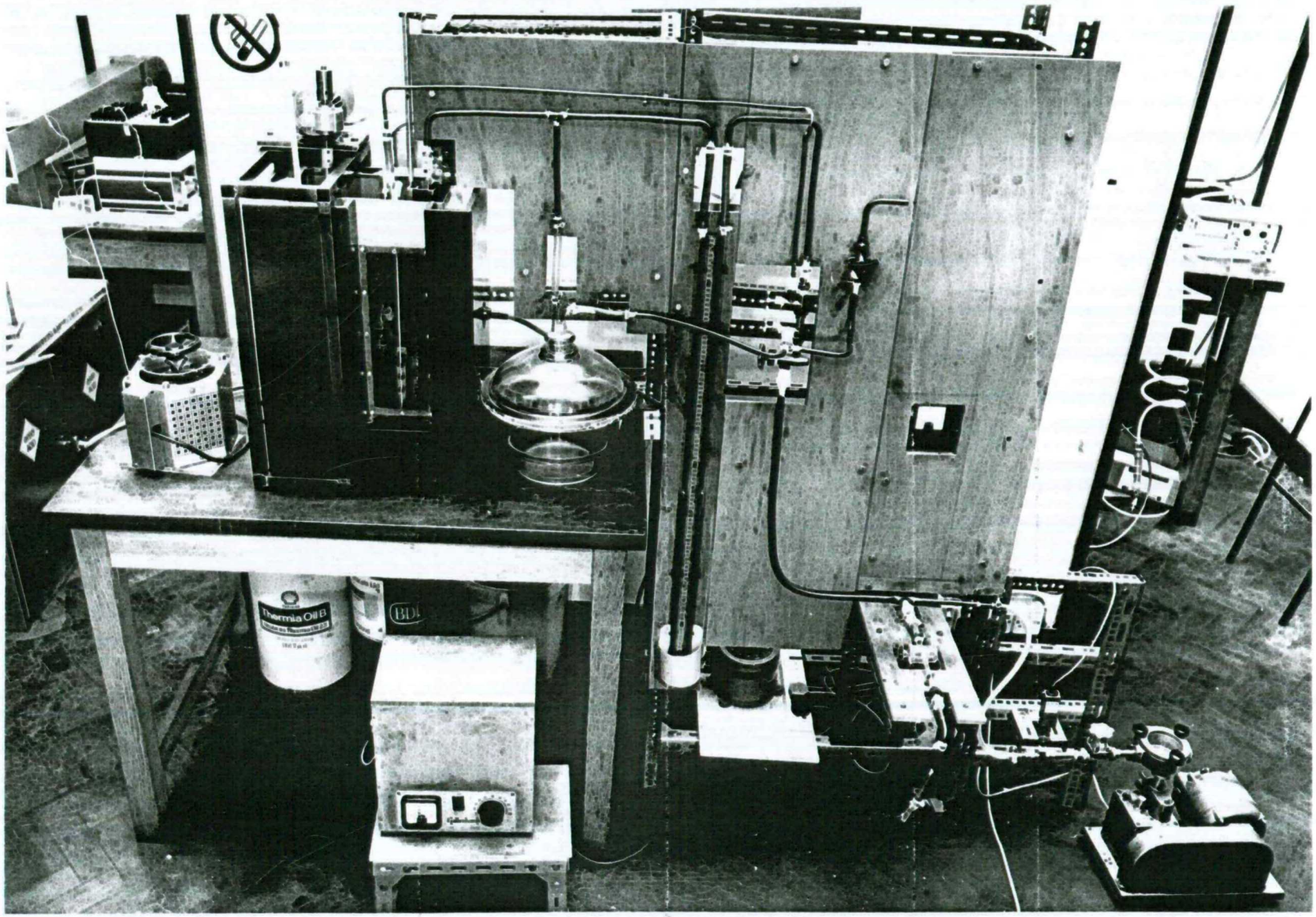
Thermia Oil B
BDH

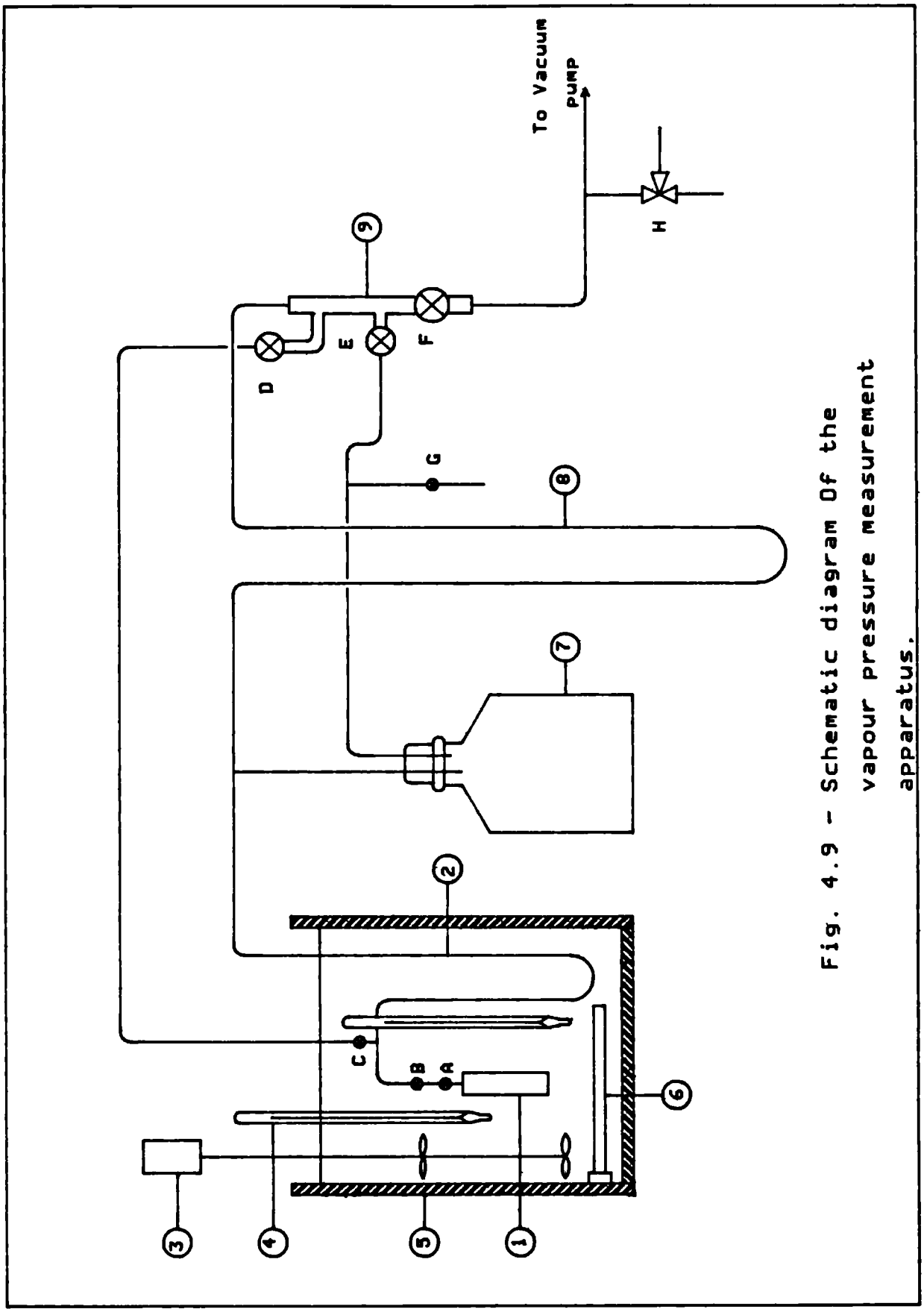

Fig. 4.9 - Schematic diagram Of the vapour pressure measurement apparatus.

Notation For Figure 4.9

1) Solution cell
2) Confining liquid manometer
3) Stirrer
4) Thermometer
5) Insulated oil bath
6) Immersion heater
7) Dessicator
8) Mercury manometer
9) Valve manifold

Figure 4.9 consisted of: a solution cell/confining liquid assembly, an oven for drying the salts under vacuum, an oil bath, a mercury manometer, a heavy duty stirrer, and a vacuum pump for evacuating the system when required (not shown in sketch).

The solution cell was a thick 31.9mm o.d, heat resisting glass tube with a flat bottom and a 29/32 ground glass joint at the top end to hold a cover which carried a valve for isolating the cell. The outlet end of the cover was a 10mm o.d glass tube with a 12/21 ground glass joint. The internal volume of the cell was approximately 114 cm^3

The confining liquid manometer was a 10mm o.d, U-shaped glass tube. The left leg which incorporated a 6mm branch off for evacuating the space between the solution in the cell and the confining liquid in the manometer, was connected to the solution cell through the 12/21 ground glass joint. The right leg was connected to the mercury manometer. The solution cell/confining liquid assembly positioned on a support was mounted on a retort stand (Figure 4.10) and could easily be separated from the other components of the apparatus and removed from the oil bath to charge the cell with new solution of different concentration.

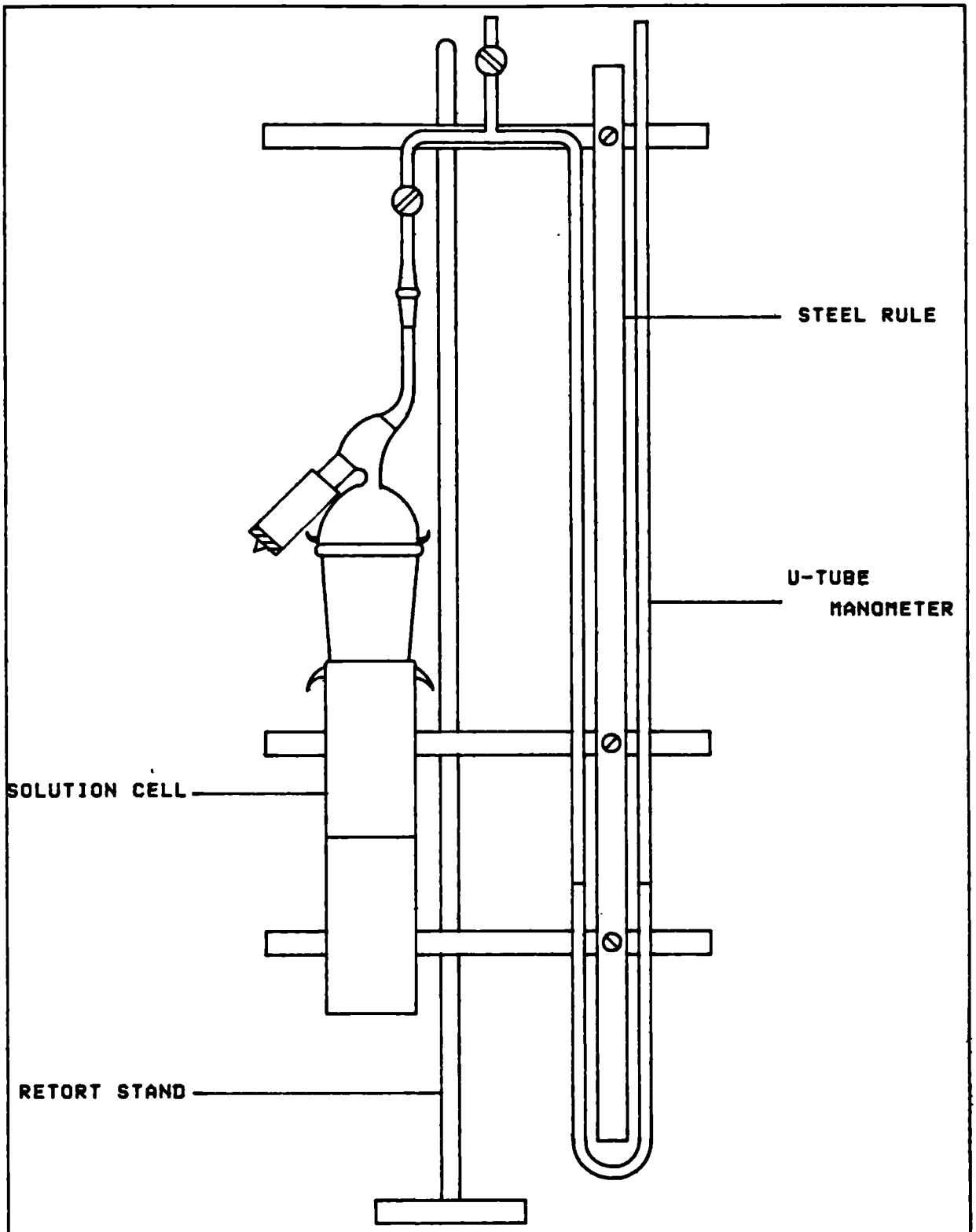

Fig. 4.10 - The solution cell/confining liquid manometer assembly.

The properties of a good confining liquid are

i) an appreciably low vapour pressure of its own at the temperatures under study

ii) the vapour of the solution should not dissolve in it

iii) it should not react chemically with the vapour of the solution especially if a gas is produced.

The liquid selected to meet these requirements was Tri-n-butyl Citrate, an odourless, nonvolatile, pale yellow, stable liquid. It is practically insoluble in and immiscible with water, with a specific gravity of 1.045 and a boiling point of approximately 233.5°C.

An empty dessicator between the confining liquid and the mercury manometers, helped to dampen any pressure fluctuations in the system. It also provided a point where the pressure between the confining liquid and and mercury in the manometers could be increased or decreased. A valve manifold (9) in the system connected the evacuation points in the left leg of the confining liquid manometer, the right leg of the confining liquid and hence the left leg of the mercury manometers, and the right leg of the mercury manometer to the vacuum pump. The solution cells were evacuated during solution preparations through a three-way valve, (H). The mercury manometer was made of a 9.00mm i.d glass tube and about 90cm high.

The solution cell/confining liquid manometer assembly was placed inside an oil bath where the solution, its vapour and the confining liquid were maintained at the same predetermined temperature by the combined operation of a heavy duty electric motor driven stirrer and two immersion heaters each of 2KW capacity. The stirrer had two sets of blades 22.86cm apart with the bottom set at a depth of 47.0cm. One of the immersion heaters was positioned close to the base of the oil bath in the horizontal plane whilst the other (not shown in the diagram) was positioned with its elements in the vertical plane.

The oil bath was a rectangular steel tank, 30.48cm x 17.78cmx48.26cm high with a viewing window, 11.4cm wide x 33cm high covered with clear Perspex. The solution cell/confining liquid assembly and a submerged thermometer could be viewed through this window. The rectangular metal tank was placed inside a 12.7mm thick wooden box with 50mm space at the bottom and sides of the tank except at the viewing window. The space between the metal tank and the wooden box was filed with fibreglass insulating materials. The metal tank was filled with 25 litres of paraffin oil to completely submerge the solution cell/confining liquid manometer assembly. Care was taken, however, not to over fill the bath as the oil level rose with increased bath temperature.

A small oven with a transverse tube was used to dry

the salts. The oven temperature could be thermostatically controlled over the range from 0°C-1250°C. The transverse tube was large enough to take the solution cell lying in the horizontal position with the cover end connected to the vacuum pump through the 3-way valve (H).

The vacuum pump was a model 25C20A, two stage, Speedivac high vacuum type with a vacuum sensor and gauge monitoring the pressure in the system continuously. Before taking any gauge reading, the gauge was always calibrated against a set current voltage.

Three calibrated mercury-in-glass thermometers were used to monitor the bath temperature which was taken as the solution temperature. One of the thermometers was completely submerged in the oil whilst the other two had part of their stems exposed and corrections were made for these.

4.3.2 The Experimental Procedure

i) Preparing the solution

The solution cell was washed in clean warm water, dried and vacuum greased. It was then weighed unevacuated. The system was isolated from the vacuum pump by closing valve F (Figure 4.9) and the cell was evacuated to 0.03mm Hg through an arm of the 3-way

valve H. It was then reweighed to within 0.01 gram still under vacuum.

Zinc bromide salt was added to the cell then placed in the oven and connected to the vacuum system through valve H. The salt was dried with an oven temperature of about 300°C whilst being evacuate until the gauge registered 0.03mm Hg. The cell was then removed from the oven, allowed to cool to room temperature and reweighed still under vacuum. Sufficient lithium bromide salt to give two moles to one mole of zinc bromide was added to the cell which was similarly dried under vacuum in the oven. The cell was then isolated and allowed to cool to room temperature and reweighed still under vacuum. The buoyancy effect was neglected as the variation in environmental temperatures under which the weighings were carried out could be neglected.

Distilled water was then added to dissolve the dried salts using the set up shown schematically in Figure 4.11. The line up to the cell isolating valve was full of water before opening the valve slowly to admit water into the cell thus minimising air leakage to the cell. However, in order to remove any air that might have got into the cell during this process the solution was frozen to about -40°C in a mixture of water ice, carbon dioxide ice and liquid methanol. The cell was then evacuated to 0.03mm Hg, the valve closed and then

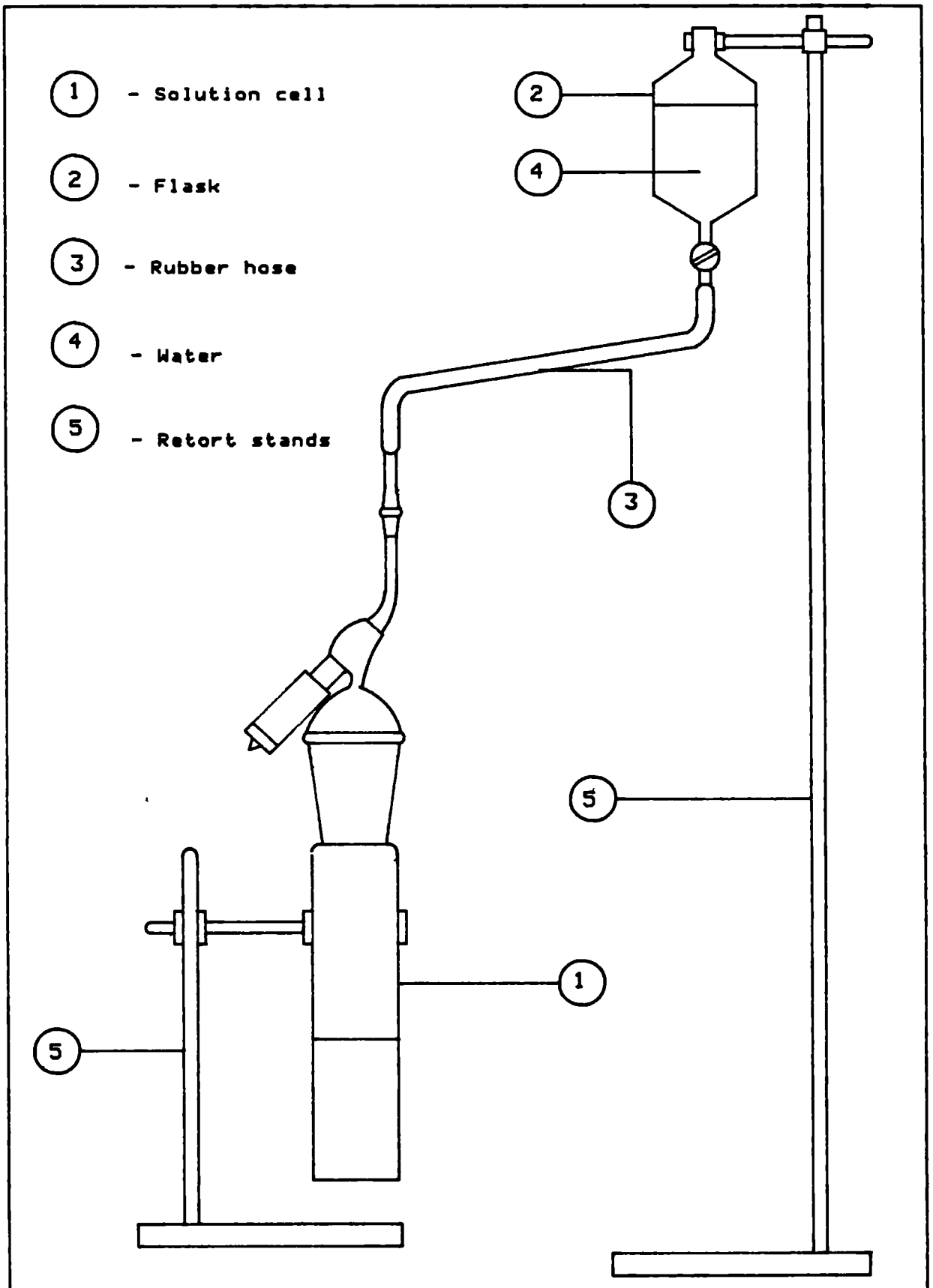

Fig. 4.11 - Diagram of the set up for adding solution solvent.

allowed to warm up to room temperature. It was cleaned and reweighed still under vacuum, to find the weight of water added. The solution was then ready to be tested.

ii) The Principle of Measurement

The principle of measurement in this work was to keep the solution vapour at the same temperature as the confining liquid which indirectly measured the pressure of the vapour. With valves C and D closed (Figure 4.9), and valves A and B opened, the pressure of the solution vapour acted on the left leg of the confining liquid manometer. This pressure was balanced by either opening (very slowly) valve G which admitted air from the atmosphere or valve E which connected the right leg of the confining liquid manometer to the vacuum pump. Once the legs of the confining liquid manometer are balanced, the pressure in the solution vapour line was the same as the pressure on the left leg of the mercury manometer.

The right leg of the mercury manometer was continuously evacuated by the vacuum pump with the pressure registered on the vacuum gauge. The pressure differential then measured by the mercury manometer was the difference in pressure between the solution vapour and the vacuum gauge readings. By this method,the effect of atmospheric pressure variations on the measurements was eliminated and the vapour pressure of the solution easily determined.

iii) The Experiment

The solution cell,still under vacuum, was connected to the confining liquid manometer and the assembly was submerged in the oil bath and connected up accordingly. With cell valve A, the air admittance valve G and valve H closed, all other valves were opened and the system evacuated to 0.03mm Hg. The vacuum pump was isolated by closing valve F, then valves C, D and E were closed. Valve A was opened to establish contact between the solution vapour and the confining liquid. Valve F was also opened to continuously evacuate the right leg of the mercury manometer.

The stirrer was switched on and also the heaters which were regulated through variacs to bring the temperature of the bath to the predetermined value. The levels of the confining liquid in the manometer were then balanced through either valve G or E. At equilibrium conditions, characterised by a constant pressure for at least fifteen minutes, readings of the thermometers in the bath, the mercury manometer differential pressure and the respective mimiscus heights in each leg, and the vacuum gauge were taken. The body temperature of the mercury manometer was also taken using thermometers taped to the body.

The pressure readings were corrected for capillary effect, temperature and gravity according to the NBS

monograph 8 (88).

4.3.3. Results

The vapour pressure of distilled water was measured using the apparatus described above and the results compared with values of Rogers and Mayhew (89). The experimental data were correlated by the equation:

$$\text{Log}_{10}P = a + b/T + c\log T + d\,T \qquad (4.5)$$

where P = the vapour pressure of water, mbar

T = the absolute temperature of water, K

a = -696.70126

b = 17298.90683

c = 281.82074

d = -0.19168

Equation 4.5 fitted the experimental data to within 0.3% (Table 4.12). The vapour pressure data of Rogers and Mayhew (89) and Olama (25) were interpolated for the experimental temperatures between 30° and 70.5°C and these values were compared with those calculated from equation 4.5 and shown in Table 4.13. Even though the results of this investigation agreed well with Olama's values, there was better agreement with Rogers and Mayhew's steam Table values. A maximum deviation of the order of 1.8% was observed in the results of this investigation and those of Rogers and Mayhew within the temperature range considered.

Solution Temperature (°C)	Vapour pressure (mbar)		Deviation (mbar)
	observed	calculated from eq 4.5	
30.3	44.20	44.11	0.09
40.1	74.75	74.61	0.14
50.0	123.80	123.48	0.32
60.0	199.02	198.63	0.39
70.5	314.67	313.93	0.74

Table 4.12 Experimental vapour pressure data for distilled water

Solution temperature (°C)	Present work (mbar)	Rogers & Mayhew steam table (mbar) (89)	Olama (25) (mbar)
30.3	44.11	43.37	43.08
40.1	74.61	74.25	74.51
50.0	123.48	123.30	124.62
60.0	198.63	199.20	198.17
70.5	313.93	319.71	-

Table 4.13 Comparison of vapour pressure data for distilled water

For the (2LiBr + $ZnBr_2$)/H_2O Solution, vapour pressure measurements were made for six solution concentrations in the range between 50% and 75% salts by weight. For each concentration the pressures were measured for 4-6 solution temperatures in the range between 20°C and 100°C. The correlating equation is similar to equation 4.5 but the constants were obtained in terms of the solution concentration by the following equations:

$$a = 2257753.065 - 145936.3077\,\xi_{4,2} + 3520.602124\,\xi_{4,2}^2 - 37.59600705\,\xi_{4,2}^3 + 0.1500350605\,\xi_{4,2}^4 \quad (4.6)$$

$$b = -68090655.59 + 4406949.076\,\xi_{4,2} - 10645.9839\,\xi_{4,2}^2 + 1138.143607\,\xi_{4,2}^3 - 4.546978226\,\xi_{4,2}^4 \quad (4.7)$$

$$c = -885445.2854 + 57217.9301\,\xi_{4,2} - 1379.976313\,\xi_{4,2}^2 + 14.73296646\,\xi_{4,2}^3 - 5.878218084E{-}2\,\xi_{4,2}^4 \quad (4.8)$$

$$d = 541.2547064 - 34.92005739\,\xi_{4,2} + 0.8408961527\,\xi_{4,2}^2 - 8.96472716E{-}3\,\xi_{4,2}^3 + 3.572181619E{-}5\,\xi_{4,2}^4 \quad (4.9)$$

These equations were used to calculate the vapour pressures of the solution at the experimental temperatures and concentrations and the results compared with observed ones as shown in Table 4.14. The maximum error was less than 3.00%. The equation constants are also shown in Table 4.15.

The graphs of $Log_{10}P$ Vs 1/T for distilled water and the solution are shown in Figure 4.12. These show generally a straight line relationship with better fits at higher salt concentrations.

The vapour pressure data for the solution were plotted against the weight fractions of the salts at temperatures of 40°C, 60°C, 80°C and 100°C as shown in Figure 4.13. These graphs make it possible to read the vapour pressure of the solutions at weight fractions other than those experimented at the plotted temperatures. The graphs confirm that for a constant concentration, the vapour pressure increases with an increase in temperature. At any temperature, the vapour pressure decreased with increased concentration, but the decrease becomes more pronounced as the temperature increased.

The vapour pressure of the solution was also plotted against the mole fractions for the same temperatures 40°, 60°, 80° and 100°C as shown in Figure 4.14. At all the temperatures, the solution exhibited a negative deviation from Raoult's law.

Concentration (%)	Solution Temp. °C	Vapour pressure (mbar)		Deviations	
		observed	calculated from eqs 4.5 - 4.9	mbar	%
50.71	20.5	17.11	17.09	-0.02	-0.12
	30.0	29.74	29.48	-0.26	-0.87
	40.1	50.34	50.49	+0.15	+0.30
	60.1	132.51	131.89	-0.62	-0.47
	80.4	312.80	312.13	-0.67	-0.21
56.89	20.5	14.57	14.32	-0.25	-1.72
	30.5	23.74	24.10	+0.36	+1.52
	50.4	69.45	67.47	-1.98	-2.85
	65.1	138.68	137.64	-1.04	-0.75
	75.0	212.96	214.21	+1.25	+0.59
	94.6	463.40	457.96	-5.44	-1.17
59.52	50.3	62.02	61.16	-0.86	-1.39
	65.3	126.87	126.11	-0.76	-0.60
	74.9	191.32	193.29	+1.97	+1.03
	94.6	417.91	408.86	-9.05	-2.17
65.40	30.7	16.08	16.01	-0.07	-0.44
	50.1	44.65	44.20	-0.45	-1.01
	70.1	110.52	110.78	+0.26	+0.24
	90.0	248.77	245.21	-3.56	-1.43
	99.8	348.49	348.02	-0.47	-0.13
70.96	40.5	14.75	14.59	-0.16	-1.08
	59.8	38.13	37.71	-0.42	-1.10
	79.8	92.61	91.58	-1.03	-1.11
	95.5	177.21	175.20	-2.01	-1.13
74.05	51.1	14.44	14.30	-0.14	-0.97
	70.1	37.70	37.33	-0.37	-0.98
	89.8	89.27	88.38	-0.89	-1.00
	96.9	120.63	119.42	-1.21	-1.00

Table 4.14 Experimental vapour pressure data for $(2LiBr + ZnBr_2)/H_2O$ solution

Concentration (%)	Calculated Fitting Equation Constants			
	a	b	c	d
50.0	661.236688	-21324.57750	-257.38565	0.16267
52.0	-527.40248	13573.44058	211.34351	-0.13323
54.0	-992.88994	26959.90779	395.66646	-0.25241
55.0	-1043.53086	28267.27784	416.12451	-0.26713
56.0	-1013.07708	27195.66683	404.59813	-0.26164
58.0	-808.2020	20895.52077	324.58106	-0.21402
60.0	-540.88932	12928.23304	219.48547	-0.14892
62.0	-316.15023	6416.52744	130.60920	-0.09198
64.0	-181.38243	2737.08811	76.67774	-0.05514
65.0	-146.79587	1912.24938	62.49590	-0.04423
66.0	-126.37017	1520.55957	53.84421	-0.03661
68.0	-83.28424	651.54671	35.68940	-0.02089
70.0	73.31805	-3731.38526	-26.77829	0.02123
72.0	526.49285	-17235.71072	-205.12279	0.13269
74.0	1516.90974	-47214.94372	-593.48041	0.37015
75.0	2304.54691	-71158.05641	-902.00385	0.55758
76.0	3342.85181	-102768.63794	-1308.55979	0.80397
78.0	6360.21560	-194742.38671	-2489.64196	1.51825
80.0	10982.51108	-335727.82296	-4298.58029	2.61078

Table 4.15 - Vapour pressure equation Constants for $(2LiBr + ZnBr_2)/H_2O$ Solution

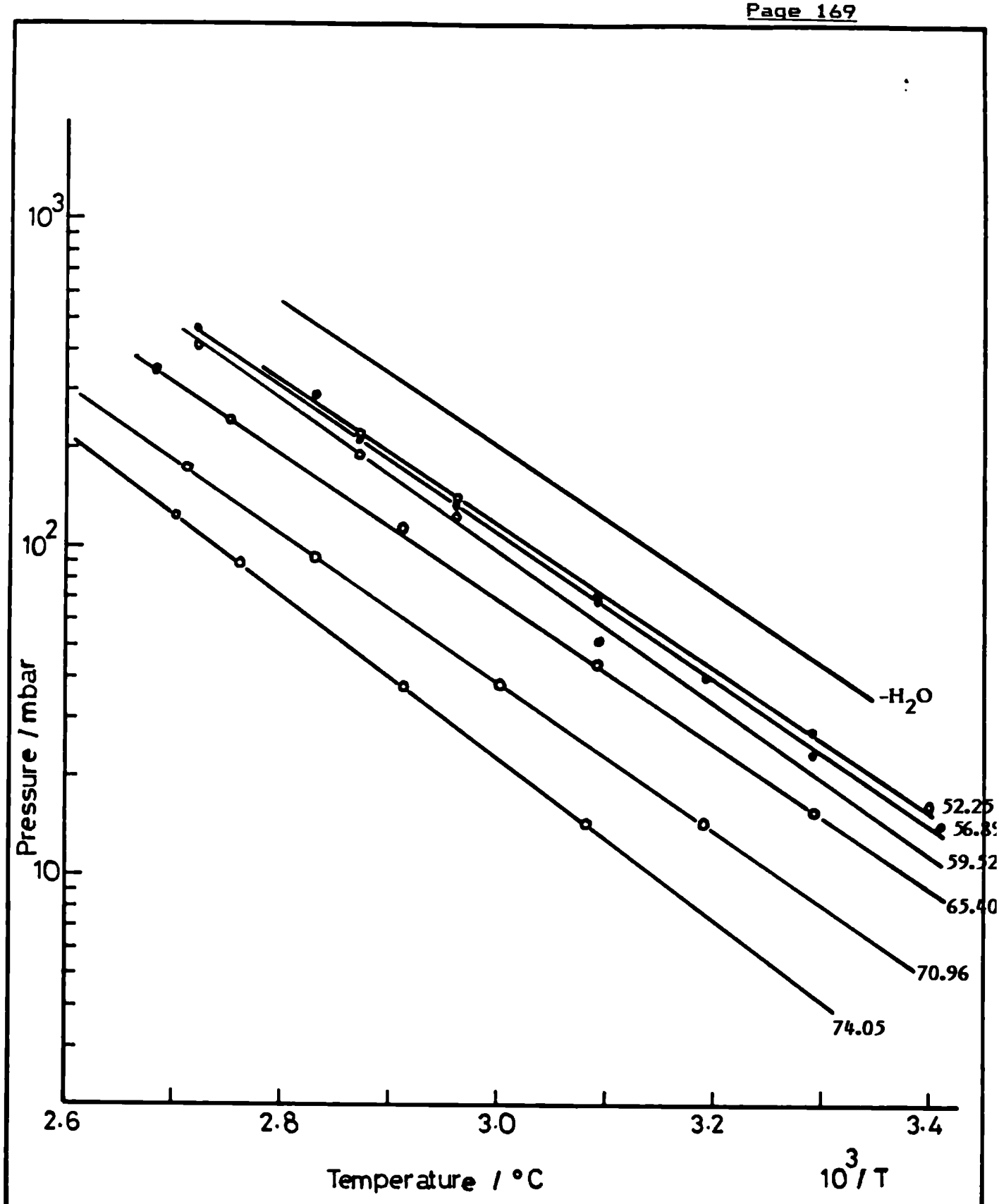

Fig. 4.12 Vapour pressure Vs inverse of temperature of (2LiBr + $ZnBr_2$)/H_2O solution

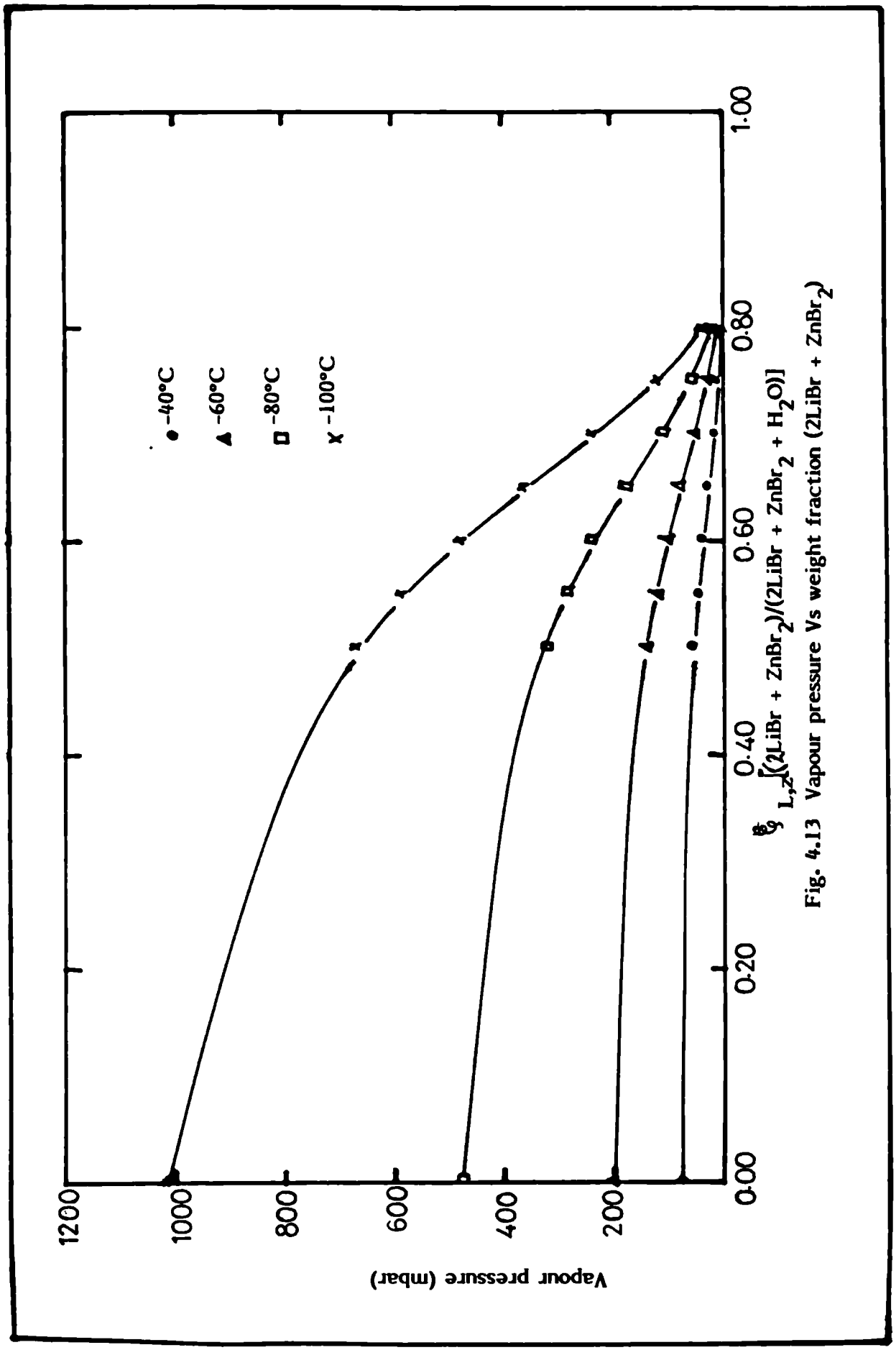

Fig. 4.13 Vapour pressure Vs weight fraction (2LiBr + $ZnBr_2$)

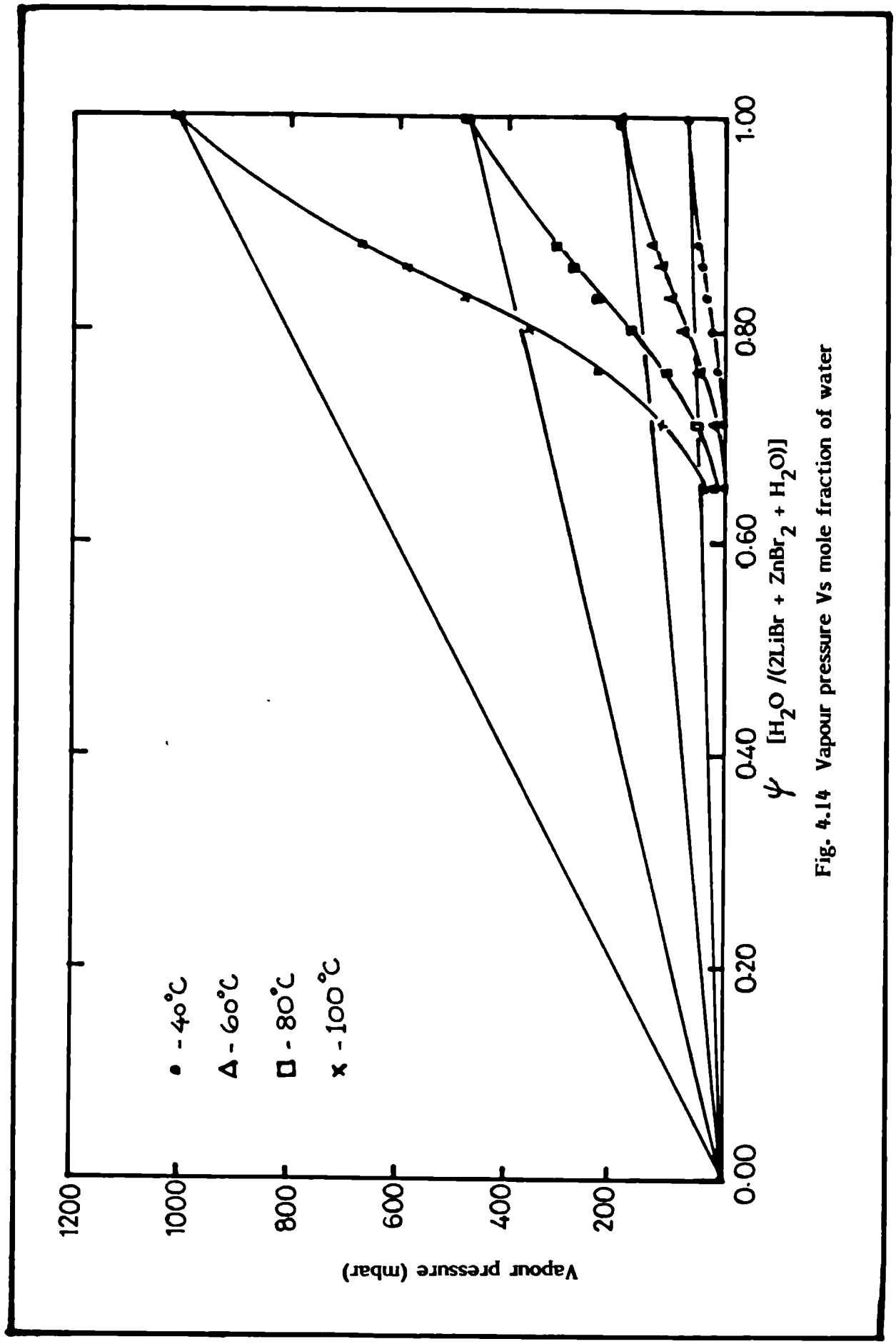

Fig. 4.14 Vapour pressure Vs mole fraction of water

4.3.4 Accuracy of Results

The major sources of error in the vapour pressure measurements could be: error in temperature readings and difficulty in maintaining constant bath temperatures;inaccuracy in weighing of solution components during solution making and error in mercury manometer readings. The design of, and the effectiveness of stirring the oil bath gave a fairly steady bath temperature with a maximum deviation of the order of 0.2°C. The accuracy of the mercury-in-glass thermometers used was within 0.1°C. Temperature measurement errors then accounted for a maximum of about 0.3°C. This error would increase the vapour pressure reading by about 1.4%.

Weighing of solution components was made to within 0.01g. Normally, the volume occupied in the solution cell/confining liquid manometer by the solution vapour would increase with increase in temperature. However, the idea of balancing both legs of the manometer tended to maintain this volume constant during the experiment. Since the confining liquid had negligible vapour pressure at the temperatures of the test, the variation in the amount of vapour escaping from the solution would be minimal. The volume occupied by the solution vapour (water vapour) was approximately 80cm^3. The mass of vapour to occupy this volume is less than 0.04g at a solution temperature of 90°C, hence the change in the

concentration of the solution could be assumed to be negligible. For pressure measurements, corrections were made for capillary effects and for temperature and gravity effects.

In general, as mentioned in the previous section, the results of this investigation for distilled water was compared with Rogers and Mayhew's (89) and Olama's (25) data. Assuming the Rogers and Mayhew's data that has been widely used to be correct, the maximum deviation was of the order of 1.8% within a temperature range of 30 - 70.5°C. The maximum error in the vapour pressure measurements is therefore believed to be of the order of 2.5% within the temperature range between 20° - 100°C. Owing to lack of data in the literature for the $(2LiBr + ZnBr_2)/H_2O$ solution, the results could not be compared.

4.3.5 Presentation of Vapour Pressure Results

i) The Equilibrium Chart

The vapour pressure of solutions are normally presented in form of plots containing the three variables, temperature, pressure and mass fraction. Any two of these could be used as the co-ordinates with the third as a parameter. Several methods of plots to give approximately straight line have been suggested, such as the plot of: log P against T; log P against 1/T and log P against 1/(T-C), where C is a

constant determined for the substance. However, these plots give nearly but not quite straight lines.

A plot that gives a straight line relationship will be very useful for interpolating or extrapolating data especially for solutions with scanty data points. The Duhring plot which also gives a nearly straight line relationship when the saturation temperatures of the refrigerant and the solution are plotted against each other at the same pressure, is now often used. Incidentally, in refrigeration plants, the saturation temperature of the refrigerant is of more significance than the actual pressure.

The Duhring equation for the $(2LiBr + ZnBr_2)/H_2O$ solution was represented by:

$$t = At' + B \qquad (4.10)$$

where t = saturation temperature of solution, °C

t' = saturation temperature of water, °C

A and B are constants for any given concentration.

A polynomial fit was made for the two constants in terms of solution concentration to obtain:

$$A = A_0 + A_1 \xi_{L,Z} + A_2 \xi_{L,Z}^2 + A_3 \xi_{L,Z}^3 + A_4 \xi_{L,Z}^4 \qquad (4.11)$$

where $A_0 = -43.048622$

$A_1 = 3.03984$

$A_2 = 7.782661E-2$

$A_3 = 8.764915E-4$

$A_4 = -3.656371E-6$

$$B = B_o + B_1 \xi_{L,Z} + B_2 \xi_{L,Z}^2 + B_3 \xi_{L,Z}^3 + B_4 \xi_{L,Z}^4 \qquad (4.12)$$

where $B_o = 1383.19423$

$B_1 = -102.114017$

$B_2 = 2.797981$

$B_3 = -3.376695E-2$

$B_4 = 1.52386E-4$

Using equations (4.10) to (4.12), the saturation temperature of water was calculated for solution temperatures between 30° and 90°C and for solution concentrations between 50% and 76%. The results were compared with the accepted values for water as a reference substance as given by Rogers and Mayhew (89) and shown in Table 4.16. Except at temperatures of 30°C for some concentrations where the error introduced by the equations was as high as 5.8%, the average error was below 2%.

The Duhring plot or equilibrium chart for the $(2LiBr + ZnBr_2)/H_2O$ solution is shown in Figure 4.15.

Table 4.16 The Equilibrium chart data

Concentration (%)	Solution Sat. temp. (°C)	Saturation temp of water, t′ (°C)		Deviation (°C)	Calculated Equation constants	
		Rogers & Mayhew	Smoothed values		A	B
50	30	23.6	24.0	+0.4	1.08597	3.9895
	40	33.3	33.2	-0.1		
	50	42.7	42.4	-0.3		
	60	60.8	60.8	0.0		
	90	79.1	79.2	+0.1		
52	30	23.7	22.7	-1.0	1.08764	5.2904
	40	32.2	31.9	-0.3		
	50	41.1	41.1	0.0		
	70	59.7	59.5	-0.2		
	90	78.5	77.9	-0.6		
54	30	22.4	21.5	-0.9	1.08587	6.6174
	40	30.7	30.7	0.0		
	50	39.6	40.0	+0.4		
	70	58.3	58.4	+0.1		
	90	77.1	76.8	-0.3		
55	30	21.6	20.9	-0.7	1.08528	7.2665
	40	30.0	30.2	+0.2		
	50	39.0	39.4	+0.4		
	70	57.8	57.8	0.0		
	90	76.5	76.2	-0.3		
56	30	20.8	20.4	-0.4	1.08553	7.9003
	40	29.4	29.6	+0.2		
	60	47.9	48.0	-0.1		
	80	66.7	66.4	-0.3		
	90	75.9	75.6	-0.3		
58	30	19.1	19.1	0.0	1.09008	9.1276
	40	28.1	28.3	+0.2		
	60	46.7	46.7	0.0		
	80	65.3	65.0	-0.3		
	90	74.2	74.2	0.0		
60	30	17.5	17.8	+0.3	1.10158	10.346
	40	26.6	26.9	+0.3		
	60	45.2	45.1	-0.1		
	80	63.4	63.2	-0.2		
	90	72.0	72.3	+0.3		
62	30	16.0	16.4	+0.4	1.12067	11.6610
	40	25.2	25.3	+0.1		
	60	43.4	43.1	-0.3		
	80	61.1	61.0	-0.1		
	90	69.6	69.9	+0.3		

Table 4.16 (continued)

64	30	14.5	14.6	+0.1	1.14661	13.2366
	40	23.4	23.3	-0.1		
	60	41.1	40.8	-0.3		
	80	58.3	58.2	-0.1		
	90	66.7	66.9	+0.2		
65	30	13.8	13.6	-0.2	1.16152	14.1894
	40	22.5	22.2	-0.3		
	60	39.8	39.4	-0.4		
	80	56.8	56.7	-0.1		
	90	65.2	65.3	+0.1		
66	30	12.8	12.5	-0.3	1.17723	15.2952
	40	21.3	21.0	-0.3		
	60	38.2	38.0	-0.2		
	80	55.1	55.0	-0.1		
	90	63.4	63.5	+0.1		
68	30	10.4	9.8	-0.6	1.20899	18.1178
	40	18.4	18.1	-0.3		
	60	34.7	34.6	-0.1		
	80	51.2	51.2	0.0		
	90	59.6	59.5	-0.1		
70	40	14.5	14.5	0.0	1.2369	22.0437
	50	22.5	22.6	+0.1		
	60	30.4	30.7	+0.3		
	80	46.7	46.9	+0.2		
	90	55.0	54.9	-0.1		
72	40	9.3	10.0	+0.7	1.25462	27.4712
	50	17.4	18.0	+0.6		
	60	25.4	25.9	+0.5		
	80	41.5	41.9	+0.4		
	90	49.7	49.8	+0.1		
74	50	11.5	12.1	+0.6	1.25437	34.8565
	60	19.9	20.0	+0.1		
	80	35.7	36.0	+0.3		
	90	43.8	44.0	+0.2		
75	50	8.2	8.5	+0.3	1.24468	39.4421
	60	16.8	16.5	-0.3		
	70	24.9	24.6	-0.3		
	80	32.6	32.6	0.0		
	90	40.4	40.6	+0.2		
76	50	4.3	4.3	0.0	1.22696	44.7151
	60	12.5	12.5	0.0		
	70	20.6	20.6	0.0		
	80	28.8	28.8	0.0		
	90	36.9	36.9	0.0		

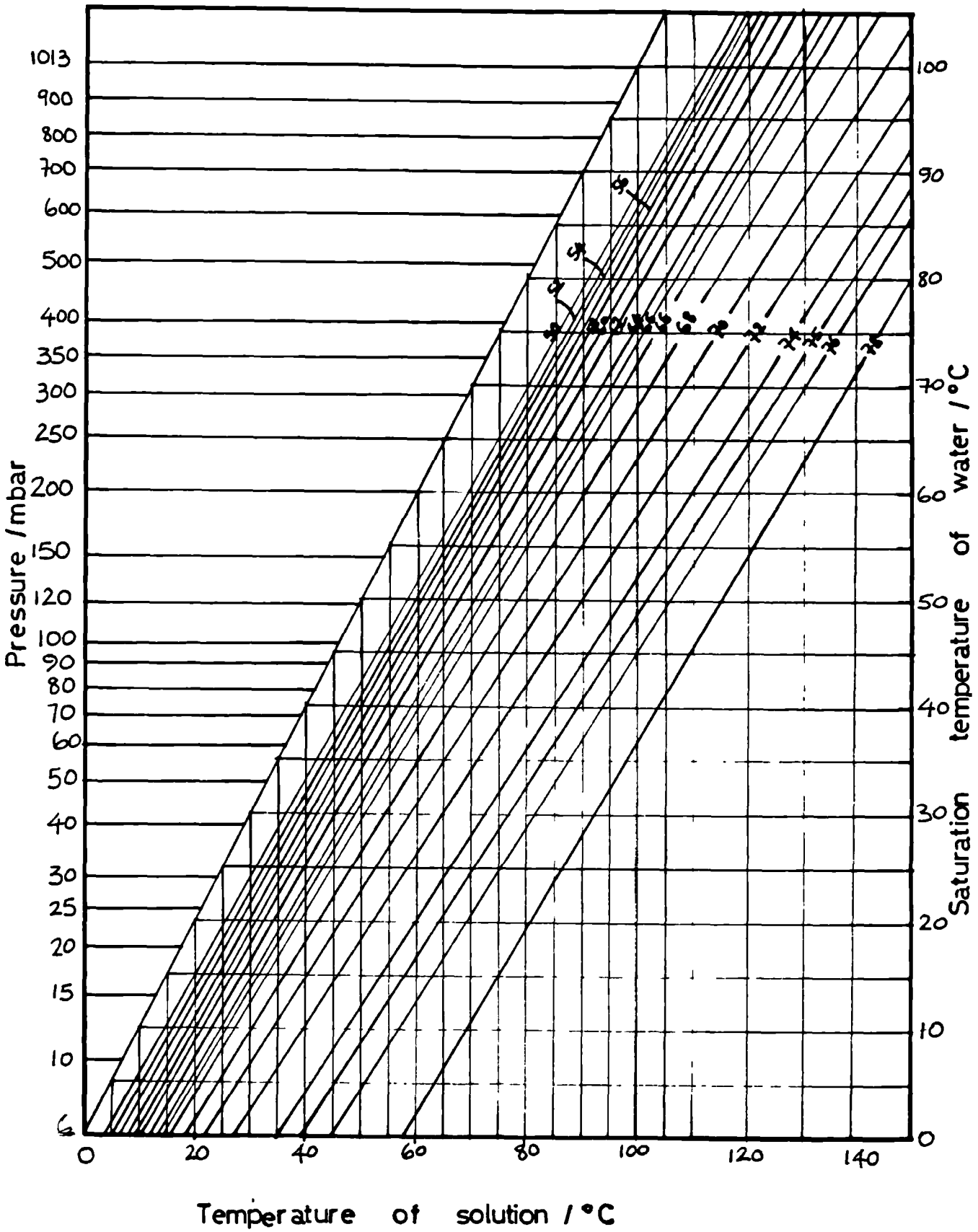

Fig. 4.15 The equilibrium chart for (2LiBr + $ZnBr_2$)/H_2O solution

ii) The enthalpy/concentration chart

a) Method

The enthalpy of solutions containing a single volatile consistent can be calculated from the following data:

i) the heat capacities of the solution at any one concentration over the entire temperature range,

ii) vapour pressure of the solution over the concentration and temperature range of interest.

The Duhring plot for the solution is also useful as the linear relationship between pressure, temperature and concentration is useful in this method. The latent heat of a solution, ΔH, can be found from the following relationship derived from the Clapeyron equation and taken from McNeely (86):

$$\Delta H = \frac{\Delta H' \; V \; T}{\Delta V' T'} \qquad (4.13)$$

where:

$\Delta H'$ = latent heat of saturated water at temperature t', (KJ/Kg)

V' = specific volume of saturated water vapour at temperature t', (m^3/Kg)

V = specific volume of superheated water vapour, (m^3/Kg)

T' = absolute saturation temperature of

water, (K)

T = absolute saturation temperature of solution, (K)

A = slope of Duhring line

t' = saturation temperature of water, (°C)

t = saturation temperature of solution, °C

The latent heat of saturated water is given by:

$$\Delta H' = H'_v - H_f \qquad (4.14)$$

H'_v is the enthalpy of saturated water vapour at t' (KJ/Kg) obtained from the simplified steam table equation converted from McNeely (80):

$$H'_v = (0.000166t' - 0.030426)P + (1.8816t' + 2500.9) \qquad (4.15)$$

H_f is the enthalpy of water at t' (KJ/Kg) obtained from the following equation also from (Ref 80):

$$H_f = 4.19t' - 0.0419 \qquad (4.16)$$

V' and V can be calculated from the following simplified steam table equations converted to SI units from McNeely (80).

$$V' = (-0.00000263t'^2 + 0.0008146t' - 0.07967) + (4.6147t' + 1260.93)/P \qquad (4.17)$$

$$V = (-0.00000263t^2 + 0.0001846t - 0.07967) + 4.6147t + 1260.93)/P \quad (4.18)$$

P being the pressure in mbar obtained from steam table (or Duhring plot) at water saturation temperature, t'.

The Duhring line slope, A, can be calculated from equation 4.11.

The saturation temperature of water, t' can be obtained from the equations:

$$t' = \frac{t-B}{A} \quad (4.19)$$

Haltenberger (90) described a method for constructing an enthalpy-concentration chart using the Duhring chart data plus heat capacity for a single concentration over the range of temperature desired. The following equation was derived from a heat and material balance of the isothermal evaporation of water from a base concentration:

$$H_1 = \frac{H_o \int_{\beta_o}^{\beta_1} \bar{H}\, d\,(1-\beta_o/\beta)}{\beta_o/\beta_1} \quad (4.20)$$

where:

H_1 = enthalpy of the solution concentration, β_1 as calculated at isotherm t, (KJ/Kg.)

H_o = enthalpy of the solution base concentration for each isotherm to be calculated, (KJ/Kg.)

$\bar{H}$ = the partial enthalpy of water in solution, KJ/Kg.

β_o = base concentration of solution for which heat capacity is known.

ρ_{f_1} = final concentration after water is added to or evaporated from base concentration.

ω = $(1 - \rho_{f_0} / \rho_{f_1})$

= total water added to or evaporated as ρ_f varies from ρ_{f_0} to ρ_{f_1}, Kg.

Setting the reference state of zero enthalpy at 0°C for water and the solution at the chosen concentration, the enthalpy of the base concentration is given as:

$$H_o = \int_0^{t_1} C_{pm} \, dt \qquad (4.21)$$

where:

C_{pm} = the heat capacity of the solution at the chosen concentration.

The partial enthalpy of water in solution, $\bar{H}$ is given by the equation:

$$\bar{H} = H_v - \Delta H \qquad (4.22)$$

H_v being the enthalpy of superheated water vapour (KJ/Kg, obtained from the steam tables or from the equation taken from Ref 80.

$$H_v = (0.000166t - 0.030426)\, P + (1.8816t + 2500.9) \qquad (4.23)$$

b) Enthalpy calculations

The base concentration used in the determination of solution enthalpy in this work was 59.75%. The National Physical Laboratory measured the heat capacity of the solution at this concentration over a temperature range between 20°C and 100°C and the smoothed values are shown in Table 4.17 below.

Solution concentration ,(%)	Solution temperature (°C)	Heat capacity (KJ/Kg K)
59.75	20	1.863
	30	1.863
	40	1.863
	50	1.864
	60	1.866
	70	1.868
	80	1.872
	90	1.877
	100	1.883

Table 4.17 Heat capacity for $(2LiBr + ZnBr_2)/H_2O$ solution at ξ_{LZ}= 59.75%.

The correlating equation was:

$$C_{pm} = A + BT + CT^2 \qquad (4.24)$$

where: A = 2.286

B = -2.789E-3

C = 4.589E-6

T = absolute temperature of solution, (K)

C_{pm} = heat capacity of the solution at constant pressure (KJ/Kg K)

Equation 4.24 was transformed to:

$$C_{pm} = a + bt + ct^2 \qquad (4.25)$$

where: a = 1.8666

b = -2.8341E-4

c = 4.589E-6

t = solution temperature, (°C)

From equations 4.21 and 4.25, the enthalpy at the base concentration was calculated for each isotherm and the results shown in Table 4.18.

Temperature (°C)	Enthalpy of solution base concentration, H_o (KJ/Kg)
20	37.3
30	55.9
40	74.5
50	93.2
60	111.8
70	130.5
80	149.2
90	168.0
100	186.8

Table 4.18 Enthalpy of base concentration at the isotherms.

From equations 4.13 - 4.19, 4.22 and 4.23, the value of $\bar{H}$ were compiled. The integral of equation 4.20 was solved for each isotherm by firstly using a microcomputer to obtain the best polynomial fit for the plot of the $\bar{H}$ against ω, then using the derived equation with a programmable Casio fx-4000P hand calculator to perform the numerical integration to obtain the area under the curve between the value of ω at $\xi = \xi_o$ and $\xi = \xi_1$ which represents the total heat added or removed from the solution as one Kg of solution changes to (1-ω)Kg at ξ_1.

Using equation 4.19, the enthalpy of solution at

each isotherm was calculated. The calculated data was correlated by the following equation:

$$h = \alpha + \beta \xi_{L,Z} + \gamma \xi_{L,Z}^{2} \qquad (4.26)$$

where α, β and γ are constants, obtained in terms of solution temperatures as follows:

$$\alpha = 90.093914 + 10.44301.t - 0.198468.t^2 + 2.614931E\text{-}3t^3 - 1.18601E\text{-}5t^4 \qquad (4.27)$$

$$\beta = -1.676825 - 0.259806.t + 6.132393E\text{-}3t^2 - 7.96672E\text{-}5.t^3 + 3.597467E\text{-}7.t^4 \qquad (4.28)$$

$$\gamma = 2.615096E\text{-}3 + 1.929348E\text{-}3.t - 4.656353E\text{-}5t^2 + 5.949482E\text{-}7.t^3 - 2.671531E\text{-}9t^4 \qquad (4.29)$$

concentration range = $50\% \leq \xi \leq 76\%$

temperature range = $20°C \leq t \leq 100°C$.

Table 4.19 shows the comparison of the solution enthalpy data obtained by the described method and those calculated by the correlating equations 4.26 - 4.29.

An enthalpy/concentration chart for the (2LiBr + $ZnBr_2$)/H_2O solution is shown in Figure 4.16 for concentrations ranging from 50 - 76% and temperatures ranging from 20° - 100°C.

Table 4.19 The (2LiBr + $ZnBr_2$)/H_2O Solution enthalpy data

Temperature t (°C)	Mass fraction $B_{L,Z}$, (%)	Solution enthalpy (KJ/Kg)		Deviation (KJ/Kg)
		Obtained from described method	Calculated from eqns. 4.26-4.29	
20	50	56.8	55.9	-0.9
	55	42.3	45.0	+2.7
A = 238.588746	60	37.1	35.5	-1.6
B = -4.999766	65	29.3	27.3	-2.0
C = 0.026909	70	18.2	20.5	+2.3
	75	13.4	15.0	+1.6
	76	16.0	14.0	-2.0
30	50	77.2	76.4	-0.8
	55	61.9	64.4	+2.5
A = 285.75947	60	55.6	54.0	-1.6
B = 5.811471	65	47.2	45.3	-1.9
C = 0.032488	70	36.0	38.1	+2.1
	75	31.1	32.6	+1.5
	76	33.7	31.7	-2.0
40	50	97.4	96.80	-0.6
	55	81.6	83.8	+2.2
A = 327.259242	60	74.1	72.7	-1.4
B = -6.434985	65	65.1	63.3	-1.8
C = 0.036525	70	53.5	55.8	+2.3
	75	48.7	50.1	+1.4
	76	51.0	49.2	-1.8
50	50	118.2	117.4	-0.8
	55	101.4	103.3	+1.9
A = 368.815164	60	92.8	91.3	-1.5
B = -7.046126	65	82.9	81.3	-1.6
C = 0.040345	70	71.1	73.3	+2.2
	75	66.0	67.3	+1.3
	76	68.2	66.3	-1.9
60	50	138.2	138.2	0.0
	55	121.3	122.9	+1.6
A = 413.307914	60	111.4	109.9	-1.5
B = -7.734368	65	100.5	99.1	-1.4
C = 0.044633	70	88.3	90.6	+2.3
	75	83.1	84.3	+1.2
	76	85.1	83.3	-1.8

Table 4.19 (Continued)

70	50	159.9	159.2	-0.7
	55	141.1	142.6	+1.5
A = 460.771746	60	130.0	128.6	-1.4
B = -8.502851	65	118.3	116.9	-1.4
C = 0.049432	70	105.7	107.8	+2.1
	75	100.0	101.1	+1.1
	76	101.8	100.1	-1.7
80	50	180.2	180.3	+0.1
	55	161.1	162.4	+1.3
A = 508.39449	60	148.6	147.2	-1.4
B = -9.268371	65	135.9	134.7	-1.2
C = 0.054144	70	122.8	124.9	+2.1
	75	116.7	117.8	+1.1
	76	118.4	116.7	-1.7
90	50	201.6	201.3	-0.3
	55	181.1	182.2	+1.1
A = 550.517552	60	167.4	165.9	-1.5
B = -9.86139	65	153.5	152.6	-0.9
C = 0.05753	70	140.0	142.1	+2.1
	75	133.6	134.5	+0.9
	76	135.0	133.3	-1.7
100	50	221.5	221.6	+0.1
	55	201.0	201.8	+0.8
A = 578.635914	60	186.2	184.8	+1.4
B = -10.026025	65	171.6	170.8	-0.8
C = 0.05771	70	157.5	159.6	+2.1
	75	150.4	151.3	+0.9
	76	151.6	150.0	-1.6

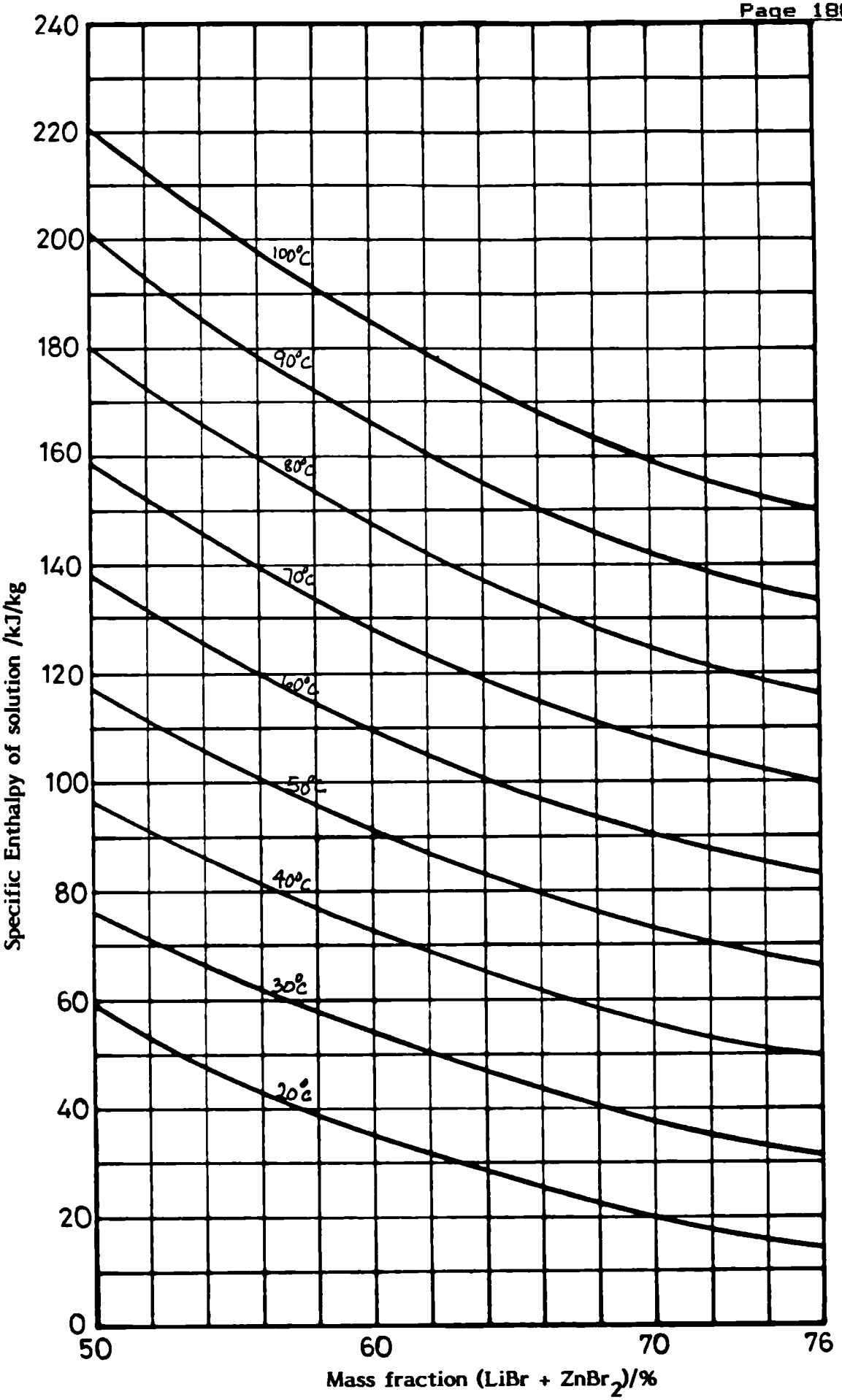

Fig. 4.16 The enthalpy/concentration chart for (2LiBr + $ZnBr_2$)/H_2O solution

4.3.6 Significance of Results

Although more of the thermal and transport properties of the (2LiBr + $ZnBr_2$)/H_2O solution need to be determined in order to completely evaluate the solution, some advantages have emerged for the solution over the LiBr-H_2O solution from the few thermodynamic properties so far investigated. The major problem of the LiBr-H_2O solution is that of limited solubility of the salt at low temperatures. The addition of one mole of zinc bromide to two moles of lithium bromide has solved the solubility problem. Hence with the (2LiBr + $ZnBr_2$)/H_2O solution, strong solution returning from the generator could be cooled to nearer the absorbing temperature without salt crystallisation. This development could eliminate some decrystallising gadgets normally associated with some lithium bromide units. The cooling of the strong solution to nearer the absorbing temperature calls for a more efficient heat exchanger to perform higher duty. Hence, the weak solution would arrive at the generator at a higher temperature, thus reducing the generator load. This would in effect result in a higher system efficiency than in a LiBr-H_2O system.

Lithium bromide is an expensive salt when compared with zinc bromide. Because of the high molecular weight of zinc bromide (225.19 compared with 86.86 for lithium bromide), a larger amount of the relatively

cheap zinc bromide is needed to make up a solution of 2 moles of lithium bromide and one mole of zinc bromide in water. At the 1986 BDH Chemicals Ltd., prices, the cost of the laboratory grade lithium bromide salt was £51.60/Kg whilst that of zinc bromide salt was £27.60/Kg. The Leverton-Clarke price for the commercial grade lithium bromide salt was £17.90/Kg. Even though the author is not aware of any commercial grade price for zinc bromide, the variation in the laboratory grade prices indicates that the price would be lower than that of lithium bromide. Hence, it would be cheaper to make a $(2LiBr + ZnBr_2)/H_2O$ solution of the same concentration with a $LiBr-H_2O$ solution. The advantages of the $(2LiBr + ZnBr_2)/H_2O$ over the $LiBr-H_2O$ system will be discussed further in Chapter Seven.

Chapter Five

The Design Of Experimental Absorption Refrigerator

5.1 The cycle specification

Before constructing any system operating on the (2LiBr + $ZnBr_2$)/H_2O solution, the performances of two systems working under the same conditions, one working on (2LiBr + $ZnBr_2$)/H_2O and the other working on LiBr - H_2O solution, were evaluated to find out whether 2LiBr + $ZnBr_2$ has any real advantages over LiBr alone in water. The major component heat loads and the heat ratios for the following four sets of cycle conditions were calculated from the appropriate Duhring plots and their respective enthalpy/concentration charts and the results shown in Table 5.1. The following conditions were assumed for each cycle.

Cycle 1 - evaporating temperature = 7°C
- absorbing temperature = 30°C
- condensing temperature = 30°C
- generating temperature = 75°C

Cycle 2 - evaporating temperature = 5°C
- absorbing temperature = 35°C
- condensing temperature = 40°C
- generating temperature = 85°C

Cycle 3 - evaporating temperature = 4°C

- absorbing temperature = 40°C

- condensing temperature = 46°C

- generating temperature = 99°C

Cycle 4 - Same operating conditions as cycle 3, but with the $(2LiBr + ZnBr_2)/H_2O$ solution cooled to the absorbing temperature. (Not possible for LiBr alone.)

In the analytical evaluation of both systems, the following simplifying assumptions were made:

i) the refrigerant and absorbent phases were in equilibrium at points in the cycle where temperatures were specified.

ii) the evaporator and condenser pressures were the same as the steam table vapour pressure values for water.

iii) no pressure drop in the cycle except at the restrictors between the condenser and the evaporator and between the solution heat exchanger and the absorber.

Cycle No.	Solution			Circulation factor	q_c	q_e	q_a	q_h	q_g	Heat Ratio
	Type	Concentration, % Weak ξ_w	Strong ξ_s	λ	(KJ/Kg)	(KJ/Kg)	(KJ/Kg)	(KJ/Kg)	(KJ/Kg)	ξ
1	A	69.7	74.6	14.22	2516.3	2388.3	2397.3	1094.9	2525.3	0.946
	B	51.3	60.8	5.4	2516.3	2388.3	2659.4	475.2	2787.4	0.857
2	A	72.4	74.0	45.25	2492.1	2342.5	2551.5	3439.0	2701.1	0.867
	B	55.0	60.0	11.0	2492.1	2342.5	3035.0	979.0	3184.6	0.736
3	A	74.0	75.6	46.25	2493.3	2315.7	2873.5	4116.3	3051.1	0.759
	B	58.0	62.7	12.34	2493.3	2315.7	2760.9	1246.3	2938.5	0.788
4	A	74.0	75.6	46.25	2493.3	2315.7	2387.8	4601.9	2565.4	0.903
	B	58.0	62.7	12.34	2493.3	2315.7	2760.9	1246.3	2938.5	0.788
A = $2LiBr + ZNBr_2 + H_2O$ B = $LiBr + H_2O$										

Table 5.1 Comparison of $LiBr/H_2O$ and $(2LiBr + ZnBr_2)/H_2O$ systems operating under the specified conditions

iv) complete heat exchange in the heat exchanger for cycles 1 and 2 and for the (2LiBr + $ZnBr_2$)/H_2O of cycle 4. For cycle 3, complete heat exchange is not possible without crystallisation of salt and a temperature of strong solution leaving the exchanger of 46°C was assumed.

In both cases, the evaporator and condenser loads were the same. However a considerable advantage is observed in the reduction of absorber and generator loads for the (2LiBr + $ZnBr_2$)/H_2O system except in cycle 3. At the same time, however, there is a considerable increase in the heat exchanger loads for the (2LiBr + $ZnBr_2$)/H_2O system.

Of great importance in absorption system calculations is the mass flow rate of the strong solution which is needed to absorb unit mass flow rate of vapour from the evaporator. This quantity called the "circulation factor", λ, is determined from the mass and material balance for the non-volatile absorbents in the solution circuit and is given as:

$$\lambda = \frac{\beta_w}{\beta_s - \beta_w} \qquad (5.1)$$

where β_w = mass fraction of weak solution, (%)

β_s = mass fraction of strong solution, (%)

Gosney (1) recommended that if heat loss from the heat exchanger can be neglected, the heat transfer rate in the generator can be obtained by drawing the boundary around the generator and heat exchanger to give for unit mass of refrigerant:

$$q_g = [(h_1 - h_4 + \lambda(h_7 - h_4)] \qquad (5.2)$$

where q_g = heat transfer in the generator (KJ/Kg)

h_1 = enthalpy of refrigerant vapour leaving the generator (KJ/Kg)

h_4 = enthalpy of weak solution leaving the solution pump (KJ/Kg)

h_7 = enthalpy of strong solution leaving the heat exchanger (KJ/Kg).

As a result of the high values of λ, for the (2LiBr + $ZnBr_2$)/H_2O solution, the second term of equation (5.2) has a significant effect on the heat required in the generator. Table 5.1 shows that the circulation factor increases with reduced evaporating temperatures for both systems. Values for the (2LiBr + $ZnBr_2$)/H_2O solution are, however, markedly higher than those of the LiBr-H_2O system. Despite the high circulation factors, however, the heat ratios are higher than those of the LiBr-H_2O system except for cycle 3 where complete heat exchange is not assumed for the heat exchangers in both systems. The high circulation factor coupled with high strong solution

exit temperature from the heat exchanger could have accounted for this difference. For the same circulation factor but allowing for lower exit, temperature of strong solution from the heat exchanger, the heat ratio becomes higher than for the LiBr-H_2O system. This is because the effect of the high circulation factor has been reduced by the lower enthalpy of the lower temperature strong solution from the heat exchanger, resulting in a reduced q_g. The temperature of the strong solution delivered to the absorber, therefore, is an important factor affecting the system efficiency, hence the nearer it is to the absorbing temperature, the higher is the heat ratio which is a measure of the system efficiency.

The higher solubility characteristics of the (2LiBr + $ZnBr_2$)/H_2O solution permits lower heat exchanger exit temperatures without salt crystallisation. At this stage, therefore, it could be said that the (2LiBr + $ZnBr_2$)/H_2O system is more promising than the LiBr-H_2O system regarding system efficiency and salt crystallisation problems.

The experimental refrigerator was designed for Cycle 1 assuming an evaporator load of 500W. Other calculated design data are as shown below:

- generator load = 527W
- absorber load = 501W
- heat exchanger load = 229W

- condenser load = 526W
- the refrigerant flow rate = 0.209 g/s
- the weak solution flow rate = 3.18 g/s
- the strong solution flow rate = 2.97 g/s
- the circulation factor = 14.22

The heat transfer surface areas for the major components were found to be:

- evaporator = 0.322m^2
- condenser = 0.15m^2
- absorber = 0.084 m^2
- heat exchanger = 0.028m^2

5.2 The Layout and Description Of The Experimental Refrigerator

5.2.1 The Layout

Figure 5.1 shows the schematic diagram of the layout of the experimental refrigerator. Plate 5.1 shows the relative positions of the components of the refrigerator whilst Plate 5.2 shows the whole layout including both instrument panels. Plate 5.3 shows the instrument panel I on which the wattmeter, electronic thermometer, vacuum gauge, the electric heater switches, the d.c. supply for the electrical relays and the manometers, are mounted. The variacs for regulating the power supply to the heaters and the vacuum pump are also located at the bottom of this panel. Other instruments such as the flowmeters, hydrometers, solution pump discharge gauge and the

thermocouple sockets are shown on the instrument panel II in plate 5.4.

The refrigerator components are mounted on angle iron frameworks. The generator in an insulated wooden box was installed at the highest level and close to it on the same level was located the condenser. This was to reduce any pressure drop in the vapour line between the two vessels. The heat exchanger was placed directly under but close to the generator and the lines between them were insulated.

The evaporator contained in an insulated wooden box was the vessel at the lowest level. The absorber was at a slightly higher level on the support frame to facilitate the direction of refrigerant vapour to it from the evaporator.

The solution pump was placed well below the absorber with no restriction in the flow of the solution to it to facilitate its priming at start ups. The highest point of each vessel was connected to a vacuum header connected to the vacuum pump.

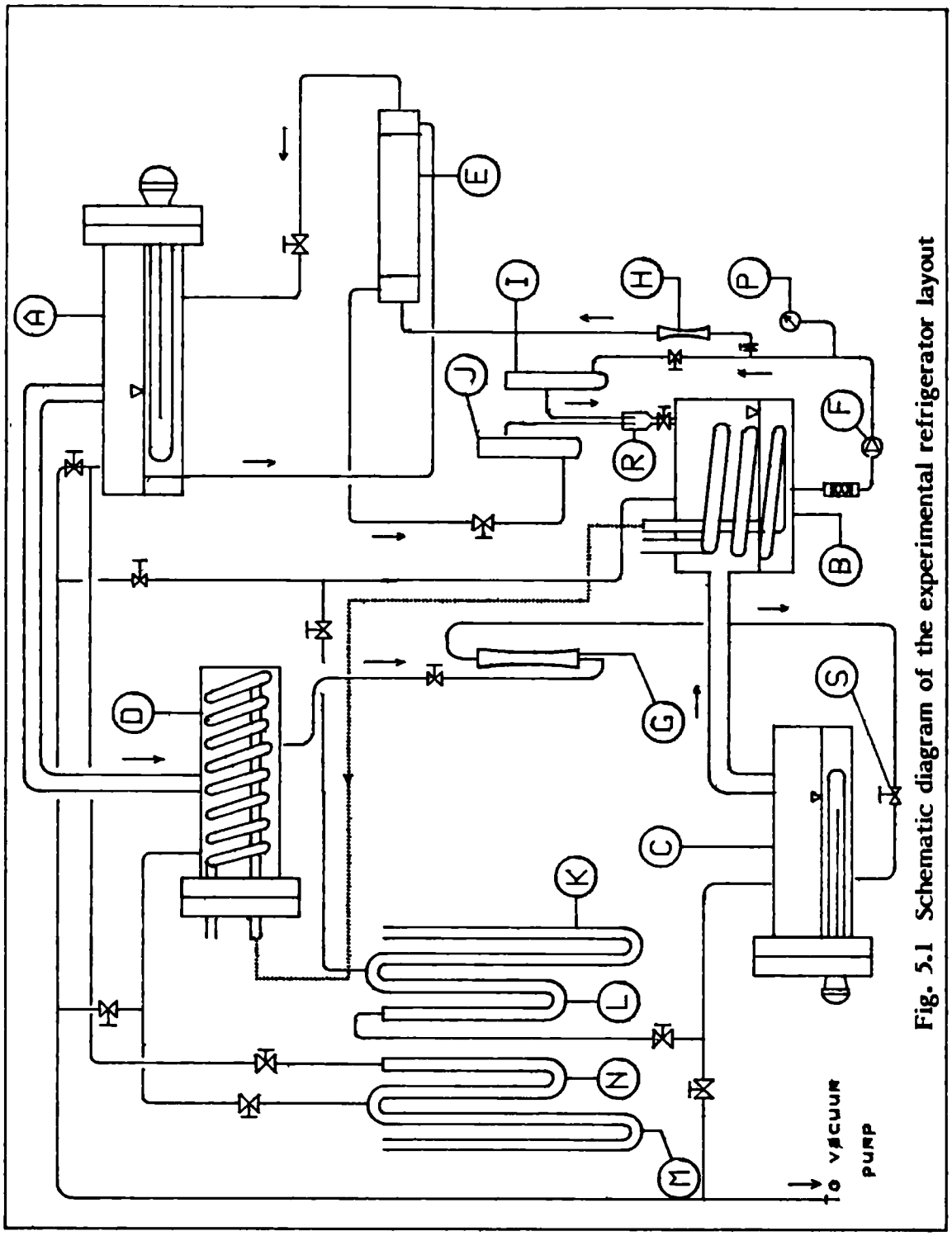

Fig. 5.1 Schematic diagram of the experimental refrigerator layout

Notation for Figure 5.1

A - Generator

B - Absorber

C - Evaporator

D - Condenser

E - Heat exchanger

F - Solution pump

G - Refrigerant flowmeter

H - Weak solution flowmeter

I - Weak solution hydrometer glass casing

J - Strong solution hydrometer glass casing

K,M- Mercury manometers

L,N- Tri-n-butyl citrate manometers

P - Vacuum gauge

R - Mixing pot

S - Regulating valve

Plate 5.1

Component Parts Of The Refrigerator

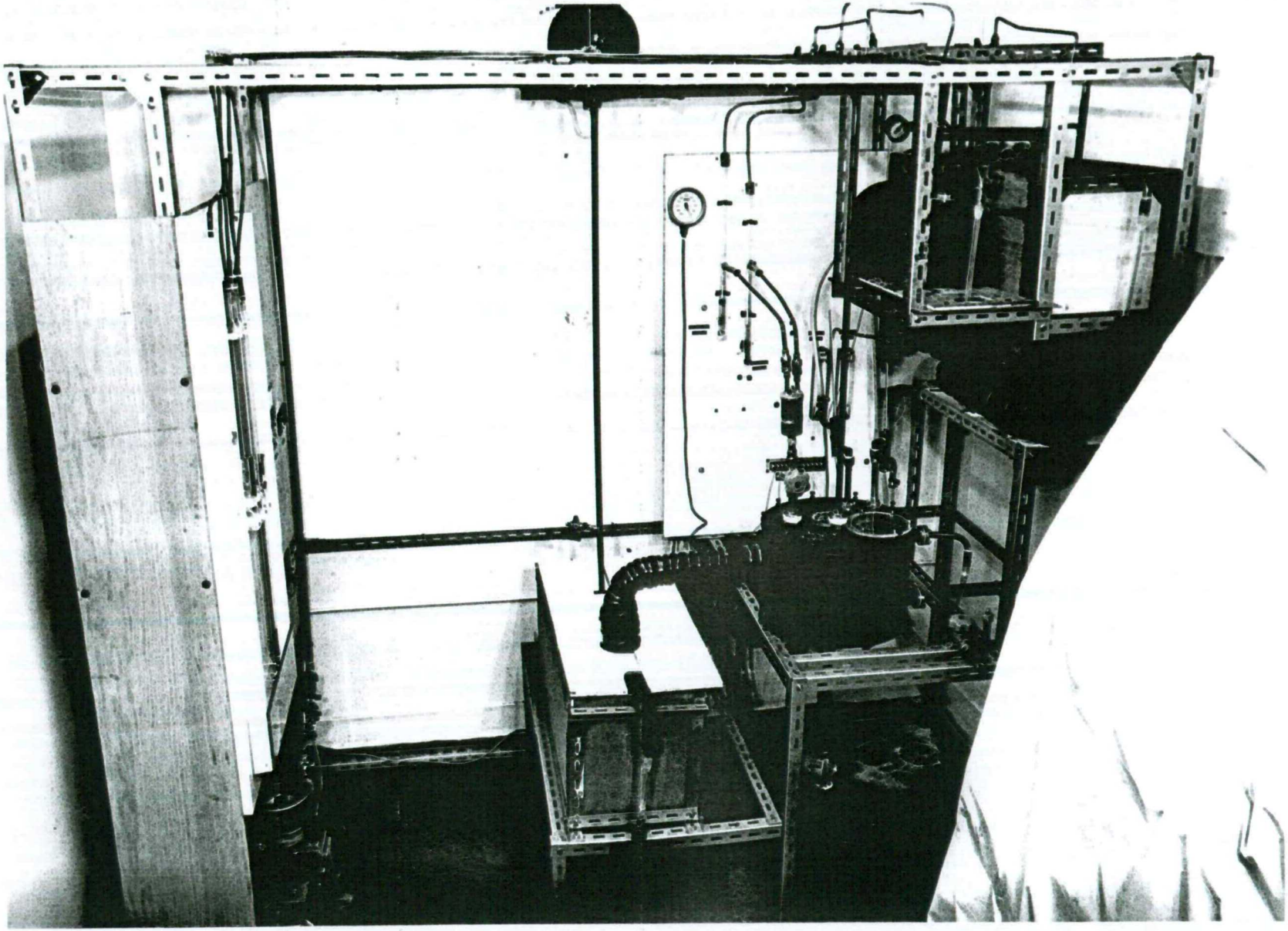

Plate 5.2

The Complete Layout Of The
Experimental Refrigerator.

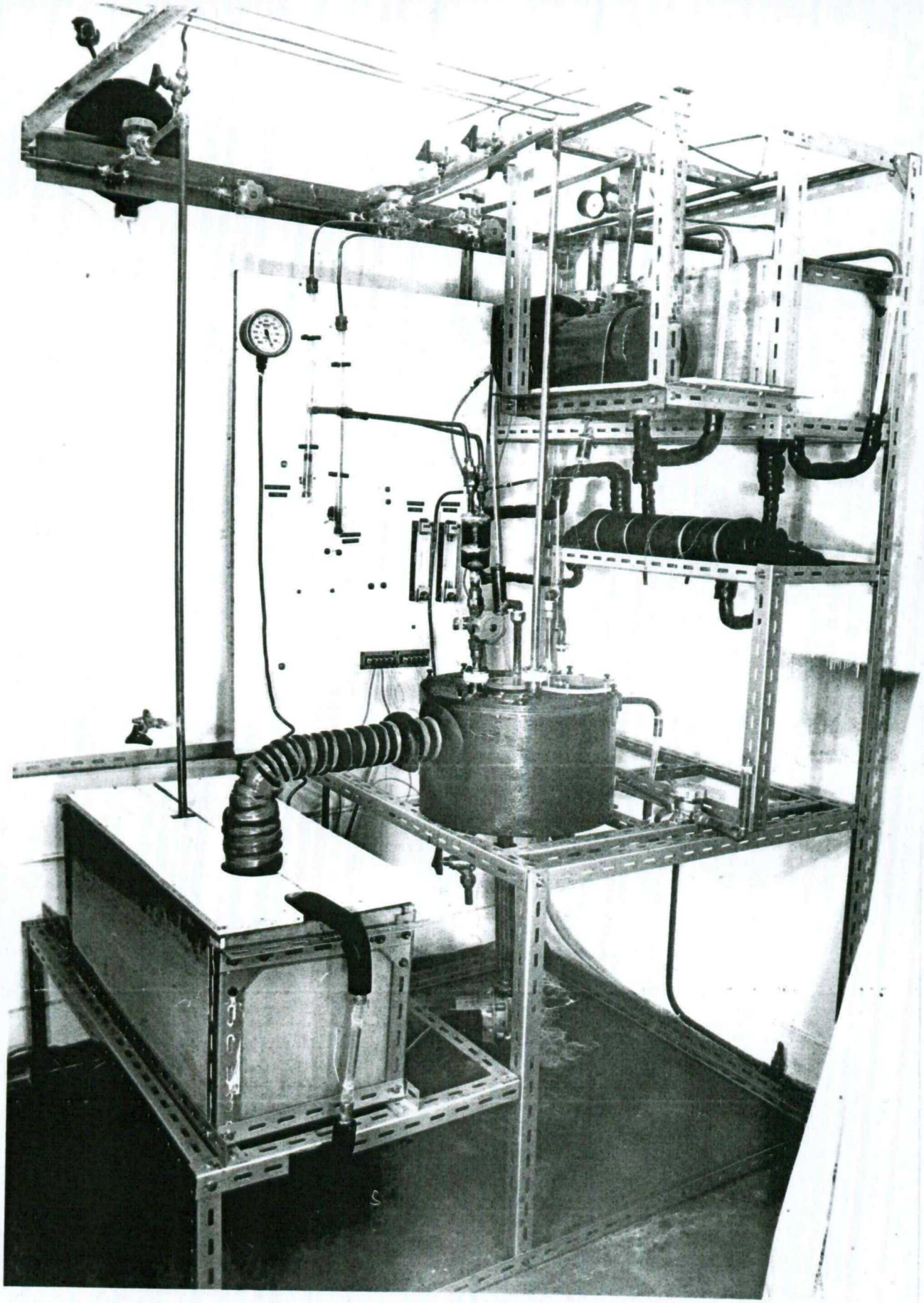

Plate 5.3

Instrument Panel I

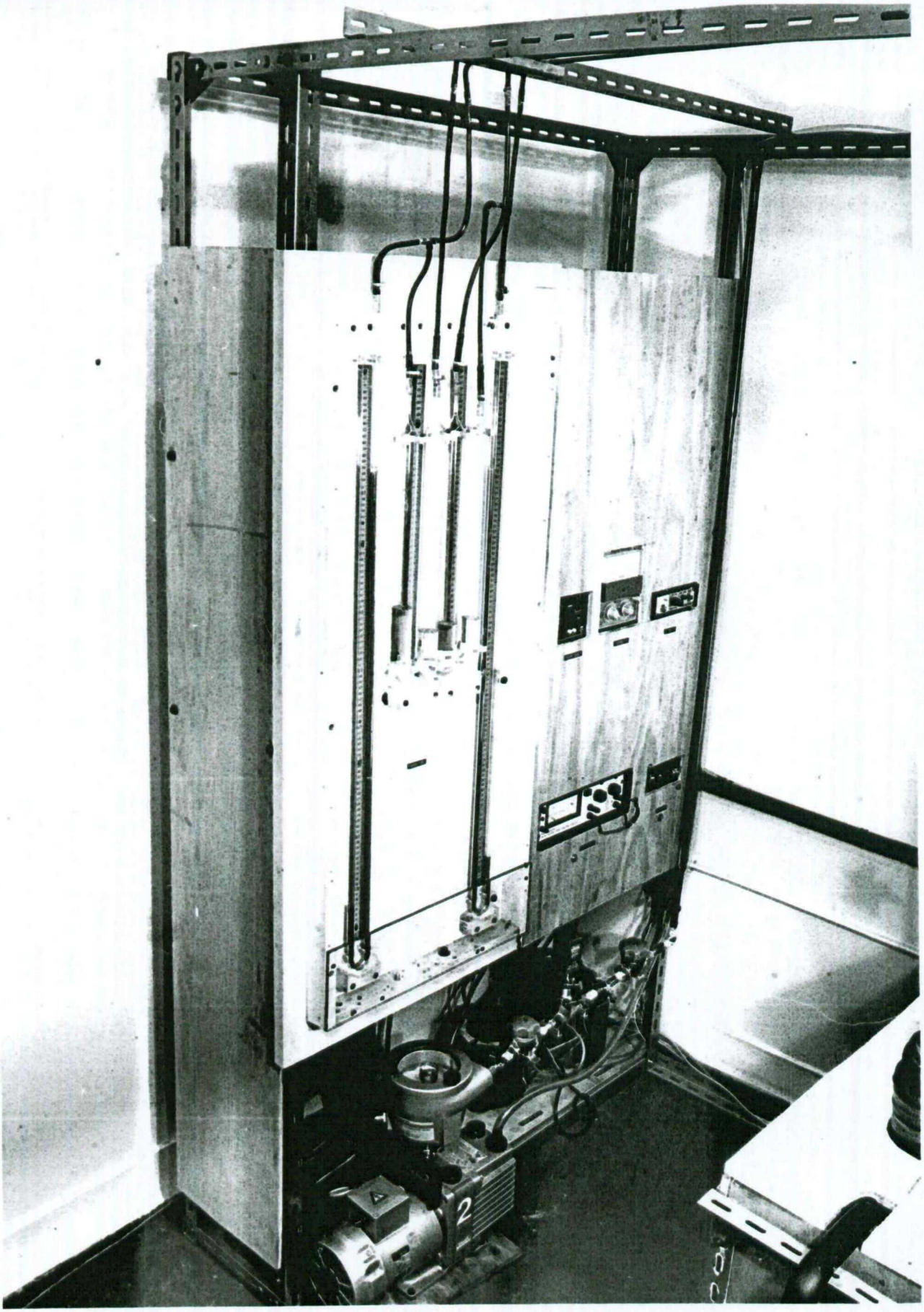

Plate 5.4

Instrument Panel II

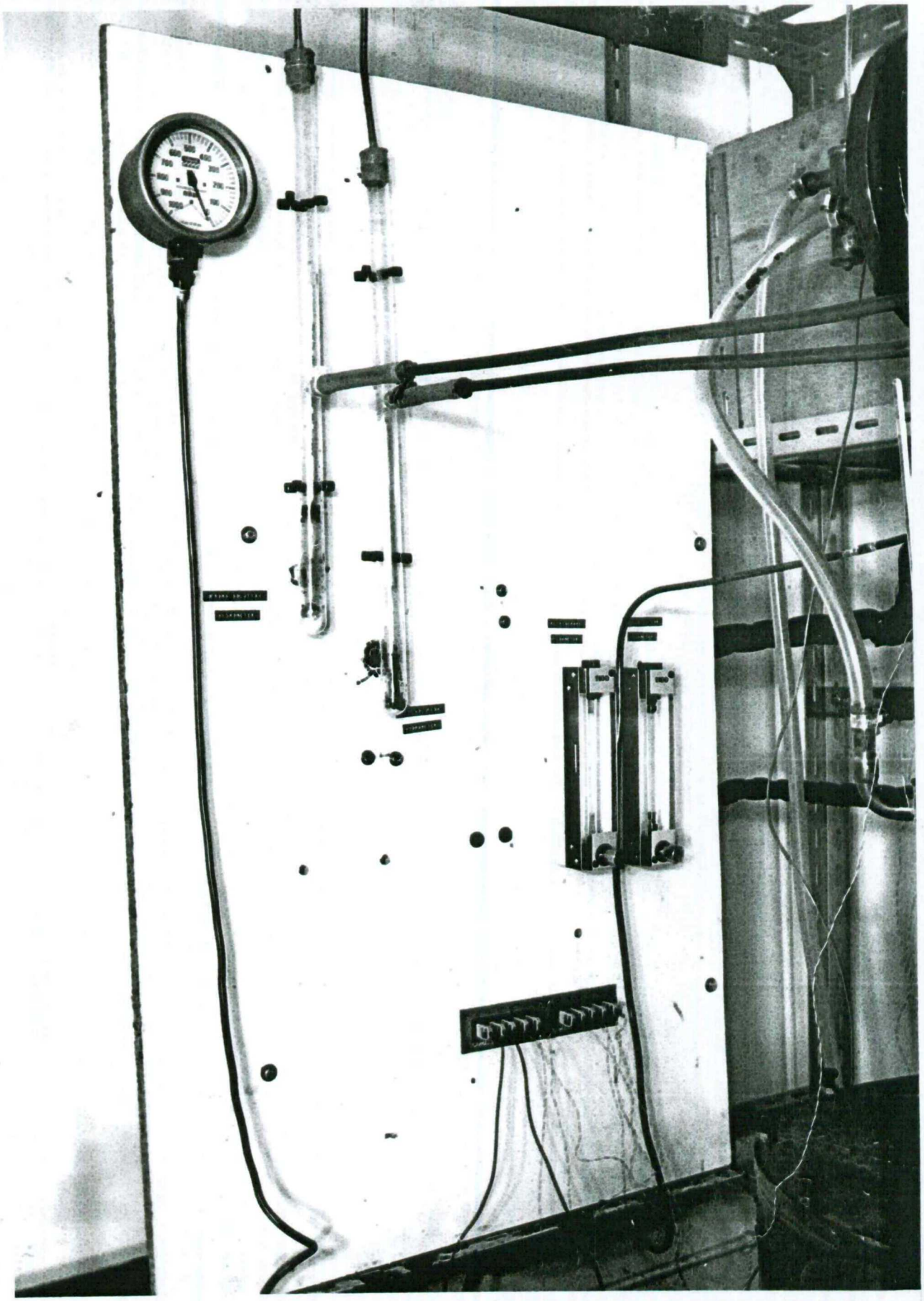

5.2.2. Description Of Refrigerator

The regeneration heat was supplied by a 1Kw electric immersion heater. Water vapour from the generator A in Figure 5.1 flowed into the condenser (D) where the heat of vaporisation was removed by cooling water flowing through the coil. The condensate then flowed through the flowmeter (G) and regulating valve (S) to the evaporator (C).

Inside the evaporator, heat was supplied by a 1Kw electric immersion heater to boil the refrigerant under very low vapour pressure (about 10mbar). The vapour given off was absorbed by the (2LiBr + $ZnBr_2$)/H_2O solution in the absorber (B). Inside the absorber, the heat of condensation of the refrigerant vapour and the heat of dilution of the absorbent were removed by cooling water flowing through the coils. As the refrigerant vapour dissolved in the absorbent, the refrigerant content and the vapour pressure of the solution increased. In order to maintain the vapour pressure of the solution at a level low enough to provide the low pressure and temperature required in the evaporator, it was necessary to continuously reconcentrate the solution. This was accomplished by pumping the weak solution with the pump (F) through the heat exchanger (E) to the generator (A). A portion of the weak solution was, however, recirculated through the absorber. The recirculated portion was

routed through a glass tube (I) that housed the weak solution hydrometer. A flowmeter (H) measured the flowrate of the weak solution to the generator.

The strong solution returning from the generator was routed through a glass tube (J) that housed a hydrometer. The hot strong solution from (J) and the relatively cold weak solution from (I) were mixed in a pot (R) before being throttled back to the absorber. The concentrated solution returning to the absorber was sprinkled over the cooling coils through a perforated tray inside the absorber, to facilitate the absorption process.

5.3 The experimental refrigerator component parts

In the manufacture of the generator, absorber, condenser and evaporator vessels, some lessons learnt from constructional problems encountered by Olama (25) and Alloush (78) who had earlier carried out similar constructions in this laboratory for experimental refrigerators utilising $(2LiBr + ZnBr_2)/CH_3OH$ as working fluids were considered. One such problem was the brazing of small diameter copper tubes directly on to relatively large steel shells. Such brazing points were frequent sources of leakages in the system that had to operate under vacuum,. To correct for this in these constructions, flanged steel nipples were machined and welded directly on to the steel vessels. The copper tubes were then brazed on to similar brass

flanges (50mm diameter). The steel and brass flanges were then bolted together with a thin PTFE gasket in between them.

For these vessels, use was made of available materials where reliability and accuracy of the experiments were not impaired.

5.3.1. The Generator

The generator, shown in Figure 5.2 was made from a mild steel pipe. One end was closed and the other end had a grooved flange. The flange cover (2) had 8 holes on a pitch diameter of 240mm. The grooved flange carried an o-ring to maintain vacuum in the vessel.

The flange cover supported the 1Kw capacity immersion heater (3) used to simulate the solar energy supply to the generator. The heater was installed in the lower portion of the horizontal shell. The vapour line connection to the condenser (4) was a 28.6mm O.D copper tube. The weak solution inlet connection from the heat exchanger (5) was a 9.5mm O.d copper tube whilst the strong solution outlet (6) was also a 9.5mm O.D copper tube installed to protrude into the shell to ensure that the immersion heater was always covered with solution to prevent element burnout. The 12.7mm connections near the closed end of the generator shell (7) were used to connect an external sight glass arrangement that indicated the level of the solution

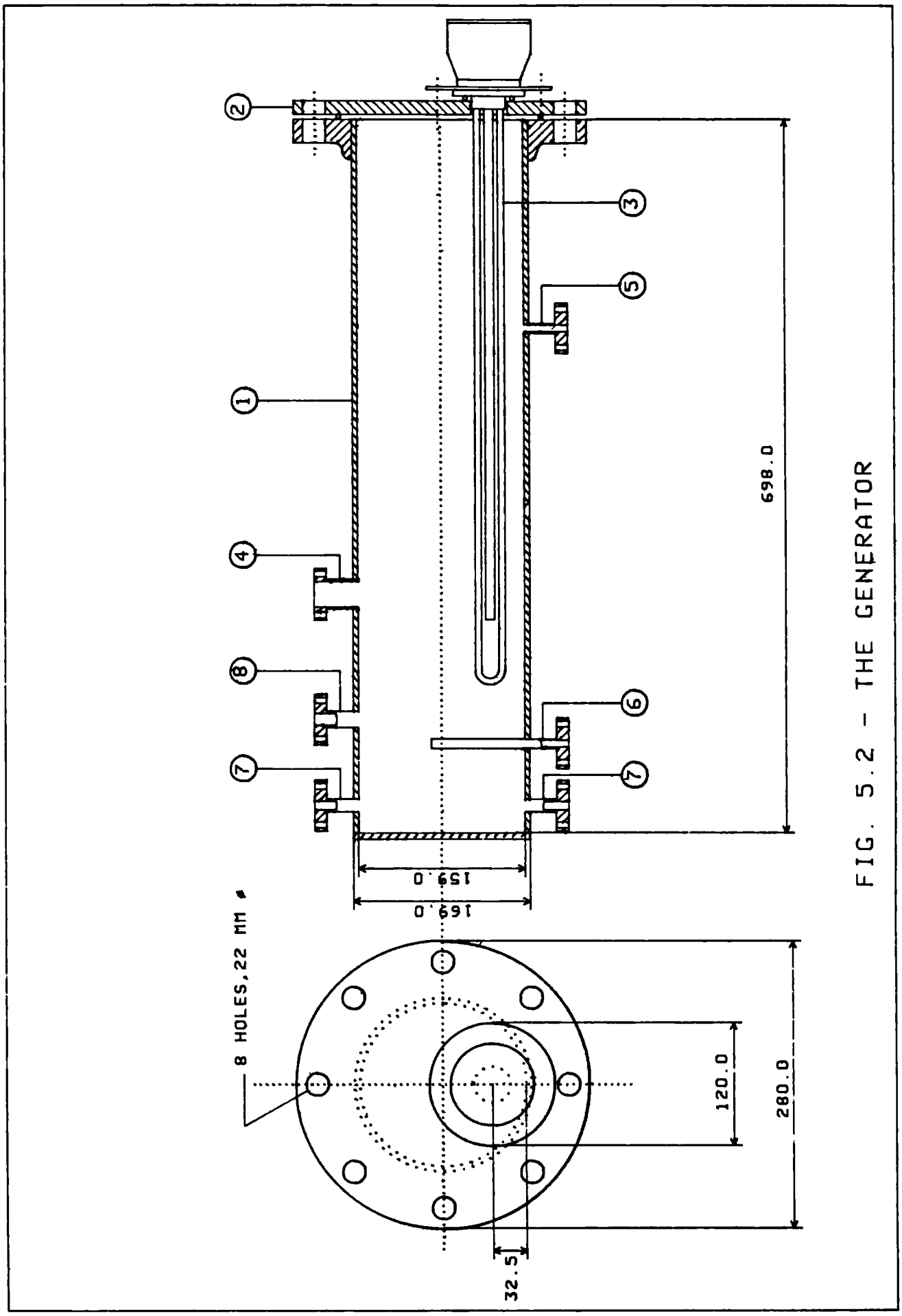

FIG. 5.2 - THE GENERATOR

Notation for Figure 5.2

1. Generator body
2. Generator flange
3. Immersion heater
4. Refrigerant vapour outlet
5. Weak solution inlet
6. Strong solution outlet
7. Connections for the level gauge
8. Vacuum connection

in the generator. The initial evacuation and subsequent purging of the generator was carried out through a 16mm O.D copper tube connected to the vacuum pump through the vacuum tube header. An isolating valve on the weak solution inlet line, between the generator and the solution heat exchanger prevented the solution from draining down at plant shut downs.

The generator was insulated with 19mm thick Armaflex insulation sheets and placed inside a wooden box where it was further covered with Fibre glass insulating materials.

5.3.2 The Absorber

Owing to the fact that there were no data available for the working fluid on which to base detailed theoretical design calculations for the absorber, the following useful assumptions were made in the estimation of the heat transfer surface required:

i) solution density, ρ= 1800 Kg/m^3

ii) specific heat capacity, C_p = 1.878 KJ/KgK

iii) specific heat of vaporisation, h_{fg} = 1485 KJ/Kg

iv) thermal conductivity, k = 0.458 W/mK

v) dynamic viscosity, μ = 13x10^{-3} Kg/ms

Based on these assumptions, a 1.7m long, 16mm O.D plain copper tube was arrived at.

The absorber body (Figure 5.3) was a 12.7mm thick cylindrical shell. Welded to the body (1) were the following flanged steel connections:

i) the refrigerant vapour inlet (5) - a 50mm I.D copper tube.

ii) the absorber solution charging inlet (6) for the 16mm O.D line.

iii) weak solution outlet (7) - a 25.4mm O.D line to which the solution pump located beneath the absorber is connected. The line protruded about 25mm into the absorber to avoid any sludge that might have accumulated at the bottom of the absorber from getting into the pump.

iv) an absorber drain connection (8) - a 16mm O.D line

(v) two 12.7mm O.D outlets, one at the base and the other at the side for the liquid level indicator.

Inside the absorber was a perforated drip tray (4), provided with three legs that rested on the absorber base on which the returned solution is directed. The solution was sprinkled down to wet the cooling coils to enhance the absorption of refrigerant vapour from the evaporator.

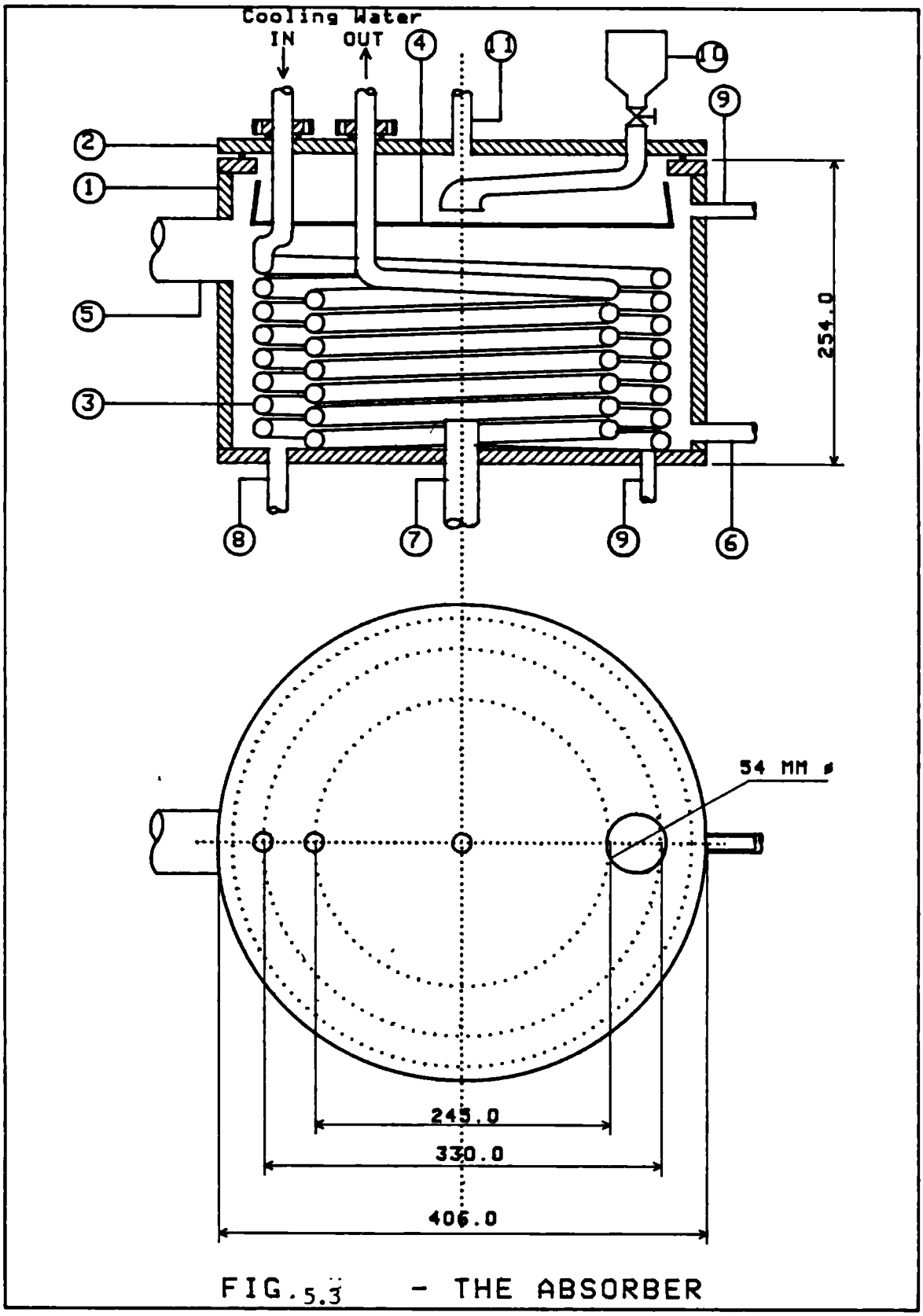

FIG. 5.3 - THE ABSORBER

Notation for Figure 5.3

1. Absorber body
2. Absorber cover
3. Cooling coils
4. Drip tray
5. Refrigerant vapour inlet
6. Absorber solution charging inlet
7. Weak solution outlet
8. Absorber drain connection
9. Connections for liquid level indicator
10. Mixing pot for returning strong solution and recirculated weak solution
11. Vacuum connection.

The absorber cover (2), with a groove to take an O-ring used in maintaining vacuum in the vessel also carried a connection for the mixing pot (10). Grooved brass flanges were brazed to the cooling coils inlet and outlet lines and the flanges with the O-rings in place were screwed on to the absorber cover.

The evacuation and subsequent purging of the absorber was carried out through a 16mm O.D line(11), connected to the vacuum pump through the vacuum line header. The cooling water temperatures were measured by mercury-in-glass thermometers in thermowells at the inlet and outlet of the cooling coils. The heat removal in the absorber was adequate as the weak solution was cooled to as low as 20°C depending on the cooling water flow rate. However, after a few minutes, the corrosive solution deposited some sludge believed to be erosions from the internal parts of the pipelines, on the drip tray, thus temporarily blocking the small perforations and restricting the dripping rate of the solution in the absorber. At this point, it was necessary to dismantle the absorber to enlarge the holes on the drip tray. This work was undertaken by an M.Sc student. A design calculation of the heat transfer surface area for the absorber is shown in Appendix B.

5.3.3. The Solution Pump

Experience in our laboratories with experimental

refrigerators utilising the $(2LiBr + ZnBr_2)/CH_3OH$ as working fluid had shown glandless pumps to perform better for solution circulation than those with mechanical seals. Therefore, for this experimental refrigerator, a glandless pump type S10, manufactured by Crane Ltd, but originally designed for hot water circulation in central heating systems, was selected to perform the dual function of recirculating the weak solution around the absorber and also transferring weak solution through the heat exchanger to the generator.

The pump had two speeds adjusted from a terminal box switch: 1700 rpm at an input power of 46W and 2500 rpm at an input power of 99W. Further regulation of the speed was possible via the manual duty regulator fitted on the pump casing. The pump with 25mm branch sizes and driven by a single phase electric motor has a cast iron casing. The impeller material was of Noryl and the shaft which also carried the rotor of the motor was made of stainless steel with self lubricating graphite sleeve bearings between the rotor and impeller, and at the far end of the rotor. The rotor rotated in the solution inside a rotor can of stainless steel construction but the stator outside the can, is dry. Particles of dirt were prevented from entering the motor can by fitting a sintered bronze filter at the impeller end of the can thus preventing seizure of the rotor.

With the pump running at 2500 rpm the flow rate is 0.68 l/s at 250 mbar head. The pump performed well under operational conditions of the refrigerator without any reaction between the solution and the graphite bearing materials as was the case with the $(2LiBr + ZnBr_2)/CH_3OH$ solution.

5.3.4 The Solution Heat Exchanger

Even though no transport data was available for the solution on which to base a more elaborate evaluation of the heat exchanger required for the system, the same values assumed in the estimation of the absorber heat transfer surface area were also used to estimate the exchanger heat transfer area. In estimating the overall coefficient of heat transfer between the fluid streams, U, a thin walled copper tube, 16mm O.D was assumed as the heat exchanger tube and a fouling resistance on outside of tube of $0.0002 m^2K/W$, generally acceptable for normal solar system design was also assumed (9/). The following equations, obtained from (9/) were used to calculate the film coefficients.

$$h_i = \frac{0.225k}{D_i} (Re)^{0.8} (Pr)^{0.4} \qquad (5.3)$$

$$h_o = \frac{0.385k}{D_o} (Re)^{0.56} (Pr)^{0.3} \qquad (5.4)$$

where: k = thermal conductivity of solution, W/mK

D_i = inner diameter of tube, m

D_o = outer diameter of tube, m

h_i = inner film coefficient, W/m^2K

h_o = outer film coefficient, W/m^2K

Re = Reynolds number

Pr = Prandtl number

Assuming fluid velocities of 1.22 m/s and 0.61 m/s for flows inside and outside the tube respectively and neglecting the unit resistance of the tube, U was found to be 1336 W/m^2K.

Other design conditions were: 75°C and 40°C hot solution inlet and outlet temperatures respectively; 30°C and 60°C warm solution inlet and outlet temperatures respectively. Applying a factor of safety of 2 to cater for deviations in assumed property values for the solution from actual values and other operational conditions, the estimated heat transfer area of the heat exchanger was $0.028m^2$.

A Dunham-Bush heat exchanger, basically designed for conventional vapour compression refrigeration system was available but it was appreciated that the area might not be enough. This exchanger was a shell and tube type with inner fin construction. The weak solution flowed through the tubes and the strong solution through the shell side. The shell was 89mm O.D and the overall length was 549mm.

The heat exchanger was insulated with a 19mm thick layer of AF/Armaflex insulation with thermal conductivity at 20°C of 0.036W/mK. Thermopockets were provided to measure the temperatures at inlets and outlets of the strong and weak solutions respectively.

Even though the heat exchanger performed well in that it increased the temperature of the weak solution entering the generator appreciably, the cooling of the strong solution from the generator was inadequate. This is probably because the heat transfer surface area of the only heat exchanger used was inadequate. However, this problem was partly solved by designing for the still warm solution from the heat exchanger to mix with the relatively cold recirculated weak solution from the absorber in a pot before being throttled into the absorber. This arrangement reduced the temperature of the mixed solution returned to the absorber to an acceptable level without the need for a second heat exchanger. For instance, the following temperatures were recorded for a particular run:

- weak solution outlet from absorber = 21.2°C
- weak solution inlet to heat exchanger = 26.4°C
- weak solution outlet from heat exchanger = 42.7°C
- strong solution inlet to heat exchanger = 53.1°C
- strong solution outlet from heat exchanger = 34.2°C.
- mixed solution to the absorber = 27.4°C

5.3.5 The Evaporator

The evaporator as shown in Figure 5.4 was made from a mild steel cylindrical shell (1), closed by a welded plate at one end and flanged at the other end. The flange cover (2) supported a 1KW immersion heater (3), installed at the lower portion to keep it continuously submerged by the liquid refrigerant. The heater was also used to simulate the heat load in the evaporator.

The saturation pressure in the evaporator was taken from steam tables using the measured evaporating temperatures. The temperature probe was installed in the flange cover through a small hole (8).

Welded to the evaporator body (1) was a 54mm O.D pipe (4) which conveyed the refrigerant vapour to the absorber. A flexible hose was used to connect this pipe to the absorber vapour line pipe to relieve any stress on the pipe connections that might be introduced as a result of misalingment between the absorber and the evaporator. Also welded to the body were: a 6mm O.D refrigerant inlet line from the condenser (5), a 16mm O.D vacuum line (7) for the evacuation of the evaporator and two 12.7mm O.D pipes (6), that were connected to the liquid level indicator.

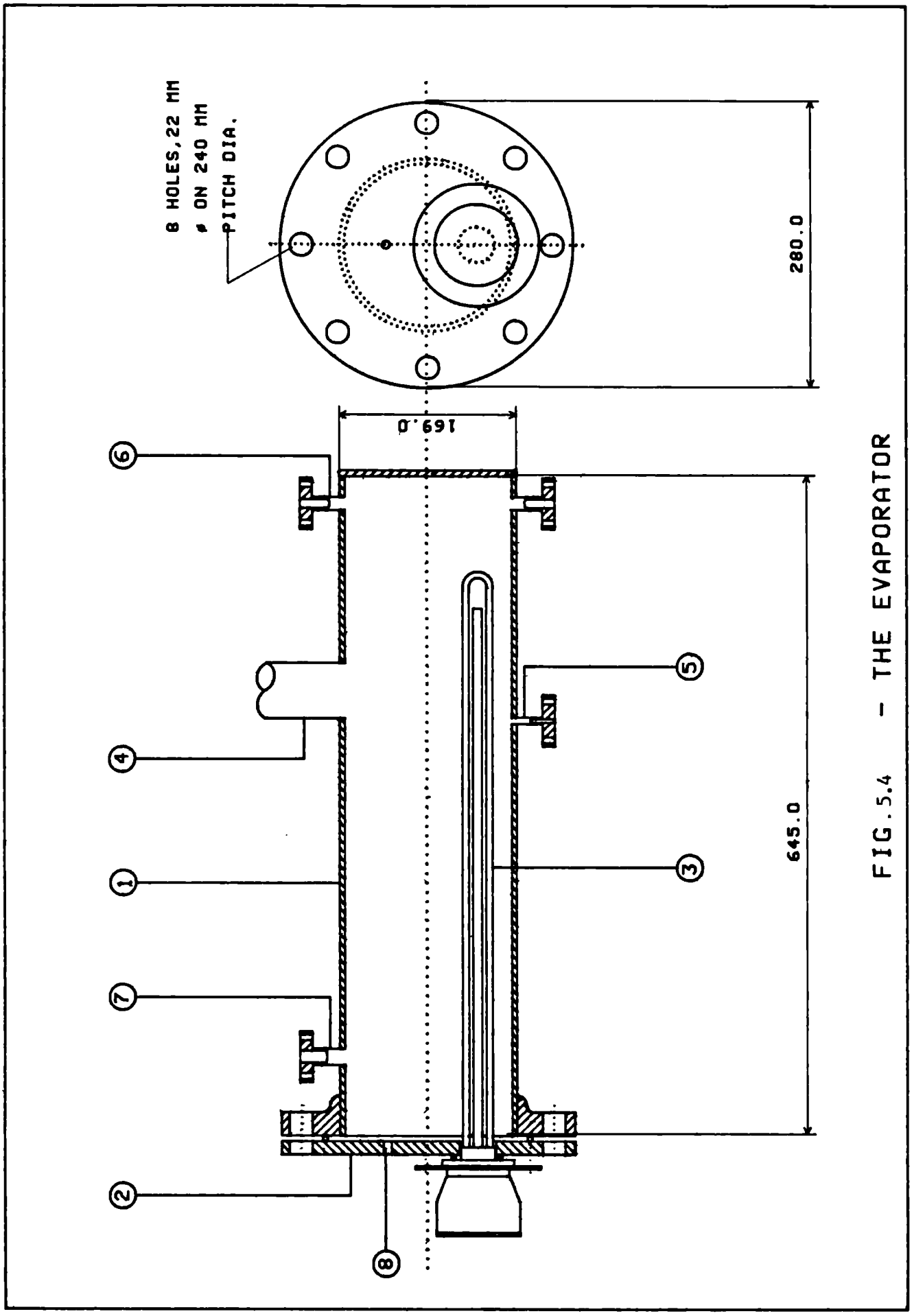

FIG.5.4 - THE EVAPORATOR

Notation for Figure 5.4

(1) - The evaporator body

(2) - Flange cover

(3) - 1Kw immersion heater

(4) - Refrigerant vapour outlet

(5) - Liquid refrigerant inlet

(6) - Connections for the level indicator

(7) - Vacuum line

(8) - Hole for the temperature probe

The whole vessel was insulated with 19mm thick Armaflex insulating sheets then placed inside a wooden box which was filled with some fibre glass insulating materials.

The performance of the evaporator was satisfactory except that its response to changing operating conditions were slow because it contained by necessity a large amount of refrigerant liquid.

The design calculation for the heat transfer surface required in the evaporator is shown in Appendix C.

5.3.6 The Condenser

The condenser, shown in Figure 5.5 was basically of the same material as the evaporator. The spirally wound cooling coil (3) was made from a 3.0m length of 16mm O.D copper tube coiled to 9 turns of 96mm pitch diameter. This coil was supported from the flange cover (2) which was bolted to the grooved flange with the O-ring in place to maintain the vacuum required in the vessel. Grooved brass flanges were brazed to the coil inlet and outlet pipes after passing them through the flange cover. With the O-rings in place the brass flanges were screwed on to the flange cover. Cooling water flowed inside the coil whilst the refrigerant vapour flowed outside it. The design calculation for the coil heat transfer surface required is shown in

Appendix D.

The saturation pressure in the condenser was taken from the steam tables using the measured condensing temperature by a probe installed through hole (8).

Welded to the condenser body (1) were the following flanged steel nipples:

i) a 28mm O.D, for vapour inlet from the generator (4).

ii) a 6mm O.D, for liquid refrigerant outlet to the evaporator (5)

iii) a 16mm O.D, for vacuum line connections (6)

iv) two 12.7mm O.D, for connecting the liquid refrigerant level indicator.

To facilitate heat rejection by the condenser, it was not insulated. The condenser operated satisfactorily as condensing temperatures lower than design values were obtained. There was some subcooling also as the cooling coil was partly immersed in the refrigerant liquid.

5.3.7 Other components used in this system

i) The immersion heaters and the control circuit

As mentioned in Chapter One, solar heated fluids pass through heating coils in the generator. In this work, no attempt was made to use solar energy directly to heat the solution. Instead, it was decided to simulate

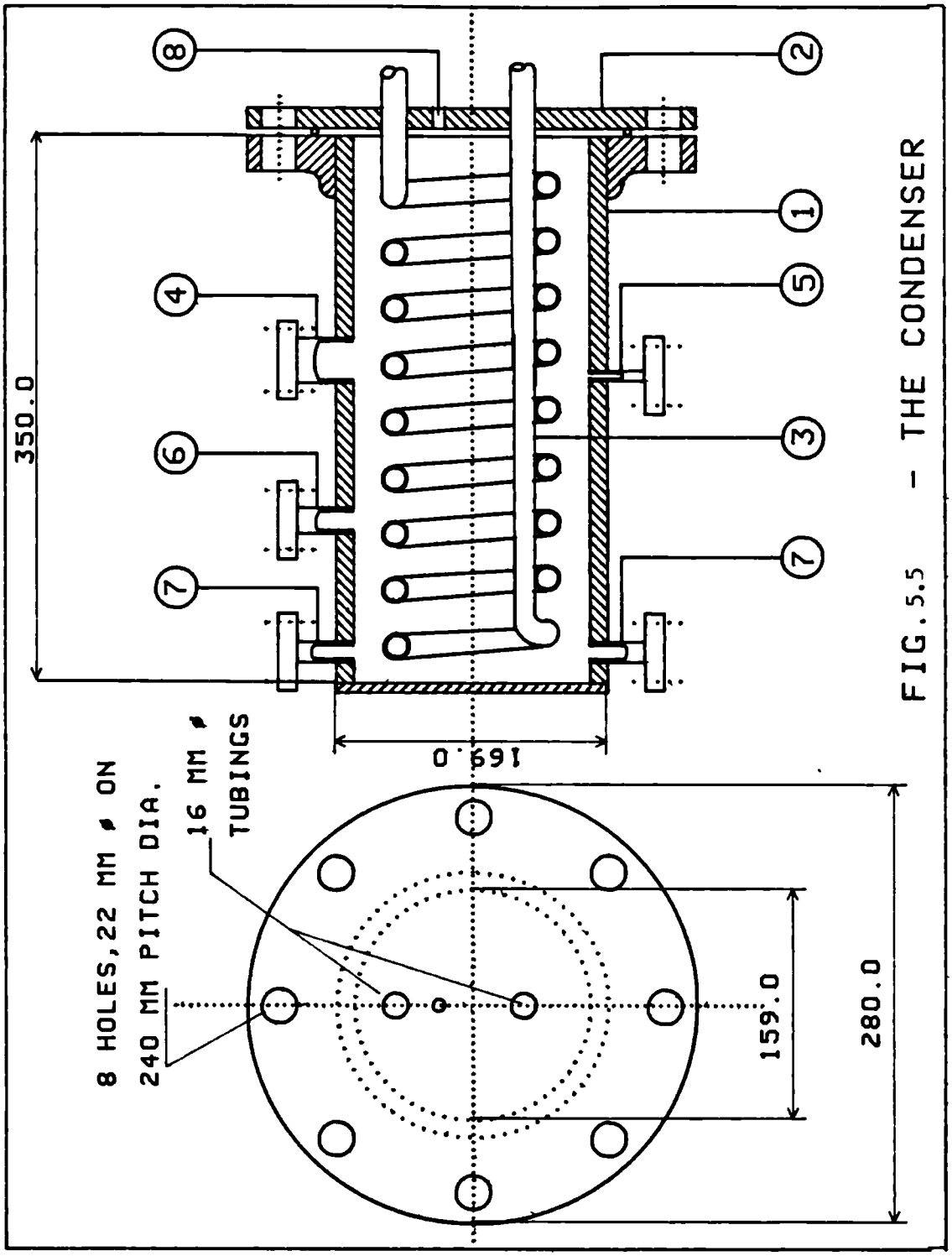

FIG. 5.5 - THE CONDENSER

Notation for Figure 5.5

(1) - The condenser body

(2) - Flange cover

(3) - Cooling coil

(4) - Refrigerant vapour inlet

(5) - Liquid refrigerant outlet

(6) - Vacuum line

(7) - Connections for the liquid level indicator

(8) - Hole for the temperature probe

the solar heating aspect with a 1Kw electric immersion heater but to show that the obtained operational temperatures were possible for conventional flat-plate solar energy collector in areas of abundant sunshine. The heat load in the evaporator was also simulated by a 1Kw electric immersion heater.

The heaters used were Eltron FMB010 type, basically designed for oil heating. Each heater was powered from a single phase supply with a maximum immersion length of 570mm. They were operated through variacs, switches and relays arranged to use only one wattmeter to indicate the power supply to each heater.

The block diagram of the control circuit is shown in Figure 5.6. The heaters were so connected that power was supplied to each of them at all times but with the use of the switches (S_1 and S_2) and two relays (RA_1, RA_2 and RB_1, RB_2),only the power supply to one of them could be routed through the wattmeter at a time. The two switch knobs were inter-connected to ensure that they were switched on at the same time. With the switches in positions b_1 and b_2, the generator heater only was connected through the wattmeter. Once the switches were moved to positions a_1 and a_2, the relay switches moved to the dotted line positions with the evaporator heater now routed through the wattmeter. The relays were connected through a 12v d.c supply as shown in the insert of Figure 5.6.

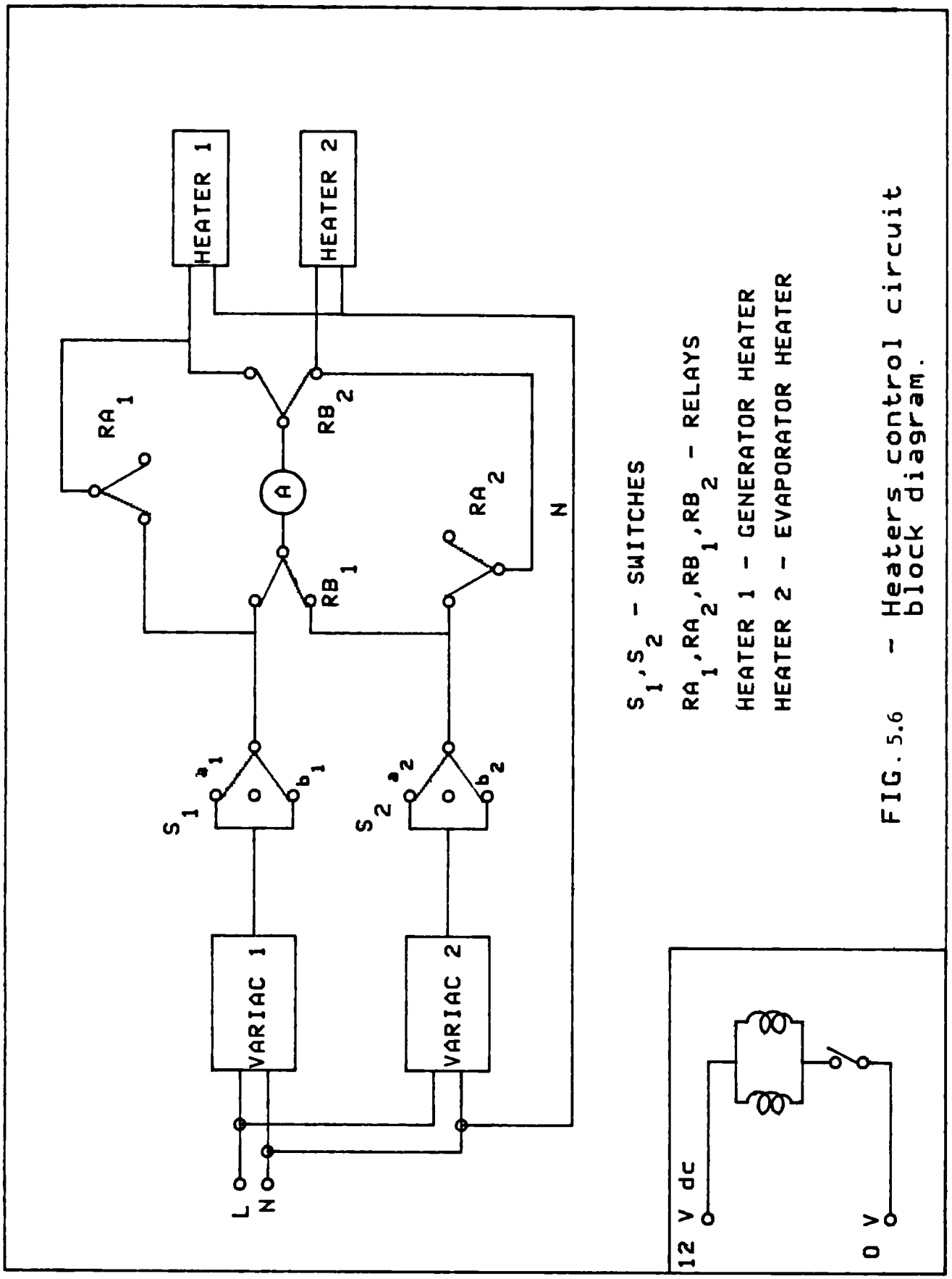

FIG. 5.6 - Heaters control circuit block diagram.

ii) The Flowmeters

Two flowmeters were used, one between the condenser and the evaporator (Figure 5.1, G) and the other between the absorber and the heat exchanger (Figure 5.1, H) to measure the flow rate of the weak solution. The flowmeters manufactured by KDG Rotameter Works, worked on the variable area principle.

The refrigerant flowmeter was factory calibrated for flow rates in the range of 0.0 - 0.46 g/s of water at 20°C. The solution flowmeter, graduated in millimetre scale was calibrated in our laboratory for solution concentration of 69. 88% for flow rates in the range of 0.76 to 3.50 g/s at 21°C.

Each of the flowmeters had a needle valve which was used to control the flow rates in addition to some vacuum valves on the affected lines.

iii) Temperature Measurements

Copper/Constantan thermocouples were used for temperature measurements in the system. Typical arrangements are shown in Figure 5.7 where the thermocouple is passed through small bore stainless steel tubes and sealed at the top with Araldite. The hot junction was thus in direct contact with the liquid whose temperature was being measured. Special temperature probes were, however, used for temperature determination in the condenser and evaporator. These

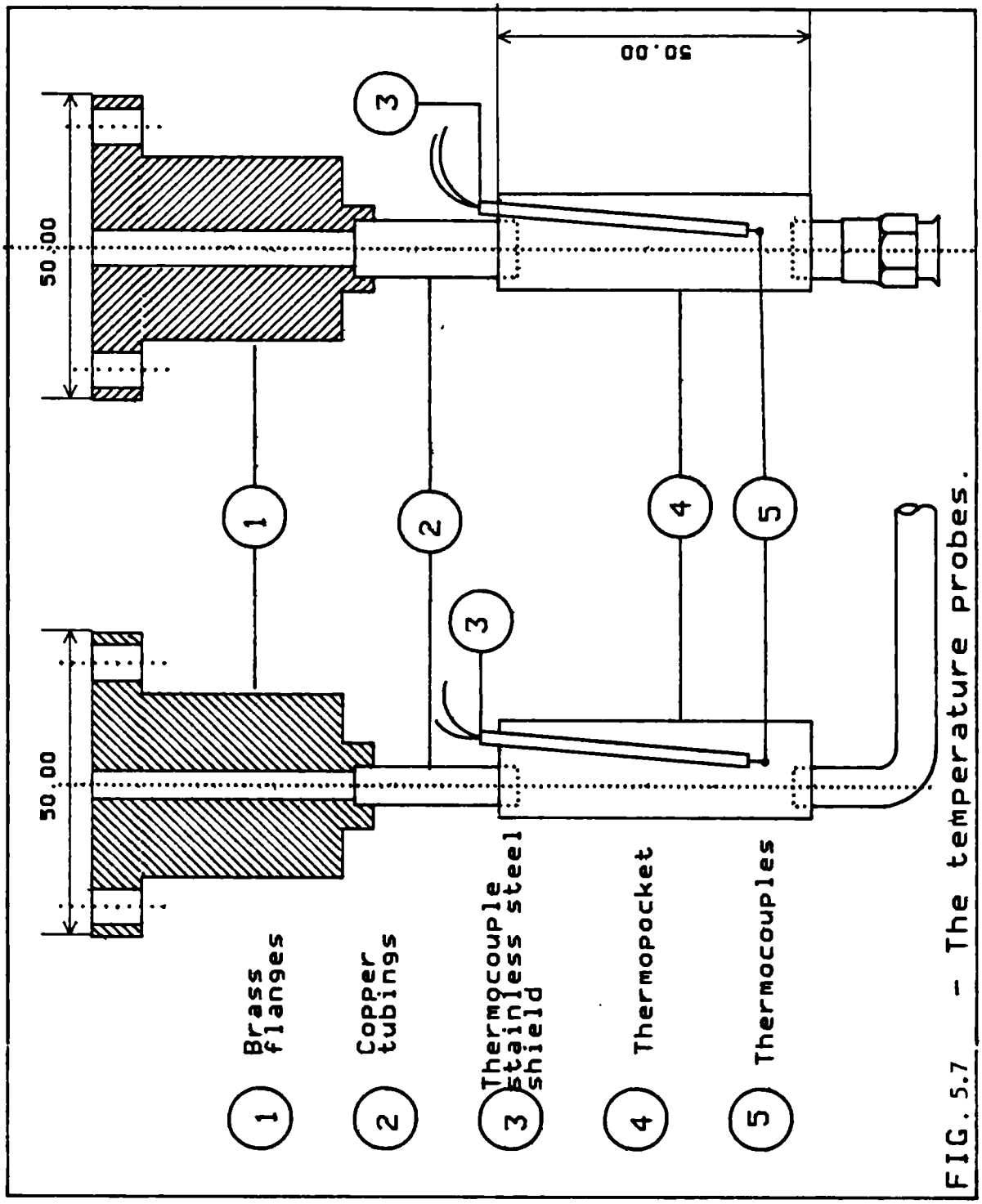

FIG. 5.7 - The temperature probes.

probe sensors were of 3mm diameter and about 10cm long with 2m lead length.

Temperature measurements were made at ten points around the system as shown in Figure 5.8, using the thermocouples. Mercury-in-glass thermometers placed inside oil-filled thermowells were, however, used for measuring the cooling water temperatures.

The cold end of each thermocouple was connected to a miniature plug. The ten miniature plugs were plugged into ten miniature sockets mounted side by side on the instrument panel II through 2-5way connector panels (plate 5.4). Using a 0.19mm diameter, ptfe insulated thermocouple wires, the panel mounted connectors were connected to a type 1625 Cormark Electronics thermometer mounted on instrument panel I (Plate 5.3). The electronic thermometer with 10-way selector units could measure in the range of $-100^{o}C$ to $+300^{o}C$ in 40 steps of $10^{o}C$ with an accuracy of $\pm 0.5^{o}C$ at $23^{o}C$. The resolution per division was $0.1^{o}C$. It was operated through a 9v dry cell battery. The thermometer incorporated a built-in reference function with a stability of $\pm 0.025^{o}C$ per ^{o}C.

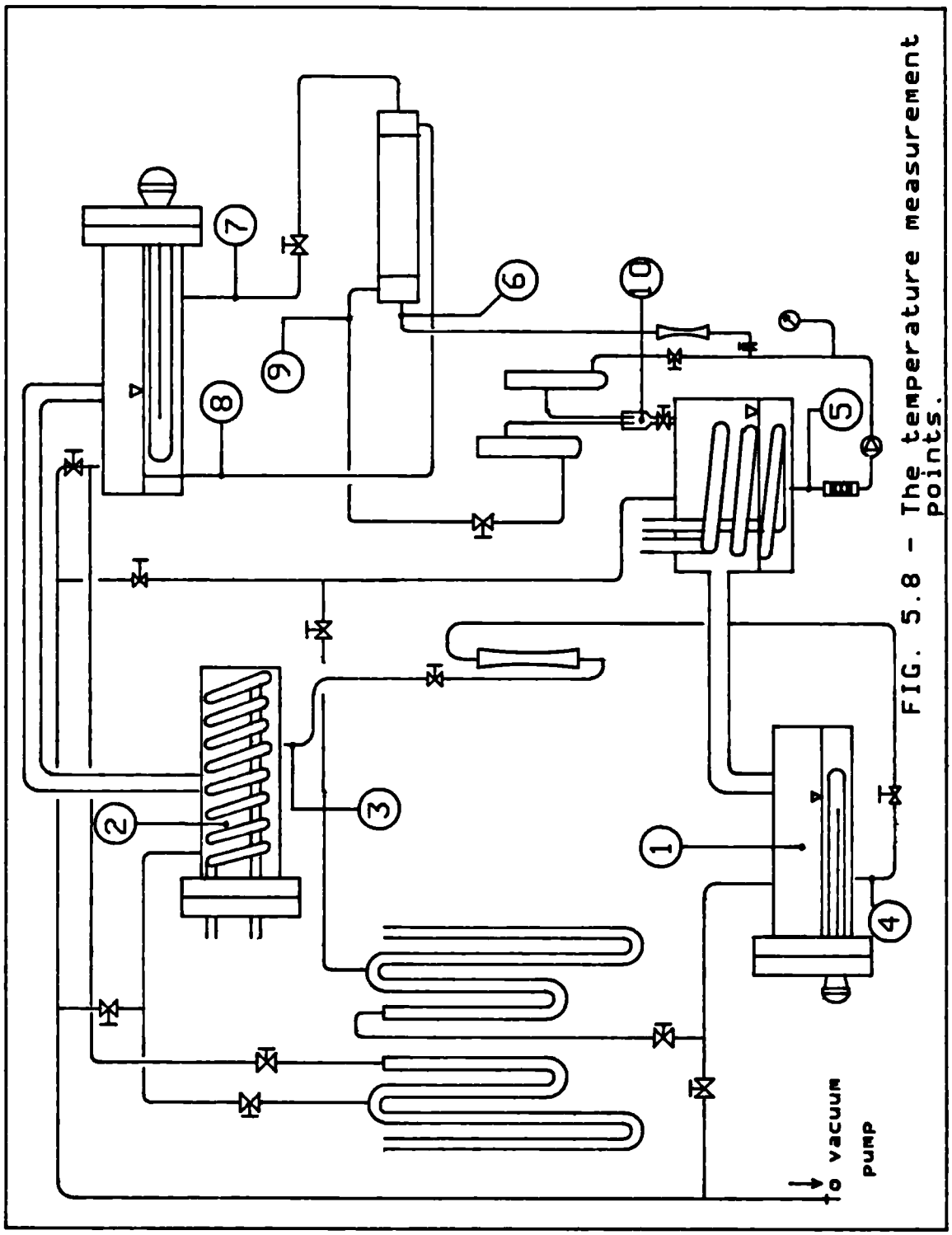

FIG. 5.8 - The temperature measurement points.

Notation for Figure 5.8

(1) Evaporating temperature

(2) Condensing temperature

(3) Liquid refrigerant from condenser

(4) Liquid refrigerant to the evaporator

(5) Weak solution from absorber

(6) Weak solution inlet to heat exchanger

(7) Weak solution inlet to generator

(8) Strong solution outlet from generator

(9) Strong solution outlet from heat exchanger

(10) Mixed solution in absorber

iv) Device for measuring mass fraction of solutions

The mass fraction of the solutions were deduced from measured temperatures and densities. Two hydrometers were used, each housed inside a glass tube closed at the bottom end and covered at the top with rubber stoppers. The solution inlets and outlets in these tubes were so arranged that there was always enough liquid to float the hydrometers. The space above the solution in each tube was connected to the vacuum line through a 6mm O.D copper tube passed through the rubber stopper.

In calibrating the hydrometers, it was found that they were too light for highly concentrated solutions. In order to be able to use them, a small weight was stuck to each with Araldite to sink them to levels where their original graduations were still usuable with a change of calibration.

In the new method, the specific gravities of the solutions as recorded by the original graduations on the hydrometers were measured for four solution concentrations ranging from 50% - 78% for the weak solution and 59% - 78% for the strong solution at solution temperatures of 20°C, 30°C, 50°C and 60°C for the weak solution and 25°C, 40°C, 50°C, and 60°C for the strong solutions. The data were fitted to obtain equations relating the solution concentration with specific gravity and the equation constants expressed

in terms of solution temperatures. So, during the experiments, the solution temperatures and the hydrometer readings were recorded and the solution concentrations calculated using equations 5.3 - 5.7 shown below:

For the weak solution hydrometer

- SG range = 1.000 - 2.000
- original weight of hydrometer = 22.99g
- added weight including weight of Araldite = 8.55g
- Total weight = 31.54g.

For the strong solution hydrometer

- SG range = 1.400 - 2.000
- original weight of hydrometer = 35.08g
- added weight including weight of Araldite = 8.51g
- Total weight = 43.59g.

The hydrometer calibration equation is assumed to be:

$$\%_{SG} = A + BS + CS^2 + DS^3 \qquad (5.3)$$

$$A = A_o + A_1 t + A_2 t^2 + A_3 t^3 \qquad (5.4)$$

$$B = B_o + B_1 t + B_2 t^2 + B_3 t^3 \qquad (5.5)$$

$$C = C_o + C_1 t + C_2 t^2 + C_3 t^3 \qquad (5.6)$$

$$D = D_o + D_1 t + D_2 t^2 + D_3 t^3 \qquad (5.7)$$

where: $\%_{SG}$ = solution mass fraction, %

S = specific gravity (as recorded by the hydrometers)

t = solution temperature, °C.

The data obtained is shown in Table 5.2 for the weak solution and in Table 5.3 for the strong solution. The constants of equations (5.4) to (5.7) are shown in Table 5.4. At any solution temperature desired, the constants of equation (5.3) can be calculated and for the recorded specific gravity reading of the hydrometer, the solution concentration can be calculated.

Solution Temperature (°C)	Specific gravity Reading S	Concentration (%)
20	1.250	50.27
	1.410	60.09
	1.620	69.70
	1.770	76.68
30	1.235	51.85
	1.400	57.56
	1.602	69.99
	1.750	75.37
50	1.222	50.26
	1.390	60.89
	1.585	71.02
	1.740	77.77
60	1.218	50.34
	1.385	61.67
	1.580	72.06
	1.730	77.57

Table 5.2 Calibration data for the weak solution hydrometer

Solution temperature (°C)	Specific gravity reading S	Concentration (%)
25	1.490	60.91
	1.580	65.43
	1.665	69.34
	1.830	75.11
40	1.480	61.69
	1.570	63.98
	1.655	68.99
	1.820	76.83
50	1.475	59.64
	1.555	63.74
	1.645	68.43
	1.790	78.15
60	1.468	59.92
	1.550	64.42
	1.633	68.50
	1.780	75.54

Table 5.3 Calibration data for the strong solution hydrometer

Equation constants	Weak solution hydrometer (Range: 1.000-2.000)	Strong solution hydrometer Range: 1.400-2.000
A_0	-12313.2861	-91016.26752
A_1	1031.01811	7057.73781
A_2	-25.552666	-167.825689
A_3	0.19621266	1.255914
B_0	24706.672	166915.5026
B_1	-2069.3603	-12956.76268
B_2	51.319606	308.480742
B_3	-0.394494	-2.311145
C_0	-16338.354	-101830.7324
C_1	1373.2165	7917.419533
C_2	-34.078176	-188.760401
C_3	0.262268	1.415988
D_0	3582.57632	20681.7805
D_1	-301.57269	-1610.364649
D_2	7.489627	38.450506
D_3	-5.7712913E-2	-0.2888343

Table 5.4 Hydrometer calibration equation constants

v) The Manometers

To monitor the pressure of the low and high sides and the pressure differentials between the evaporator and absorber on the low side and between the generator and the condenser on the high side, two pairs of U-tube manometers were used. Each pair consisted of a mercury manometer for absolute pressure measurements and a larger diameter manometer filled with Tri-n-butyl citrate, a solution that is practically insoluble and immiscible with water, to measure the pressure differences between the two vessels meant to be at the same pressure. Referring to Figure 5.1, manometers K and L were used for the low pressure side and M and N for the high pressure side.

However, before charging the system, it was noticed that there was leakage in the manometers M and N for the high pressure side. All attempts to locate and arrest this leakage failed despite changing most parts of the lines. The two manometers were therefore, isolated from the system and a bourdon tube vacuum gauge was connected to the condenser charging port to monitor the high side pressure in addition to the saturation pressure obtained from the temperature measurements inside the condenser.

The low pressure side manometer, K and L which were found to be leak-free were in use during the experiment. K was the mercury manometer whilst L was

the Tri-n-butyl citrate manometer for measuring pressure differences between the evaporator and the absorber.

vi) The Vacuum Pump and Gauge

A reliable vacuum pumping system is essential for initial evacuation and subsequent purging of the refrigeration system. The pumping system used consisted of a vacuum pump, a gauge head and a vacuum gauge.

The vacuum pump employed was a two-stage rotary pump, mode E2M2 manufactured by Edwards High Vacuum. It had a displacement of 47 l/min and the ultimate vacuum was $1x10^{-3}$mbar without gas ballast or $3x10^{-2}$ mbar with gas ballast. The maximum water vapour pumping rate for the pump was 0.5g/min.

The vacuum gauge otherwise known as the controller was also an Edwards instrument, model 503, which operated in conjunction with a single Pirani gauge head type PRM 10CR. The pressure range covered was 1000 to 10^{-3}mbar.

With the PRM 10CR gauge head, which is specifically designed for operating for a long period in the presence of highly corrosive gases, the hairpin filament of special material is suspended along the axis of the gauge head envelope. Compensation for

ambient temperature is provided by a coil bonded to the outside of the envelope. The low thermal capacity of the coil material gives a fast response time to a step change in pressure.

The vacuum gauge had a relay facility with two set points variable over the range 100 to 10^{-3}mbar to provide differential switching. Switching indication was given by two LEDs which also served as power supply indication. The gauge was mounted on panel I (Plate 5.3)

Chapter Six

The Experimental Refrigerator -

Operation and Results

6.1 Operation

The whole system was evacuated to 0.6mbar absolute pressure and the major components then charged separately as follows:

i) Generator

6 litres of 74.6% concentrated solution. Of this, 1 litre was to fill the shell side of the heat exchanger, whilst the remaining 5 litres ensured that the electric heating element was continuously covered with solution.

ii) Absorber

9.6 litres of 69.7% concentrated solution. This took care of the tube side of the heat exchanger and the weak solution pipelines ensuring there was always enough solution in the absorber for recirculation.

iii) Evaporator

6.0 litres of distilled water to keep the heating element continuously covered.

iv) Condenser

1.0 litre of distilled water.

The operational procedure of the refrigerator was as follows:

The generator heater was switched on and the power supply routed through the wattmeter. The cooling water to the absorber coils was turned on. The solution pump was then switched on and the flow rate of the portion to the generator and the recirculated portion were adjusted accordingly using the appropriate valves. Once refrigeration started, the evaporator heater was switched on and adjusted accordingly. During this period, the power supply to the evaporator was routed through the wattmeter.

When equilibrium conditions had been obtained, characterised by constant evaporating and condensing temperatures and constant solution flow rates for at least 45 minutes, the following readings were recorded:

i) the evaporating, condensing, generating and absorbing temperatures and temperatures at the various points in the cycle.

ii) the generator and evaporator heat loads.

iii) the apparent specific gravity of the strong and weak solutions asrecorded by the hydrometer.

iv) the refrigerant and weak solution flow rates.

v) the cooling water inlet and outlet temperatures to and from the cooling coils.

vi) the evaporator absolute pressure from the mercury manometer and the condenser gauge pressure.

6.2 Results and performance of the experimental refrigerator

6.2.1 Results

Seven sets of readings were taken at different evaporating and generating conditions before the perforated holes on the drip tray inside the absorber became temporarily blocked by sludge removed from the internal parts of the pipework by the corrosive fluid. These data are shown in Table 6.1. The first set of readings was taken at zero evaporator load when the evaporating temperature was 8.9°C.

For runs 2 to 7, the evaporator load varied from 40 - 160W whilst the generator load varied from 120 - 400W. The high side pressure varied between 27 and 33mbar, whilst the low side pressure varied between 11 and 15mbar.

Table 6.1 - Performance data for the Experimental Refrigerator

	Run Number						
	1	2	3	4	5	6	7
Evaporator temperature, °C	8.9	9.5	10.4	11.8	13.2	12.8	12.6
Condenser temperature, °C	22.2	23.3	25.9	23.2	22.3	22.7	25.5
Temperature of refrigerant outlet from condenser, °C	22.05	23.15	23.75	23.25	22.35	22.5	24.2
Temperature of refrigerant inlet to evaporator, °C	18.5	16.85	17.3	20.15	19.6	18.9	18.8
Temperature of weak solution from absorber, °C	22.6	21.2	24.5	21.3	21.2	20.5	19.6
Temperature of weak solution inlet to H.E, °C	25.2	26.4	26.0	30.3	22.8	22.3	22.25
Temperature of weak solution inlet to generator, °C	41.7	42.7	51.3	60.7	42.4	53.3	52.7
Temperature of strong solution outlet from generator, °C	51.3	53.1	63.6	61.8	63.75	68.7	64.7
Temperature of strong solution outlet from H.E, °C	38.3	34.2	40.7	32.8	41.6	42.4	40.4
Temperature of mixed solution to the absorber, °C	27.4	27.4	31.2	25.35	28.1	25.0	24.9
Refrigerant flow rate, g/s	0.03	0.03	0.06	0.03	0.06	0.06	0.06
Weak solution flow rate, g/s	1.55	0.32	1.22	1.82	2.66	2.17	1.49
Weak solution hydrometer reading	1.630	1.620	1.650	1.620	1.640	1.600	1.600
Strong solution hydrometer reading	1.755	1.760	1.750	1.755	1.725	1.730	1.770
Weak solution mass fraction, $\%_{\omega(aq)}$ %	70.56	69.90	71.76	69.91	70.79	68.90	68.79
Strong solution mass fraction, $\%_{s(aq)}$ %	74.64	74.25	74.66	73.92	73.32	73.63	75.54
Actual circulation factor, λ_{act}	50.67	9.67	19.33	59.67	43.33	35.17	23.83

Table 6.1 (continued)

	Run Number						
	1	2	3	4	5	6	7
* Equilibrium circulation factor, λ_{eq}	8.29	6.01	9.43	4.92	2.77	2.52	2.59
Evaporator heater load, W	0	40	80	120	160	160	160
Generator heater load, W	40	120	200	240	280	320	400
Evaporating pressure, mb	11.4	11.87	12.61	13.83	15.17	14.78	14.59
Condensing pressure, mbar	26.75	28.60	33.41	28.43	26.92	27.58	32.63
Cooling water inlet temp. to absorber coils, °C,	17.1	17.5	18.2	16.5	16.5	16.2	15.5
Cooling water outlet temp. from absorber coils, °C	22.5	22.0	25.0	19.8	20.5	19.5	19.0
Cooling water outlet temp. from condenser coil, °C	22.8	22.1	25.2	21.5	21.0	21.2	21.4
Actual heat ratios, ξ_{act}	-	0.33	0.4	0.5	0.57	0.5	0.4
Theoretical heat ratios, ξ_{th}	0.978	0.978	0.966	0.971	0.977	0.973	0.973

* Based on Solution conditions at measured temperatures

A glance at the experimental results, however, revealed that the cooling capacity of the heat exchanger employed was inadequate, if the strong solution temperature was to be cooled to or nearer the absorber temperature. However, the mixing before delivery to the absorber, of the recirculated weak solution and the relatively hot strong solution returning to the absorber helped in lowering the temperature of the strong solution to nearer the absorber temperature.

Table 6.1 shows the circulation factors calculated using the measured mass fractions and the theoretical ones calculated using the equilibrium mass fractions. For the calculation of the theoretical heat ratios (ξ_{th}), the circulation factors based on equilibrium mass fractions and the experimental temperatures were used. Complete heat exchange between the two solution streams in the heat exchanger was also assumed.

6.2.2. The performance of the Experimental Refrigerator

The actual heat ratios were calculated neglecting the pump power which was very small compared with the generator load. Figure 6.1 shows a plot of the actual and theoretical heat ratios against the evaporating temperature. Within the range of the evaporating

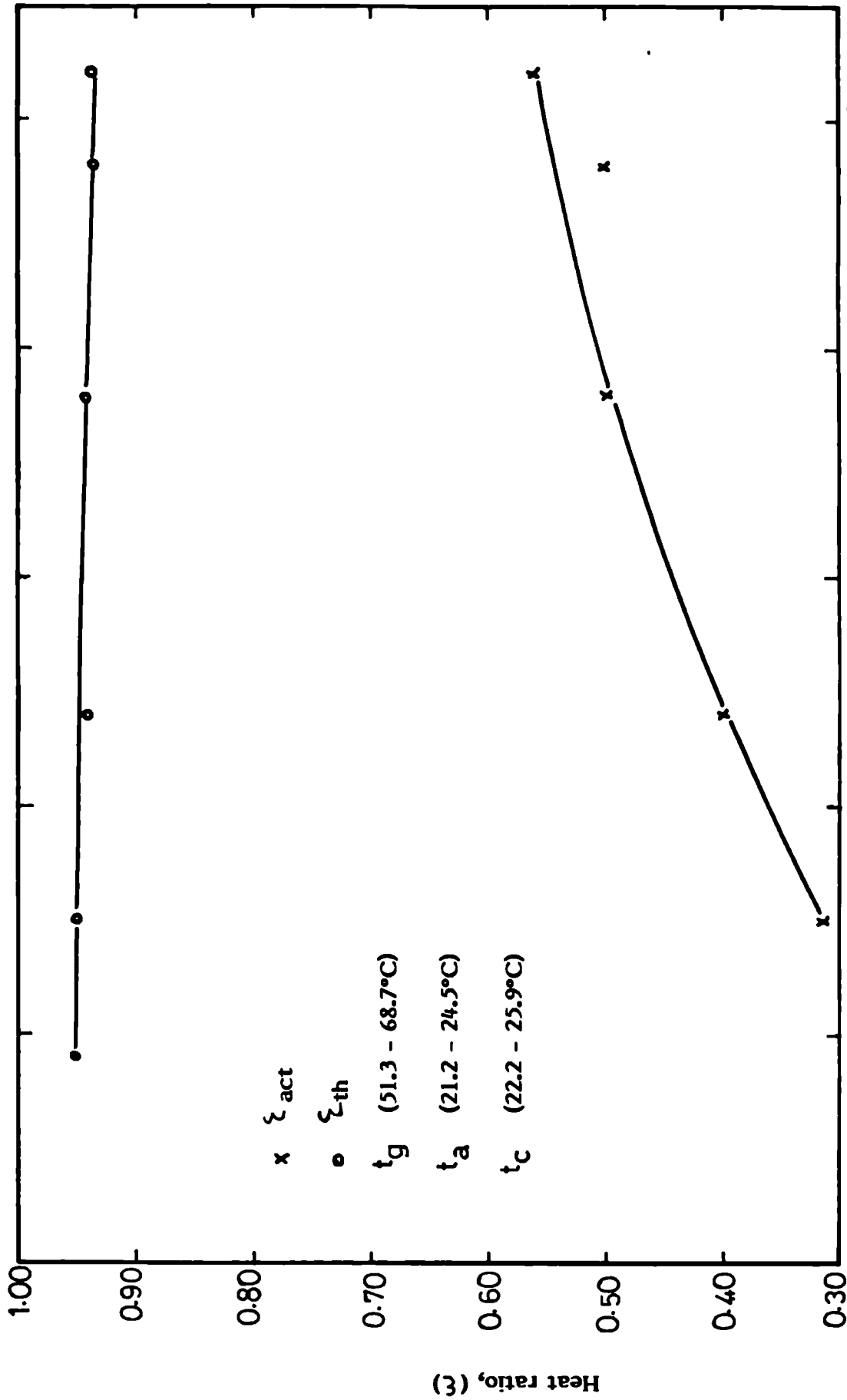

Fig. 6.1 Heat ratio (ξ) Versus Evaporator temperature (t_e) for the experimental refrigerator

temperatures considered, the actual heat ratio increased with an increase in evaporating temperature whereas the theoretical heat ratio was almost constant with only a slight decrease as the evaporating temperature increased. However, the actual heat ratios were much lower than the theoretical ones.

Two methods were used in calculating the theoretical heat ratios. In one of the methods, the equilibrium mass fractions at the measured temperatures were used. Complete heat exchange was also assumed. For the other method, the measured mass fractions and temperatures were used. Even though complete heat exchange was not assumed in this case, the temperature of the strong solution to the absorber was taken as that at the mixing pot where the still warm strong solutions from the heat exchanger and the relatively cold weak solution recirculated through the absorber were mixed. The theoretical heat ratios calculated by these methods are shown in Table 6.2.

The heat ratios based on equilibrium conditions were found to be higher than those based on measured mass fractions. The differences resulted from:

i) deviation from saturation conditions at exits from the absorber and the generator
ii) incomplete heat exchange between the fluid streams in the heat exchanger
iii) the effect of the solution pump

Run Number	1	2	3	4	5	6	7
Temperature of weak solution leaving absorber, °C	22.6	21.2	24.5	21.3	21.2	20.5	19.6
Temperature of strong solution leaving generator, °C	51.3	53.1	63.6	61.8	63.75	68.7	64.7
Measured mass fraction of solution leaving absorber, ,%	70.56	69.90	71.76	69.91	70.79	68.90	68.79
Equilibrium mass fraction of solution leaving absorber, ,%	63.0	60.7	66.0	61.0	54.5	54.0	53.0
Degree of departure from saturation at absorber exit, K	7.56	9.2	5.76	8.91	16.29	14.9	15.79
Measured mass fraction of solution leaving generator, ,%	74.64	74.25	74.66	73.92	73.32	73.63	75.54
Equilibrium mass fraction of solution leaving generator, ,%	70.60	70.8	73.0	73.4	74.2	75.4	73.50
Degree of departure from saturation at generator exit, K	4.04	3.45	1.66	0.52	-0.88	-1.77	1.94
Circulation factor based on measured mass fraction,	17.29	16.07	24.74	17.43	27.98	14.57	10.19
Equilibrium circulation factor,	8.29	6.01	9.43	4.92	2.77	2.52	2.59
Theoretical heat ratio based on measured mass fraction,	0.918	0.908	0.859	0.920	0.845	0.919	0.927
Theoretical heat ratio based on equilibrium mass fraction,	0.978	0.978	0.966	0.971	0.977	0.973	0.973

Table 6.2 - Measured and equilibrium circulation factors and theoretical heat ratios

i) Deviation from Saturation Conditions

The heat energy in the generator is due to:

i) an appreciable portion required to vaporise the refrigerant which is almost directly proportional to the refrigerant quantity;

ii) the heat of dilution, relatively small in amount and also proportional to the refrigerant quantity. This is usually expressed as the amount of heat added to or rejected from the solution per unit weight of water;

iii) a portion of the heat used for sensible heating the absorbent solution flowing through the generator from inlet to outlet temperature. This part of the total heat is not proportional to the quantity of refrigerant but is proportional to the mass flow of the solution and to the temperature increase.

The heat energy in the absorber also arises from: the heat of condensation of the refrigerant vapour; sensible heats and heat of solution. Deviation from saturation conditions could affect these heat components in the generator and hence the system heat ratios. The variation in mass fractions between the measured and equilibrium values are shown in Table 6.2. For all the runs, the equilibrium mass fractions were found to be lower than the experimental values,

hence, specific enthalpy values for the equilibrium mass fractions were higher than the experimental values. For the weak solutions, there was a marked difference between the mass fraction values of the experimental and equilibrium data especially for the runs where the evaporator loads were kept constant whilst the generator load increased. This could have resulted from inadequate absorption inside the absorber. Even though the heat transfer area was oversized, the rate of heat and mass transfers through the film on the cooling coil seemed not to be in the right proportion. During the last few runs when quite high variations were observed between the equilibrium and experimental mass fraction data, the drip tray perforated holes must have started to close up thus resulting in inadequate wetting of the cooling coil surface and hence in reduced absorption rate. Furthermore, the solution leaving the absorber must have been subcooled.

Even though the measured mass fractions for the strong solution was higher than the equilibrium values, the variation was slight. This variation, however, indicated some superheating of the solution in the generator. The solution is quite viscous. At the high salt concentrations encountered in the generator, therefore, the viscosities are quite high and some superheating could result in vaporising the refrigerant component owing to lack of turbulence in the boiling fluid.

The equilibrium mass fractions showed higher concentration gaps between the weak and strong solutions hence circulation factors were smaller than the experimental values.

ii) Incomplete Heat Exchange

This means that the strong solution leaving the heat exchanger is at a higher temperature than the weak solution leaving the solution pump. The strong solution would arrive at the absorber at a higher temperature than the absorbing temperature, resulting in a wastage of thermal energy that could have been utilised to improve the system efficiency. The heat loss due to incomplete heat exchange was estimated and shown in Table 6.3. For runs 5 to 7 when the evaporator load was kept constant at 160W and the generator load varied from 280 - 400 W, the heat loss due to incomplete heat exchange was fairly high, even though the heat exchanger efficiency only varied between 54 and 57%. These runs also coincided with those where the equilibrium circulation factors were quite low. As a result of high circulation factors and incomplete heat exchange, the second term of equation (5.2) played a significant role on the heat load in the generator and hence on the reduced experimental heat ratios.

Run Number	1	2	3	4	5	6	7
Evaporator temperature, °C	8.9	9.5	10.4	11.8	13.2	12.8	12.6
Generating temperature, (t_g)/°C	51.3	53.1	63.6	61.8	63.75	68.7	64.7
Temperature of weak solution entering heat exchanger, (t_a)/°C	25.2	26.4	26.0	30.3	22.8	22.3	22.25
Temperature of strong stream leaving heat exchanger, (t_v)/°C	38.3	34.2	40.7	32.8	41.6	42.4	40.4
Flow rate of strong stream ($m_s = m_w - m_r$), g/s	1.52	0.29	1.16	1.79	2.6	2.11	1.43
Efficiency of heat exchanger, $[\eta_{ex} = (t_g - t_v)/(t_g - t_a)]$	0.50	0.71	0.61	0.92	0.54	0.57	0.57
Heat loss due to incomplete heat exchange, $Q_{ex,L}$/W	37.4	4.2	32.0	8.4	91.8	79.7	48.8

Table 6.3 - Estimated heat loss due to incomplete heat exchange

iii) The Effect Of The Solution Pump

It was observed that the temperature of the weak solution entering the heat exchanger was much higher than its temperature at the exit from the absorber for most of the runs. For a particular run, the difference in temperature was up to 9°C. This rise in temperature was due to the pump heat being removed by the solution, since the rotor of the pump motor rotated inside the solution. The pump heat and the theoretical pump power for each run were estimated and the results shown in Table 6.4.

Even though the theoretical pump power was small and was rightly neglected in heat ratio calculations, the pump heat was relatively higher. The pump heat preheated the solution which reduced the heat exchanger load and also the heat loss due to incomplete heat exchange. However, part of the solution was recirculated and the rise in temperature affected the temperature of the strong solution returning to the absorber. This pump heat effect and incomplete heat exchange between the fluid streams in the heat exchanger prevented the strong solution from arriving at the absorber at the absorbing temperature and hence contributed to the difference between the theoretical heat ratios. As a result of the inadequate area of the heat exchanger utilised in the system, the disadvantage of the rise in solution temperature due to the pump heat outweighed the advantages it had in

reducing the exchanger load. Consequently, even though the solution pump was reliable, the inclusion of it is not the most suitable in small systems. Utilising the bubble pump principle for the transfer of solution from the absorber to the generator could therefore be a better alternative.

The less of the two theoretical heat ratios was found to be still higher than the actual heat ratios as shown in Table 6.5. The differences could have resulted from:

i) extraneous heat gains
ii) experimental errors
iii) non-steady conditions of operation

Since there is no perfect heat insulator, even though the generator and evaporator were well insulated, there would be some heat loss from the generator as the internal temperature was higher than the environmental temperature. Similarly, there would be some heat gain into the evaporator from the surroundings as the internal temperature was lower than the environmental temperature. The effects of these would be higher heat gains into the evaporator at reduced evaporating temperatures and for the generator, less energy than supplied by the heater would be available for regeneration. The heat loss from the generator and the heat gains to the evaporator were estimated and shown in Table 6.5. In

Run Number	1	2	3	4	5	6	7
Temperature of weak solution leaving the absorber, °C	22.6	21.2	24.5	21.3	21.2	20.5	19.6
Temperature of weak solution entering heat exchanger, °C	25.2	26.4	26.0	30.3	22.8	22.3	22.25
Weak solution flow rates, g/s	1.55	0.32	1.22	1.82	2.66	2.17	1.49
Condensing pressure, mbar	26.75	28.60	33.41	28.43	26.92	27.58	32.63
Evaporating pressure, mbar	11.4	11.87	12.61	13.83	15.17	14.78	14.59
Pump heat, W	7.6	3.1	3.4	30.8	8.0	7.3	7.4
Theoretical pump power, W	1.3×10^{-3} $\cdot02$	3×10^{-4}	1.4×10^{-3}	1.5×10^{-3}	1.7×10^{-3}	1.5×10^{-3}	1.5×10^{-3}

Table 6.4 - Estimated pump heat and theoretical pump power

Run Number	2	3	4	5	6	7
Generating temperature, °C	53.1	63.6	61.8	63.75	68.7	64.7
Heat supplied to generator, W	120	200	240	280	320	400
Est. conduction heat loss from generator to surrounding, W	11.6	15.3	14.7	15.4	17.2	15.7
Heat loss due to incomplete heat exchange, Q_{exL} , W	4.2	32.0	8.4	91.8	79.7	48.8
Net heat utilised for generation, W	104.2	152.7	216.9	172.8	223.1	335.5
Evaporating temperature, °C	9.5	10.4	11.8	13.2	12.8	12.6
Evaporator load, W	40	80	120	160	160	160
Estimated conduction heat gain to evaporator, W	4.0	3.6	3.2	2.7	2.8	2.9
Total evaporator load, W	44.0	83.6	123.2	162.7	162.8	162.9
* Theoretical heat ratio, ξ_{th}	0.908	0.859	0.920	0.845	0.919	0.927
Actual heat ratio, $\xi_{act.}$	0.33	0.4	0.5	0.57	0.5	0.4
Actual heat ratio considering heat losses and gains	0.422	0.547	0.568	0.942	0.730	0.486

* Based on actual mass fraction and measured temperatures

Table 6.5 - Effects of heat loss in generator and heat gain in evaporator on heat ratio

the estimates, the generator and evaporator shells were represented by a steel cylinder with an inner layer of 19mm thick Armaflex insulating material whilst the fibre glass insulation in the wooden boxes were represented by another layer of 76mm thick cylindrically shaped insulation of fibre glass material. Equation (6.1) taken from ASHRAE Handbook of Fundamentals, 1985, was used to estimate the heat flow.

$$q_s = \frac{t_{is} - t_{os}}{\left[r_s \ln\left(r_1/r_i\right)\right]/k_1 + \left[r_s \ln\left(r_s/r_1\right)\right]/k_2 + R_s} \quad \text{..(6.1)}$$

where: q_s = heat transfer per unit area of insulation outer surface, W/m²

R_s = surface resistance assumed to be 0.09, m²C/W

k_1, k_2 = thermal conductivities of insulation, W/mc

t_{is} = inner surface temperature of insulation equal to the temperature of fluid in the container, °C

t_{os} = outer surface temperature of insulation assumed to be the ambient air temperature taken as 21°C.

r_i = inner radius of insulation

= outside radius of steel pipe, m

r_1 = outer radius of intermediate layer of insulation, m

r_s = outer radius of insulation, m

The experimental heat ratios were recalculated considering the effects of heat loss from the generator, heat again in the evaporator and losses due to incomplete heat exchange. The results are shown in Table 6.5. The new values were higher than those without these considerations but are still lower in some cases than the theoretical values. Even though the available data is too scanty to draw any conclusion at this stage, the experimental heat ratios could be seen to improve at higher evaporating temperatures.

Furthermore there were still more heat transfers between some of the system components and the environment that had not been considered, such as heat loss from the heat exchanger, and connecting pipes. The inaccuracies in the assumptions made for the transport properties of the solutions, used in estimating the absorber heat transfer area could also have contributed to the inadequacies that resulted in the deviation between the theoretical and actual heat ratios.

Experimental errors could contribute to the difference between theoretical and actual heat ratios. Heat ratios, ξ , were calculated using the equation:

$$\xi = \frac{h_4 - h_2}{(h_1 - h_6) + \lambda(h_7 - h_6)} \qquad \ldots\ldots (6.1)$$

where:

h_1 = enthalpy of superheated refrigerant vapour leaving the generator, KJ/Kg.

h_2 = enthalpy of liquid refrigerant leaving the condenser, KJ/Kg

h_4 = enthalpy of refrigerant vapour leaving the evaporator, KJ/Kg

h_a = enthalpy of weak solution leaving the solution pump which is approximately equal to the enthalpy of weak solution leaving the absorber, KJ/Kg

h_s = enthalpy of strong solution returning to the absorber, KJ/Kg

λ = circulation factor

Any error in the determination of temperature and mass fraction would affect the enthalpy values which will in effect affect the calculated heat ratios. The circulation factor is a function of the mass flow rates and the mass fractions. The actual circulating factors were found to be much higher than calculated circulation factors (Table 6.1). Since the mass balance for water and the salts in the absorber cannot be wrong, there could have been some error in the mass flow rate readings which yielded the high actual circulation factors or in the determination of actual mass fractions.

Before taking any reading it was necessary that the system operated under steady conditions for at least 45 minutes. Taking readings under non-steady

conditions could affect the accuracy in the temperature, mass flow rate and mass fraction readings and result in inaccurate calculated heat ratios.

For the tests, special consideration was given to low regeneration temperatures (51.3 - 68.7°C). The variation in the absorbing and condensing temperatures were also slight being 21.2 - 24.5°C and 22.2 - 25.9°C respectively. It was noted, however, that for this novel working fluid ($2LiBr - ZnBr_2 - H_2O$), refrigeration was achieved during the experiment with a generating temperature as low as 53°C but with quite low cooling water temperature.

6.3 Program Of The Experiments

The operation of the experimental refrigerator was firstly, by varying both generator and evaporator loads to find out if refrigeration could be achieved at low regenerating temperatures. Then keeping the evaporator load constant whilst the generator load increased to check the effect on heat ratios and evaporating temperature. It was during the later part of the experiment that the perforated holes in the drip tray got blocked resulting in the need to dismantle the absorber to enlarge the holes. However, the performance of the refrigerator before this development has been discussed in the preceding section.

Other planned operations if the operational problem had not occurred are shown below.

i) to keep the evaporator load constant whilst the generator load decreases. It is expected that under this condition, the actual heat ratio and the evaporating temperature shall increase.

ii) to maintain constant generating temperatures of 75°C and 65°C respectively and find the effects on the evaporating temperatures whilst the absorbing and condensing temperatures remain almost constant.

Chapter Seven

Conclusions And Suggestions For Further Work

7.1 Conclusions

In Chapter One, the advantages of $LiBr-H_2O$ over the NH_3-H_2O systems, especially for air conditioning and other chilling applications were discussed. However, the solution of the crystallisation problems in the $LiBr-H_2O$ system is the major objective of this work. Hence the addition of one mole of zinc bromide to two moles of lithium bromide to make up the absorbent of the $2LiBr-ZnBr_2-H_2O$ system has resulted in solving the solubility problem of the $LiBr-H_2O$ system.

The heat ratio of the $2LiBr-ZnBr_2-H_2O$ system is here compared with those of the $LiBr-H_2O$ system working under the same conditions. Those of the NH_3-H_2O system have not been included because it has already been established that the heat ratios of $LiBr-H_2O$ systems are far superior to those of the NH_3-H_2O for evaporating temperatures above 5°C which is the range covered in this comparison. The operating conditions chosen are shown in Table 7.1. Cycles A, B and C are for evaporating temperatures of 5°C whilst cycles D, E and F are for 10°C evaporating temperature. Other operating conditions of D, E and F are similar to A, B and C respectively. The absorbing and condensing

temperatures of 35°C and 40°C respectively, are typical in some tropical countries where underground water is available or even some temperate countries when cooling towers are used.

The calculated theoretical heat ratios are shown in Table 7.2. In these calculations it was assumed that the weak solution leaving the absorber and the strong solution leaving the generator were under saturation conditions. Furthermore, complete heat exchange between the two streams of fluids in the heat exchanger was also assumed, in which case, the absorbing temperature and the temperature of the strong solution returning to the absorber were the same. McNeely's (80) data was used for the $LiBr-H_2O$ system calculations. It will not be possible to operate Cycles A and D for the $LiBr-H_2O$ system if the returning strong solution is cooled to the absorbing temperature as the state point will be too close to the crystallisation line which may give rise to salt crystallisation in the solution return pipeline to the absorber. However, it is possible to operate the $LiBr-ZnBr_2-H_2O$ system under these conditions.

Cycles	Operating temperatures, °C			
	Evaporating temperature t_e	Absorbing temperature t_a	Condensing temperature t_c	Generating temperature t_g
A	5	35	40	95
B	5	35	40	85
C	5	20	25	65
D	10	35	40	95
E	10	35	40	85
F	10	20	25	65

Table 7.1 - Description of operational cycles

Refrigeration system	Cycle	Evaporating temp (°C)	Theoretical heat ratio, ξ_{th}
$LiBr-H_2O$	A	5	-
	B	5	0.83
	C	5	0.887
	D	10	-
	E	10	0.845
	F	10	0.906
$2LiBr-ZnBr_2-H_2O$	A	5	0.915
	B	5	0.928
	C	5	0.957
	D	10	0.922
	E	10	0.933
	F	10	0.965

Table 7.2 - Heat ratio comparison

In all the cycles, the theoretical heat ratios for the2LiBr-$ZnBr_2$-H_2O system are higher than those of the LiBr-H_2O system. The circulation factor for each cycle is of course, relatively higher for the2LiBr-$ZnBr_2$-H_2O system than for the LiBr-H_2O system and this implies a higher heat exchanger load. However, with the high solution concentrations usable with the 2LiBr-$ZnBr_2$-H_2O system, the enthalpies of the weak solution from and the strong solution returning to the absorber are lower in value than the enthalpies at the concentrations usable for the LiBr-H_2O system operating under the same conditions. This suggests that the thermal properties of a working fluid in an absorption system play a more important role on the system efficiency than merely the circulation factor.

Recently, Sanyo Electric Trading Company, started the manufacture of a range of double-effect absorption chiller/heaters that utilise two generators and two heat exchangers. A theoretical heat ratio of unity had been reported for a particular model BUW-280AB but this was achieved in two stages of regeneration. For the2LiBr-$ZnBr_2$-H_2O system, a theoretical heat ratio of 0.965 was obtained at 10°C and 65°C evaporating and generating temperatures respectively, in a single stage operation.

Some manufacturers, notably Trane Ltd, use automatic decrystallisers on their units which are normally factory assembled and effectively sealed to exclude

air, which promotes corrosion from the system. These additions add to the cost of the plants even though they are not directly involved with the production of cold. Even though effective sealing of a plant operating on the new fluid is necessary, to reduce corrosion which the system is also liable to, the addition of automatic decrystallisation is practically unnecessary. This would result in lower cost of the plant. Krueger et al, (92) reported that lithium chromate when used in a solution of pH 9-10.5, was an effective corrosion inhibitor in $LiBr-H_2O$ systems. It is believed that the same corrosion inhibitor would be useful in the $LiBr-ZnBr_2-H_2O$ system. It will be necessary, however, to carry out some tests to ascertain this fact.

There seems to be two uses for the $LiBr-ZnBr_2-H_2O$ system:

i) in conventional air conditioning systems to eliminate the possibility of salt crystallisation

ii) in solar operated air conditioning or refrigeration systems in parts of the world with abundant sunshine

Even though the evaluation of the system is still at its early stage, the information obtained so far suggests that the system would be a better alternative to the $LiBr-H_2O$ system, even in conventional vapour absorption systems. The fact that high solution

concentrations can be used without the risk of crystallisation of salts in the system allows for the cooling of the strong solution from the generator to nearer the absorbing temperature resulting in reduced generator and absorber loads. Furthermore, even though the circulation factors are higher, results of our analysis show that the effect of cooling the strong solution to the absorber to absorbing temperature has a more significant effect on heat ratio than circulation factor. To get the benefit of the higher heat ratio, however, a larger heat exchanger is required but the gain in reduced generator and absorber surface areas should more than offset the extra cost of heat exchanger area.

At about 64°C regeneration temperature a refrigeration temperature of 10.4°C was obtained. The low regeneration temperature of this system therefore makes it suitable for solar energy operations bearing in mind the fact that the efficiency of solar energy collectors increase with decreased absorber temperatures. It should be noted, however, that the absorbing and condensing temperatures need to be quite low to be able to utilise regeneration temperatures much below 85°C. Solar operated absorption refrigeration systems utilising the $2LiBr-ZnBr_2-H_2O$ solution will be useful in poor developing countries with abundant sunshine and where water is readily available for cooling purposes. With such a system utilising the bubble pump principle to transfer weak

solution from the absorber to the generator, it would operate free of electricity thus further enhancing its usefullness in remote parts of developing countries where electricity supply is either inadequate or not available at all.

In Table 7.2, the generating temperatures of 65° and 85°C can be conveniently obtained from conventional flat-plate solar collectors. The heat ratios of the $2LiBr-ZnBr_2-H_2O$ are found to be superior to those of the $LiBr-H_2O$ system. Hence the $2LiBr-ZnBr_2-H_2O$ system could be a better substitute for the $LiBr-H_2O$ system for solar operations. Furthermore, Alloush (78) compared the theoretical heat ratios for $LiBr-H_2O$, $LiBr-CH_3OH$ and $2LiBr-ZnBr_2-CH_3OH$ systems operating under the same conditions of 5°C, 70°C, 25°C and 20°C evaporating, generating, absorbing and condensing temperatures respectively. The comparison showed the $LiBr-H_2O$ system to be the best with $\xi_{th} = 0.866$ followed by the $2LiBr-ZnBr_2-CH_3OH$ system with $\xi_{th} = 0.83$ and then the $LiBr-CH_3OH$ with $\xi_{th} = 0.775$. Since the evaporating temperatures of this work were above 5°C, the theoretical heat ratios of the $2LiBr-ZnBr_2-H_2O$ should be superior to those of $2LiBr-ZnBr_2-CH_3OH$ system. The $2LiBr-ZnBr_2-H_2O$ system may, therefore, be considered to be the most suitable for solar operated absorption refrigeration for air conditioning and other chilling applications.

7.2 Suggestions For Further Work

The results obtained so far from the evaluation of the $2LiBr-ZnBr_2-H_2O$ solution suggest it could be a better working fluid for absorption refrigeration systems than $LiBr-H_2O$ solution. However, based on the problems encountered in the operation of the experimental refrigerator, the following suggestions should help to improve the system performance.

It is suggested that in order to make an elaborate design of the absorber and heat exchanger, better knowledge of transport properties such as density, viscosity and thermal conductivity are essential.

The subcooling of the solution leaving the absorber could have resulted from the fact that the rates of transfer of heat and mass through the film on the cooling coil are not in the right proportion. This could occur if adequate heat is transferred through the film which is impervious to water diffusion. In such a case, the outlet temperature would show a lot of subcooling. Since there is no data available on the rate at which water diffuses into the film, this problem needs further investigation.

The absorber needed to be dismantled after only seven runs because the corrosive liquid blocked the perforated holes of the drip tray with sludge from the

internal parts of the pipes. This development resulted in reduced wetting of the surface of the cooling coil and hence reduced the absorption rate in the absorber. The perforated holes on the tray need to be enlarged so that any sludge could fall to the bottom of the absorber. After all, the suction line to the solution pump protruded about 25mm into the absorber to make sure that no sludge is sucked into the pump. A more compact absorber incorporating a not too large cooling coil and with a drip tray of adequate hole size is, therefore, required for the small loads contemplated in the system. Furthermore, suitable corrosion inhibitors for the solution have to be investigated.

The temperature of the strong solution from the heat exchanger showed that the only heat exchanger employed was undersize. More heat exchange surface area is therefore required if the strong solution is to be cooled to the absorbing temperature to counteract the effect of high circulation factor.

References

1) Gosney, W.B.,
PRINCIPLES OF REFRIGERATION.
Cambridge University Press, 1982

2) El-Shamarka, S.,
AN INVESTIGATION OF METHANOL AND INORGANIC BROMIDES FOR THERMALLY OPERATED HEAT PUMPS.
Ph.D Thesis, SME, Cranfield Institute of Technology, 1981.

3) Johnson, S.E.,
A LOOK AT TODAY'S ABSORPTION REFRIGERATION.
ASHRAE Journal, September 1960, pp 55-69.

4) Farber, E.A.,
THE DIRECT USE OF SOLAR ENERGY TO OPERATE REFRIGERATION AND AIR CONDITIONING SYSTEMS.
Technical Progress Report No.15, Engineering Progress of the University of Florida, Gainsville, November, 1965

5) Yellott, J.I.,
UTILISATION OF SUN AND SKY RADIATION FOR HEATING AND COOLING OF BUILDINGS.
ASHRAE Journal, December, 1973, pp 31-42.

6) Prigmore, D. and Barber, R.,
COOLING WITH THE SUN'S HEAT - DESIGN CONSIDERATIONS AND TEST DATA FOR A RANKINE CYCLE PROTOTYPE.
Solar Energy, Vol 17, 1975, pp 185-192

7) Kakabaev, A. and Davletov, A.,
A FREON-EJECTOR SOLAR REFRIGERATION.
Gelioeknika, Vol 5, 1966, p.42

8) Champoussin, J.C. and Hostache, G.,
PERFORMANCES D'UN SYSTEME TRITHERME A EJECTEUR A BASSE TEMPERATURE DE BOUILLEUR.
XVI International Congress of Refrigeration (Paris 1983) proceedings Tome II, pp 381-387

9) Eichhorn, R.L.,
THERMOELECTRIC REFRIGERATION.
Refrigerating Engineering, June 1958, pp 31-35.

10) Kreider, J.F. and Kreith, F.,
SOLAR HEATING AND COOLING - ACTIVE AND PASSIVE DESIGN.
2nd Edition, Hemisphere Publishing Corporation 1982, Chapter 10.

11) Vella, G.J., Harris, L.B. and Goldsmid, H.J.
A SOLAR THERMOELECTRIC REFRIGERATOR.
Solar Energy, Vol. 18, 1976, pp 355-359.

12) Field, R.L.,
PHOTOVOLTAIC THERMOELECTRIC REFRIGERATOR FOR MEDICINE STORAGE FOR DEVELOPING COUNTRIES.
Solar Energy, Vol. 25, 1980, pp 445-447.

13) Sofrata, H.,
A THERMO-ELECTRIC REFRIGERATOR POWERED BY PHOTOVOLTAIC SOLAR COLLECTORS.
Applied Energy, 18, (1984), pp 137-142.

14) Swartman, R.K. and Swaminathan, C.,
SOLAR POWERED REFRIGERATION.
Mechanical Energy (ASME), June, 1971, pp 22-24.

15) Swartman, R.K.; Ha, V and Newton, A.J.,
SURVEY OF SOLAR POWERED REFRIGERATION.
Paper No. 73-WA-SOL-6, ASME, 1974.

16) Duffie, J.A. and Sheridan, N.R.,
LITHIUM-BROMIDE WATER REFRIGERATORS FOR SOLAR OPERATION.
Inst. Of Engrs. Aus. Trans. Mech., and Chem. M.C.I., 1965, pp 79-88.

17) Manohar Prasad,
OPTIMUM GENERATOR TEMPERATURE FOR Li-Br WATER ABSORPTION SYSTEM.
Int. Inst. of Refr. Commissions D1, D2, E1, E2, Mons, Belgium, 1980, pp 265-272.

18) Porter, J.M.,
THE USE OF COMMERCIALLY AVAILABLE ABSORPTION UNITS ON SOLAR POWERED COOLING SYSTEMS.
ASHRAE Trans., Vol. 82, 1976, Pt1, pp 943-949.

19) Alloush, A. and Gosney, W.B.,
AN ABSORPTION SYSTEM USING METHANOL PLUS LITHIUM AND ZINC BROMIDES FOR REFRIGERATION USING SOLAR HEAT.
XVIth Int. Cong. Ref., Paris, 1983, pp 339-345.

20) Kakabaev, A and Khandurdyev, A.,
ABSORPTION SOLAR REFRIGERATION UNIT WITH OPEN REGENERATION OF SOLUTION.
Gelioteknika, Vol.5, No.4, 1969, pp 28-32.

21) Collier, R.K.,
THE ANALYSIS AND SIMULATION OF AN OPEN CYCLE ABSORPTION REFRIGERATION SYSTEM.
Solar Energy, Vol.23, 1979, pp 357-366.

22) Kumar, P. and Devotta, S.,
ANALYSIS OF SOLAR ABSORPTION COOLING SYSTEMS WITH LOW GENERATOR TEMPERATURES.
Int. J. Refrig., Vol.8, 1985, pp 356-359.

23) Hainsworth, W.R.,
REFRIGERANTS AND ABSORBENTS.
Part I, Refrig. Eng., 48, pp 97-100; Part II, Ibid, 48, pp 201-205, 1944.

24) Buffington, R.M.,
QUALITATIVE REQUIREMENTS FOR ABSORBENT-REFRIGERANT COMBINATIONS.
Refrig. Eng., 57, pp343, 1949.

25) Olama, M.A.,
EVALUATION OF SOME METHANOL-SOLUTIONS FOR ABSORPTION REFRIGERATION.
Ph.D Thesis, Dept of Mechanical Engrg., King's College, London University, 1980.

26) Bokelmann, H., Renz, M. and Steimle, F.,
WORKING FLUIDS FOR LOW PRESSURE ABSORPTION SYSTEM.
16th International Congress of Refrigeration (Paris 1983) proceedings TOME II, pp 281-287.

27) Macriss, R.A.,
SELECTING REFRIGERANT-ABSORBENT FLUID SYSTEMS FOR SOLAR ENERGY UTILISATION.
ASHRAE Trans., Vol. 82, Pt.1, 1976, pp 975-988.

28) Vamvakidis, S.I.,
SOLUBILITY OF ABSORBENTS IN REFRIGERANTS.
M.Sc Thesis, Dept of Mechanical Engieering, King's College, London University, 1978.

29) Pennington, W.,
HOW TO FIND ACCURATE VAPOUR PRESSURE OF LiBr-H_2O SOLUTIONS.
Refrig. Eng., 63, 1955, pp 57-61

30) Neal, W.E.J. and Pabon-Diaz, M.,
SOLAR ENERGY FOR REFRIGERATION AND AIR CONDITIONING.
Refrigeration and Air Conditioning, April 1978, pp.59.

31) Cheremisinoff, P.N. and Regino, T.C.,
PRINCIPLES AND APPLICATION OF SOLAR ENERGY.
Ann Arbor Science Publishers Inc., 1978.

32) Hollands, K.G.T.,
DIRECTIONAL SELECTIVITY, EMITTANCE AND ABSORPTION PROPERTIES OF VEE CORRUGATED SURFACES.
Solar Energy, Vol.7, No.3, 1963. pp 108-116.

33) Soin, R.S.; Sangameswar Rao, K.; Rao, D.P.; and Rao, K.S.,
PERFORMANCE OF FLAT-PLATE SOLAR COLLECTOR WITH FLUID UNDERGOING PHASE-CHANGE.
Solar Energy, Vol. 23, 1979, pp 69-73

34) Schreyer, J.M.,
RESIDENTIAL APPLICATION OF REFRIGERANT-CHARGED SOLAR COLLECTOR.
Solar Energy, Vol. 26, 1981, pp 307-312.

35) Kishore, V.V.N.; Gandhi, M.R. and Rao, K.S.,
ANALYSIS OF FLAT-PLATE COLLECTORS CHARGED WITH PHASE-CHANGING FLUIDS.
Applied Energy, 17, 1984, pp 133-149.

36) Kishore, V.V.N.; Gandhi, M.R.; Marquis, C.H., and Rao, K.S.,
TESTING FLAT-PLATE COLLECTORS CHARGED WITH PHASE-CHANGING FLUIDS.
Applied Energy, 17, 1984, pp 155-168.

37) Adegoke, C.O.,
RADIATIVE CHARACTERISTICS OF SURFACES.
M.Sc Thesis, Cranfield Institute of Technology, School of Mechanical Engineering, 1978.

38) Thomason, H.E.,
SOLAR HEATED HOUSES USES 3/4 h.p FOR AIR CONDITIONING.
ASHRAE Journal, Vol.4, Nov 1962, pp 58-62.

39) Rehbinder, G.,
THERMAL INTERACTIONS BETWEEN WATER AND ROCK IN AN UNDERGROUND HOT-WATER STORE.
Applied Energy, 20, 1985, pp 103-116.

40) Choda, A. and Read, W.R.W.,
THE PERFORMANCE OF A SOLAR AIR HEATER AND ROCKPILE THERMAL STORAGE SYSTEM.
Paper No. 4/48, I.S.E.S., Conf., Melbourne, 1970.

41) Goldstein, M.,
SOME PHYSICAL CHEMICAL ASPECTS OF HEAT STORAGE.
Paper S/7, U.N. Conf on New Sources of Energy, Rome, 1961.

42) Speyer, E.,
SOLAR BUILDINGS IN TEMPERATE AND TROPICAL CLIMATES.
Paper S/8, U.N. Conf on New Sources of Energy, Rome, 1961.

43) Telkes, M.,
SOLAR HEAT STORAGE.
Paper No.64 - WA/Sol-9, ASME, New York, 1964.

44) Tamblyn, R.T.,
THERMAL STORAGE: A SLEEPING GIANT.
ASHRAE Journal, June 1977, pp 53-57.

45) Jaffrin, A. and Cadier, P.,
LATENT HEAT STORAGE APPLIED TO HORTICULTURE.
Solar Energy, Vol. 28, No.4, 1982, pp 313-321

46) Talbert, S.G.; Frieling, D.H.; Eibling, J.A. and Nathan, R.A.
DESIGN REQUIREMENTS FOR A VIABLE PHOTOCHEMICAL SOLAR HEATING AND COOLING SYSTEM.
Solar Energy, Vol. 17, 1975, pp 367-372

47) Kudish, A.I. and Wolf, D.,
A COMPACT SHALLOW SOLAR POND HOT WATER HEATER.
Solar Energy, Vol. 21, 1978, pp 317-322

48) Tabor, H.,
SOLAR PONDS.
Solar Energy, Vol. 27, 1981, pp 181-194

49) Kangas, M.T and Lund, P.D.,
DYNAMIC EFFECTS IN A SALINITY-GRADIENT SOLAR-POND HEATING SYSTEM.
Applied Energy, 20, 1985, pp 189-205

50) Neilson, C.E.; Rabl, A.; Watson, J. and Weiler, P.
FLOW SYSTEM FOR MAINTENANCE OF SALT CONCENTRATION GRADIENT IN SOLAR PONDS - TEST IN ISOTHERMAL POND.
Solar Energy, Vol. 19, 1977, pp 763-766

51) Beniwal, R.S.; Singh, R.V. and Chaudhary, D.R.,
HEAT LOSSES FROM A SALT GRADIENT SOLAR POND.
Applied Energy, 19, 1985, pp 273-285.

52) Padillo, R.,
SOLAR COLLECTION SYSTEMS - THE RATIONALE.
ASHRAE Journal, June, 1977, pp. 42-46.

53) Bisset, J.B. and Monaghan, P.F.,
DESIGN STUDY ON SOLAR ENERGY SYSTEMS FOR COMMERCIAL BUILDINGS.
ASHRAE Trans. Pt.1, 1979, pp 252-267.

54) Farber, E.A.,
THE USE OF SOLAR ENERGY FOR HEATING WATER.
Paper S/1, U.N. Conf on New Sources of Energy, Rome, 1961. pp 24-35

55) Bhardwaj, R.K.; Gupta, B.K. and Prakash, R.,
PERFORMANCE OF A FLAT-PLATE SOLAR COLLECTOR.
Solar Energy, Vol. 11, (3 & 4), 1967, pp 160-162

56) Husain, M.S.; Tiwari, G.N. and Garg, H.P.,
PERFORMANCE OF A SOLAR COLLECTOR/STORAGE WATER HEATER.
Applied Energy, 20, 1985, pp 301-316.

57) Gilman, S.F.,
SOLAR ENERGY - PRESENT AND FUTURE.
ASHRAE Journal, Vol. 20, Nov 1978, pp 33-36.

58) Bliss, R.W.,
THE PERFORMANCE OF AN EXPERIMENTAL SYSTEM USING SOLAR ENERGY FOR HEATING, AND NIGHT RADIATION FOR COOLING A BUILDING.
Paper S/30, U.N. Conf on New Sources of Energy, Rome, 1961, pp 148-157.

59) Thomason, H.E.,
SOLAR SPACE HEATING, WATER HEATING, COOLING IN THE THOMASON HOME.
Paper S/3, U.N. Conf on New Sources of Energy, Rome, 1961, pp 224-231.

60) Dunkle, R.V.,
A METHOD OF SOLAR AIR CONDITIONING.
Trans. (Mech and Chem) Inst. of Engineers, Australia, MC-1, 1965, pp 73-78.

61) Williams, D.A.; Chung, R.; Lof, G.O.G.; Fester, D.A. and Duffie, J.A.,
COOLING SYSTEMS BASED ON SOLAR REFRIGERATION.
Refrig. Engrg., November 1958, p.33.

62) Trombe, F. and Foex, M.,
THE PRODUCTION OF COLD BY MEANS OF SOLAR RADIATION.
J. Solar Energy, Sci and Eng, Vol. 1,1, 1957, p.51.

63) Chinnappa, J.C.V.,
EXPERIMENTAL STUDY OF THE INTERMITTENT VAPOUR ABSORPTION REFRIGERATION CYCLE EMPLOYING THE REFRIGERANT-ABSORBENT SYSTEMS OF AMMONIA-WATER AND AMMONIA-LITHIUM NITRATE.
Solar Energy, Vol.V, No.1, 1961, pp 1-18.

64) Chinnappa, J.C.V.,
PERFORMANCE OF AN INTERMITTENT REFRIGERATOR OPERATED BY A FLAT-PLATE COLLECTOR.
Solar Energy, Vol.6, No.4, 1962, pp 143-150.

65) Desa, V.G.,
SOLAR ENERGY UTILISATION AT DACCA.
Solar Energy, Vol.8, No.3, 1964, pp 83-90.

66) Farber, E.A.; Flannigan, F.M.; Lopez, L. and Polifka, R.W.
OPERATION AND PERFORMANCE OF THE UNIVERSITY OF FLORIDA SOLAR AIR CONDITIONING SYSTEM.
Solar Energy, Vol.10, No.2, 1966, pp 91-95.

67) Chung, R.,
LETTER TO THE EDITOR ON 'A CASE FOR A SOLAR ICE-MAKER'.
Solar Energy, Vol.7, No.4, 1963, p187.

68) Sargent, S.L. and Beckman, W.A.,
THEORETICAL PERFORMANCE OF AN AMMONIA-SODIUM THIOCYANATE INTERMITTENT ABSORPTION REFRIGERATION CYCLE.
Solar Energy, Vol.12, No.2, 1968, pp 137-146.

69) Muradov, D. and Shadiev, O.,
TESTING OF A SOLAR ABSORPTION REFRIGERATOR.
Gelioteknika, Vol.7, No.3, pp 33-35.

70) Clausen, N.E. and Worsoe-Schmidt, P.,
SOLAR ABSORPTION REFRIGERATION UTILISING SUSPENDED SOLID ABSORBENTS.
IIR - XVIth Intern. Conf. of Refrigeration, Paris, 1983, pp 373-379.

71) Buffington, R.M.,
ABSORPTION REFRIGERATION WITH SOLID ABSORBENTS.
Refrigerating Engineering, Sept. 1933, p137.

72) Eiseman, B.J.,
WHY REFRIGERANT 22 SHOULD BE FAVOURED FOR ABSORPTION REFRIGERATION.
ASHRAE Journal, December 1959, pp 45-50.

73) Thieme, A. and Albright, L.F.,
SOLUBILITY OF REFRIGERANTS 11, 21 AND 22 IN ORGANIC SOLVENTS CONTAINING A NITROGEN ATOM AND IN MIXTURES OF LIQUIDS.
ASHRAE Journal, July 1961, pp 71-75.

74) De Silva, P.A.,
ENGINE WASTE HEAT AS A SOURCE OF ENERGY FOR REFRIGERATING SYSTEMS.
Ph.D Thesis, Department of Mechanical Engineering, King's College, University of London, 1970.

75) Borde, I.; Yaron, I. and Jelinek, M.,
CYCLE ANALYSIS OF REFRIGERATION AND HEAT PUMPING ABSORPTION SYSTEMS UTILISING LOW GRADE ENERGY WITH SOME NEW WORKING FLUIDS.
IIR - XVIth Intern. Conf. of Refrigeration, Paris, 1983, pp 253-260.

76) Aker, J.E.; Squires, R.G. and Albright, L.F.,
AN EVALUATION OF ALCOHOL SALT MIXTURES AS ABSORPTION REFRIGERATION SOLUTIONS.
ASHRAE Trans. Vol.71, Part I, 1965.

77) Grosman, E.R. and Ya.Zhuravlenka, V.,
INVESTIGATION OF AN ABSORPTION REFRIGERATION MACHINE OPERATING ON A SOLUTION OF METHANOL AND LITHIUM BROMIDE.
Kholodil naya Technika (USSR), Vol.45, 1968.

78) Alloush, A.,
ABSORPTION REFRIGERATOR FOR SOLAR HEAT APPLICATION
Ph.D Thesis, Department of Mechanical Engineering, King's College, University of London, 1983.

79) Lower, H.,
THERMODYNAMISCHE UND PHYSIKALISCHE EIGENSHCAFTEN DER WASSRIGEN LITHIUMBROMID - LO SUNG.
Technischen Hochischule, Karlsruhe, 1960.

80) McNeely, L.A.,
THERMODYNAMIC PROPERTIES OF AQUEOUS SOLUTIONS OF LITHIUM BROMIDE.
ASHRAE Trans, Pt.I, 1979, pp 413-434.

81) Duffie, J.A. and Sheridan, N.R.,
LITHIUM BROMIDE - WATER REFRIGERATORS FOR SOLAR OPERATION.
Trans. Inst. of Engineers, Australia, Vol. MC-1, 1965, pp 79-88.

82) Grossman, G.; Bourne, J.R.; Ben-Dror, J.; Kimchi, Y. and Vardi, I.
DESIGN IMPROVEMENTS IN LiBr ABSORPTION CHILLERS FOR SOLAR APPLICATIONS.
ASME Trans, Journal of Solar Energy Engineering, Vol.103, 1981, pp 56-61.

83) Zhang, X.Y. and Yu-Chi. B.,
UTILISING LOW TEMPERATURE HOT WATER AS HEAT SOURCE OF TWO STAGE LiBr ABSORPTION REFRIGERATION.
Proceedings of XVith Int. Cong. of Refrigeration, Paris, 1983, pp 297-301.

84) Carey, C.O.B.; Khahra, J.S. and Smith, I.E.,
THE SODIUM HYDROXIDE/WATER ABSORPTION HEAT PUMP.
Proceedings of XVith Int. Cong. of Refrigeration, Paris, 1983, pp 269-274.

85) Gutkowski, K.M. and Ryduchowski, K.W.,
SOLAR ABSORPTION SYSTEM FOR AIR CONDITIONING
Int. J. Refrig., Vol.9, January, 1986, pp 39-42.

86) Daniels, F.; Williams, J.W.; Bender, P.; Alberty, R.A.; Cornwell, C.D. and Harriman, J.E.
EXPERIMENTAL PHYSICAL CHEMISTRY.
McGraw Hill Book Company, 1970, Chapter 23.

87) Worthing, A.G. and Geffner, J.,
TREATMENT OF EXPERIMENTAL DATA.
John Wiley and Sons, Inc., New York. 9th Edition, 1955.

88) National Bureau Of Standards, U.S. Monograph 8, 1960.
MERCURY BAROMETERS AND MANOMETERS.

89) Rogers, G.F.C. and Mayhew, Y.R.,
THERMODYNAMIC AND TRANSPORT PROPERTIES OF FLUIDS
Basil Blackwell, publisher, 1980.

90) William Haltenberger, Jr.,
ENTHALPY-CONCENTRATION CHARTS FROM VAPOUR PRESSURE DATA.
Industrial and Engrg. Chemistry, June, 1939, pp 783-786

91) Mueller Associates, Inc.,
ACTIVE SOLAR THERMAL DESIGN MANUAL.
ASHRAE Special Project, No.40.

92) Krueger, R.H.; Dockus, K.F. and Rush, W.F.,
CORROSION INHIBITION IN LITHIUM BROMIDE ABSORPTION REFRIGERATION SYSTEMS
ASHRAE Journal, December, 1962, pp.67-73.

Appendix A

Pressure Correction For Boiling Point Measurements

One difficulty in the method used for the boiling point measuremenst is the sensitivity of the boiling point to changes in barometric pressure during the time of the experiments. The pressure-dependence of the boiling points can, however, be estimated from the Clapeyron-Clausius equation in the form:

$$\frac{dP_B}{dT} = \frac{P_B H}{RT^2} \qquad \ldots (A.1)$$

where: P_B = the barometric pressure

T = the boiling point

H = heat of vaporisation

Defining the boiling point elevation constant, $K_b = RT^2M/H$ gives:

$$dT = \frac{K_b\ dP_B}{M\ P_B} \qquad \ldots (A.2)$$

M being the molecular weight of the solvent.

A change in barometric pressure dP_B produces a change in boiling point dT.

Now $P_{\bullet}$ = 760 mmHg and K_b for water as solvent is 505. This value of K_b varies slightly with pressure, i.e., for water, the correction is 0.1/mm which should be added to K_b when the baromatric pressure is above 760mm and subtracted if it is below 760mm.

With all the parameters on the right hand side of equation A-2 known, the changes in boiling point, dT, as a result of changes in barmetric pressure was calculated.

Appendix B

Absorber Design Calculations

The cooling capacity, Q_a, of the observer can be expressed as:

$$Q_a = UA_a \Delta t_m \qquad \ldots (B.1)$$

where:

U = the overall heat transfer coefficient, W/m^2K

A_a = absorber cooling coil external surface area, m^2

Δt_m = the logarithmic mean temperature difference, K

The U-value can be obtained from the equation:

$$\frac{1}{U} = \frac{1}{h_o} + \frac{X_w}{k_w} + \frac{1}{h_i} \qquad \ldots (B.2)$$

where:

h_o = outside film heat transfer coefficient, W/m^2K

h_i = inside film heat transfer coefficient, W/m^2K

X_w = thickness of tube wall, m

k_w = thermal conductivity of tube wall, W/mK

Since k_w for copper is large compared with X_w and h_i is very large compared with h_o, it may be assumed that:

$$U \simeq h_o \qquad \ldots (B.3)$$

Using Ramm's formular for laminar flow over horizontal tubes taken from (78):

$$N_u = 0.67\, R_a^{0.11} \left(Pr\frac{\sigma}{\nu}\right)^{0.33} \qquad \ldots (B.4)$$

where:

N_u = Nusselt number

$$= \frac{h\sigma}{k}$$

σ = reduced film thickness

$$= \left(\frac{\mu^2}{\rho^2 g}\right)^{1/3}$$

k = thermal conductivity of the solution, 0.458 W/mk

ρ = solution density, 1800 Kg/m³

g = gravitational acceleration, 9.81 m/s²

μ = dynamic viscosity of the solution, 13×10^{-3} Kg/ms

Z = characteristic length = π d/2 = 2.513×10^{-2}m

R_e = Reynolds number

$$= \frac{4\Gamma}{\mu}$$

where: Γ = mass flow of condensate per unit breadth

$\triangleq 3.58\times10^{-4}$ Kg/ms assuming a coil pitch diameter of 300mm

P_r = Prandtl number

$$= \frac{\mu C_p}{k}$$

where C_p = specific heat of the solution

= 1.878 KJ/Kg K

Hence,

$P_r = 53.31$ $R_e = 0.11$, $\sigma = 1.745\times10^{-4}$m

$$h_o = 0.67 \times \frac{k}{\sigma} (R_e)^{0.11} (P_r \frac{\sigma}{z})^{0.33} \quad \ldots(B.5)$$

$$= 0.67 \times \frac{0458}{1.745\times10^{-4}} (0.11)^{0.11} \left(53.31 \times \frac{1.745 \times 10^{-4}}{2.513\times10^{-2}}\right)^{0.33}$$

$\therefore h_o = 993.74$ W/m²K

from equation (B.1)

$$A_e = \frac{Q_e}{h_o \Delta t_m}$$

Δt_m can be taken as the temperature difference between the absorbing temperature (t_{abs}) and the cooling water

temperature, t_w, as the cooling water temperature is not expected to vary much.

Hence,

$$A_a = \frac{Q_a}{h_o(t_{sat} - t_w)}$$

Assuming a cooling water temperature of 18°C,

$$A_a = \frac{501}{993.74(30 - 18)}$$

$$= 0.042m^2$$

Considering the size of the available shell for the absorber and the possibility of handling higher load, the heat transfer surface area was doubled to $0.084m^2$. This was 1.7m of 16.mm O.D copper tube.

However, for absorption processes, mass transfer is equally as important as heat transfer. If, for instance, the solution film on the cooling coil is impervious to water diffusion, even though the hear transfer may be adequate, the mass transfer through the film may be inadequate. Unfortunately there is no available data on the rate at which water diffuses into the film.

Appendix C

Evaporator Design Calculations

In the evaporator, a pool of distilled water is boiled off under reduced pressure by an immersion heater. The evaporation process can therefore be represented as nucleate pool boiling.

The data for nucleate pool boiling are best correlated by the following relation developed by Rohsenow.

$$\frac{C_{p_f}(t_s - t_{sat})}{h_{fg}} = C_{s,f}\left(\frac{C_p/\mu}{k}\right)_f^{1.7}\left[\frac{Q/A}{\mu_f h_{fg}}\left(\frac{\sigma}{g(\rho_f-\rho_g)}\right)^{0.5}\right]^{0.33} \quad \ldots\ldots(C.1)$$

$C_{s,f}$ is an empirically determined constant depending on the way in which the liquid wets the heating surface.

Values for water are:

- water with nickel or brass: C = 0.006
- water withplatignum, copper or stainless steel:
  C = 0.013

From equation (C.1)

$$Q/A = q_s = \mu_f h_{fg} \left[\frac{g(\rho_f - \rho_g)}{\sigma}\right]^{1/2} \left(\frac{C_{pf}\,\Delta t_e}{C_{s,f}\, h_{fg}\, Pr_f^{1.7}}\right)^3 \quad \cdots (C.2)$$

where σ = surface tension of the liquid, N/m

μ_f = viscosity of refrigerant liquid, NS/m²

g = the local gravitational acceleration, m/s²

$C_{s,f}$ = a coefficient depending on liquid-surface combination which vary typically from 0.0027 to 0.013.

Δt_e = excess temperature = $(t_s - t_{sat})$

t_s = temperature of the surface (°C)

t_{sat} = saturation temperature corresponding to the liquid pressure, °C.

q_s = heat flux, W/m²

Pr = Prandtl number = $\left(\frac{C_p \mu}{k}\right)_f$ of the liquid

Assuming an evaporating temperature of 7°C, the evaporating pressure is 10mbar. The evaporation design load is 500W.

Considering equation (C.2) and a saturation temperature of 7°C

μ_f = 1427 x 10^{-6} N.s/m²

h_{fg} = 2484.3 KJ/Kg

σ = 74.8x10^{-3} N/m

$\rho_f = 1/v_f = 999.9\ Kg/m^3$

$\rho_g = 1/v_g = 7.746 \times 10^{-3}\ Kg/m^3$

$C_{p_f} = 4.1997\ KJ/Kg\ K$

$Pr_f = 10.55$

$C_{s,f} = 0.013$

Assuming $\Delta t_s = 45°C$, $Q/A = 1555.07\ W/m^2$

for Q = 500W, the area A, required is $0.322m^2$

Using a 159.00 i.d pipe as shell, the length of shell required:

$$L = A/\pi D_i = \frac{0.322}{\pi \times 0.159} = 644.6mm$$

A 159.00mm i.d steel pipe, 645mm long was therefore used as the evaporator.

Appendix D

Condenser Design Calculations

For a water cooled condenser,

$$Q_c = UA_o \Delta t \qquad (D.1)$$

where Q_c = the condenser heat load, W

Δt = the overall temperature difference, K

U is the overall heat transfer coefficient based on the outside surface area A_o of the condenser tube and is calculated from the equation:

$$U = \frac{1}{\frac{1}{h_o} + R_o + R_m + R_i \frac{A_o}{A_i} + \frac{1}{h_i}\frac{A_o}{A_i}} \qquad ...(D.2)$$

where:

R_o = Unit fouling resistance on outside of tubing, m^2K/W

R_i = Unit fouling resistance on inside of tubing, m^2k/W

R_m = Unit resistance of tubing

A_o/A_i = ratio of outside tube surface to inside tube surface

h_o = average unit-surface conductance of the fluid on the outside of tubing, W/m^2K

h_i = average unit-surface conductance of fluid inside tubing, W/m^2K

h_o can be estimated from the equation:

$$h_o = 0.725 \left[\frac{k_f^3 \rho_f^2 g h_{fg}}{N D \mu_f \Delta t} \right]^{1/4} \quad \ldots . (D.3)$$

where:

N = number of tubes in a vertical row

t_f = mean condensate film temperature

k_f = thermal conductivity of the condensate film evaluated at $t_f = 1/2\ (t_c - t_w)$, W/mK

ρ_f = density of the condensate film evaluated at t_f , kg/m^3

μ_f = viscosity of the condensate film evaluated at t_f , $N\ s/m^2$

Δt = temperature differential, °C

$= (t_c - t_w)$

t_w = tube wall temperature, °C

t_c = condensation temperature, °C

D = diameter of tube, m

The waterside coefficient is expressed by the Dittus-Boelter equation:

$$\frac{h_i D}{k} = 0.023 \left(\frac{DU\rho}{\mu} \right)^{0.8} \left(\frac{C_p \mu}{k} \right)^{0.4} \quad (D.4)$$

where: $\frac{h_i D}{k}$ = N_u, the Nusselt Number

$\frac{Du\rho}{\mu}$ = R_e, the Reynolds Number

$\frac{C_p \mu}{k}$ = P_r, the Prandtl Number

from equation (D.4),

$$h_i = \frac{0.023k}{D}\left(\frac{Du\rho}{\mu}\right)^{0.8}\left(\frac{C_p\mu}{k}\right)^{0.4} \quad \ldots(D.5)$$

The calculations for the heat transfer area in the condenser was based on the following assumptions:

- condensing temperature = 30°C
- condensing pressure = 42.42 mbar
- water inlet temperature = 21°C
- water outlet temperature = 25°C
- tubing o.d = 16mm
- tubing i.d = 14.17mm

Asuming a temperature drop of 1°C through the condensing film,

t_f = 1/2 (30 + 29) = 29.5°C

at which the properties of saturated water are:

C_{pf} = 4.1792 KJ/KgK

μ_f = 806.5 x 10^{-6} kg/m.s

ρ_f = 995.75 kg/m^3

h_{fg} = 2431.2 KJ/kg

k_f = 617.3 x 10^{-6} KW/mK

$$h_o = 0.725\left[\frac{k_f^3\,\rho_f^2 . g . h_{fg}}{N.D . \mu_f . \Delta t}\right]^{0.25}$$

$$= 0.725\left[\frac{(617.3 \times 10^{-6})^3 \times 995.75^2 \times 9.81 \times 2431.2}{2 \times 0.016 \times 806.5 \times 10^{-6} \times 1}\right]^{0.25}$$

= 15.621 KW/m^2K

Heat rejected by the condenser, $Q_c = 526W$

Bulk temperature of water, $t_w = \frac{21 + 25}{2}$

$= 23^oC$

at which the properties for water are:

$\rho = 997.5\ Kg/m^3$

$C_p = 4.1817\ KJ/KgK$

$k = 607.8 \times 10^{-6}\ KW/mK$

$\mu = 932 \times 10^{-6}\ Kg/m.s$

Water flow rate, is $= \frac{Q_c}{\rho c_p \Delta t}$

$= \frac{526}{997.5 \times 4.1817 \times 10^3 \times 4}$

$= 3.153 \times 10^{-3}\ m^3/s$

Velocity of water in pipe:

$u = \dot{v}/A = 4\dot{v}/\pi d^2$

$= \frac{4 \times 3.153 \times 10^{-3}}{\pi \times 0.01417^2}$

$= 0.20\ m/s$

$P_r = \frac{\mu C_p}{k} = \frac{4.187 \times 932 \times 10^{-6}}{607.8 \times 10^{-6}}$

$= 6.41$

$Re = \frac{D_i u \rho}{\mu} = \frac{0.01417 \times 0.2 \times 997.5}{932 \times 10^{-6}}$

$= 3033.17$

$h_i = 0.023 \frac{k}{D_i} (R_e)^{0.8} (P_r)^{0.4}$

$= \frac{0.023 \times 607 - 8 \times 10^{-6}}{0.01417} (3033.17)^{0.8} (6.41)^{0.4}$

$= 1.2658\ KW/m^2K$

$\frac{A_o}{A_i} = \frac{D_o}{D_i} = 1.129$

$$\frac{1}{U} = \frac{1}{h_o} + R_o + \frac{r_o}{k}\ln\left(\frac{D_o}{D_i}\right) + R_i\left(\frac{D_o}{D_i}\right) + \frac{1}{h_i}\left(\frac{D_o}{D_i}\right)$$

$$= \frac{1}{15621} + 0.0002 + \frac{0.016}{2 \times 401} \ln 1.129 + 0.00005 \times 1.129 + \frac{1.129}{1265.8}$$

$$= 1.7229 \times 10^{-3}\ m^2K/W$$

$\therefore$ U = 580.43 W/m²K

The bare tube surface area required:

$$A_o = \frac{Q_c}{U\Delta t_m}$$

$$\Delta t_m = \frac{(30 - 21) - (30 - 25)}{\ln (30-21) / (30 -25)}$$

$$= 6.80K$$

$$A_o = \frac{525.13}{580.43 \times 6.80}$$

$$= 0.133m^2$$

The length of tube required:

$$L = A_o/\pi D_o = 0.133/\pi \times .016$$

$$= 2.65m$$

To account for variations in actual operational conditions, a tubing length of about 3.00m was used and the 16.00mm o.d tubing was coiled into 9 turns of 96.00mm pitch diameter.